TECHNISCHE UNIVERSITÄT MÜNCHEN

Lehrstuhl für Biochemische Pflanzenpathologie

Nitric Oxide Signalling in *Arabidopsis thaliana*:
Redox Modification in Mitochondria and Regulation of Transcription

Maria Cristina Palmieri

Vollständiger Abdruck von der Fakultät Wissenschaftszentrum Weihenstephan für Ernährung, Landnutzung und Umwelt der Technischen Universität München zur Erlangung des akademischen Grades eines

Doktors der Naturwissenschaften

genehmigten Dissertation.

Vorsitzender: Univ.-Prof. Dr. C. Schwechheimer

Prüfer der Dissertation: 1. Univ.-Prof. Dr. J. Durner
2. Univ.-Prof. Dr. E. Grill

Die Dissertation wurde am 01.04.2009 bei der Technischen Universität München eingereicht und durch die Fakultät Wissenschaftszentrum Weihenstephan für Ernährung, Landnutzung und Umwelt am 10.11.2009 angenommen.

Parts of this thesis are already published, or publication is in progress, respectively.

Palmieri MC, Lindermayr C, Bauwe H, Durner J (2009)
Glycine decarboxylase associated plant defence responses and cell death are mediated by S-nitrosylation and glutathionylation (submitted; corresponds to **PART I**)

Palmieri MC, Sell S, Huang X, Scherf M, Werner T, Durner J, Lindermayr C (2008)
Nitric oxide-responsive genes and promoters in *Arabidopsis thaliana*: a bioinformatics approach. J Exp Bot 59: 177-186 (corresponds to **PART II)**

Zemojtel T, Frohlich A, Palmieri MC, Kolanczyk M, Mikula I, Wyrwicz LS, Wanker EE, Mundlos S, Vingron M, Martasek P, Durner J (2006)
Plant nitric oxide synthase: a never-ending story? Trends Plant Sci 11: 524-525; author reply 526-528 (not in this thesis)

Contents

PART II: NITRIC OXIDE RESPONSIVE GENES AND PROMOTERS IN *ARABIDOPSIS THALIANA*: A BIOINFORMATICS APPROACH

List of Figures and Tables

Abbreviations

All abbreviations are introduced in the text, but a list of them is included here for easy reference:

A	Net CO_2 assimilation
AAN	Aminoacetonitrile
ABA	Abscisic acid
AEC	Anion exclusion chromatography
AOX	Alternative oxidase
ANOVA	Analysis of variance
AtNOA1	*Arabidopsis thaliana* NO-associated 1
Biotin–HPDP	N-(6-(Biotinamido)hexyl)-3'-(2'-pyridyldithio)-propionamide
bZIP	Basic region/leucine zipper motif
cADPR	Cyclic ADP-ribose
CA	Cinnamic acid
C_4H	Cinnamic acid-4-hydroxyl
CHS	Chalcone synthase
Ci	Intracellular CO_2 concentrations
cPTIO	Carboxy-2-phenyl-4,4,5,5-tetramethylimidazolinone-3-oxide-1-oxyl
cGMP	Cyclic guanosine monophosphate
DAF-2FM DA	Diaminofluorescein diacetate
DTNB	Nitrobenzoicacid
DTT	Dithiothreitol
EDRF	Endothelium derived relaxing factor
GDC	Glycine decarboxylase complex
GSH	Glutathione reduced
GSNO	S-nitroso-l-glutathione
GSNOR	GSNO reductase
GST	Glutathione S-transferase
HR	Hypersensitive response
$H_2DCF-DA$	Dichlorofluorescein diacetate
IRGA	Infrared gas analyzer
L1BX	L1 box

LC-ESI-MS/MS	Liquid chromatography associated with mass spectrometry
MALDI-MS/MS	Matrix assisted laser desorption/ionization time of flight mass spectrometry
MEF	Mitochondria enriched fraction
Nano-HPLC-MS$^{2/3}$	nano–high-performance liquid chromatography/mass spectrometry
NEM	N-ethylmaleimide
Ni-NOR	Nitrite-NO oxidoreductase
NO	Nitric oxide
NO$^+$	Nitrosonium cation
NO$^-$	Nitroxyl radical
NOR-3	(±)-(E)-ethyl-2-[(E)-hydroxyimino]-5-nitro-3-hexeneamide
NOS	Nitric oxide synthase
NR	Nitrate reductase
OBF	TGA/ocs element binding factors
ocs	Octopine synthase
PAL	Phenylalanine ammonia lysase
PHE	Phenylalanine
PR	Pathogenesis related protein
PTP	Permeability transition pore
PVDF	Polyvinylidene difluoride membrane
ROS	Reactive oxygen species
RubP	Ribulose bisphosphate
SA	Salicylic acid
SDS-PAGE	Dodecyl sodium sulphate-polyacrylamide gel electrophoresis
SEC	Size exclusion chromatography
sGC	Soluble guanylate cyclase
SHAM	Salicylhydroxamic acid
SOD	Superoxide dismutase
SNP	Sodium nitroprusside
TFBS	Transcription factor binding site
Tukey's post-hoc	Tukey Honestly Significantly Different test
XOR	Xanthine oxidoreductase
ZE-FFE	Free-flow electrophoresis in zone electrophoresis mode
Γ	CO_2 compensation point
Γ*	Photosynthetic CO_2 compensation point in absence of respiration in the light
$\Delta\Psi_m$	Transmembrane potential

Abstract

The role of nitric oxide (NO) in several signalling routes and in response to different stimuli has been investigated and recognised as fundamental in plants. Despite the proved importance of NO, little is known about signalling pathways downstream of it. Given the ability of NO to react with a range of target molecules, it is likely that there are several cellular 'NO sensor' able to act as signal transducers.

Analyses of NO-dependent processes in plant and animal systems have demonstrated that protein S-nitrosylation – the covalent attachment of NO to cysteine residues - is one of the dominant regulation mechanisms for many proteins. At the same time, a growing body of evidence suggests that mitochondria play an essential role in the NO-signal transduction in plants. Using the biotin switch method in conjunction with nano liquid chromatography and mass spectrometry we identified candidate proteins for nitrosylation in *Arabidopsis thaliana* leaves mitochondria. Among the pool of metabolic and stress-related proteins we found the glycine decarboxylase complex (GDC) as target for S-nitrosylation and S-glutathionylation. GDC is a key enzyme of the photorespiratory C2 cycle in C3 plants which as been previously described to be involved in plant defence responses. In our hands, gas exchange measurements demonstrated that the bacterial elicitor harpin, a strong inducer of reactive oxygen species and NO, inhibits GDC. The specific inhibitor of GDC, aminoacetonitrile (AAN), was able to mimic the stress and/or harpin induced mitochondrial depolarization, H_2O_2 production and cell death in *Arabidopsis thaliana* cell cultures. These findings indicate an involvement of the mitochondrial photorespiratory system as regulator in NO-signal transduction in Arabidopsis.

Besides the regulation of metabolic enzymes, NO can control physiological processes directly by encroaching upon gene transcription. Studies on the transcriptional changes induced by NO permitted to identify genes involved in different functional processes such as signal transduction, defence and cell death, transport, basic metabolism, reactive oxygen species production and degradation. The co-expression of these genes can be explained with

a co-operation of a set of transcription factor that bind common region in the promoter of the regulated genes. Here it is report about searching for common transcription factors binding site (TFBS) in promoter regions of NO-regulated genes, based on microarray analyses. Using Genomatix Gene2Promotor and MatInspector, seven families of TFBS occurred at least 20% more often in the promoter regions of the responsive genes in comparison to the promoter regions of the control genes were identified. Most of these TFBSs, such as ocs element-like sequences and WRKY, were already reported to be involved in particular stresses response. Furthermore, the promoter regions of genes involved in JA biosynthesis for common TFBS module were analyzed, since some genes, responsible for JA biosynthesis, are induced by NO and an interaction between NO- and JA-signalling has already been described.

In sum, the present work focuses on two aspect of the NO-plant interaction with the intention of better understanding the signalling cascade down-stream this molecule. Studying the relation between NO and mitochondria via analysing the S-nitrosylated protein pool, an important role for the glycine decarboxylase complex during plant-stress responses was discovered. Moreover, using a bioinformatic approach it was possible to analyze the relation between NO and plant transcriptome from a different and not conventional point of view. Such analyses of common TFBS and promoter modules in NO-regulated genes may be a fist step to provide the basis to understand regulatory networks involved in gene expression profiles.

1 Introduction

1.1 NITRIC OXIDE SIGNALLING

Nitric oxide (NO) is a high reactive molecule with the ability to diffuse and permeate cell membrane (Delledonne et al., 1998; Wendehenne et al., 2001). NO was first studied in 1772 by Joseph Priestly, who called it "nitrous air", and discovered as a colorless, toxic gas. In 1987, vascular 'endothelium derived relaxing factor' (EDRF) was identified as NO by team headed by Salvador Moncada in UK (Palmer et al., 1987). This finding is regarded as the groundbreaking one serving as a cornerstone for subsequent research on NO. From then on, NO became the sources of intensive and exciting research in animal. Further investigations led to the finding that NO is a multifunctional effectors in numerous mammalian physiological processes, including the relaxation of smooth muscle, inhibition of platelet aggregation, neural communication and immune regulation (Schmidt and Walter, 1994). In 1998 three scientists (Robert F. Furchgott, Louis J. Ignarro and Ferid Murad) won the Nobel Prize for discovering nitric oxide's role in cell signalling. Since then, NO has become one of the most researched molecules in medical topics in recent history. The use of NO is not confined to the animal kingdom. The ability of plants to accumulate and metabolize NO has been known for some time (Nishimura et al., 1986). Moreover, studies conducted several years ago suggested that many aspects of NO signalling are shared by plants and animals. NO is now recognized as one of the most versatile mediators in bacteria, protozoa, animal and plant.

1.1.1 NO Chemistry

NO is a gaseous free radical that contains an unpaired electron in its π_2 orbital, but remains uncharged. Because of its free radical nature, it can adopt an energetically more favourable electron structure by gaining or losing an electron, so that NO can exist as three interchangeable species: the radical ($NO\cdot$); the nitrosonium cation (NO^+); and the nitroxyl radical (NO^-) (Stamler et al., 1992). NO is sparingly soluble in water (0.047cm^3 cm^{-3} H_2O; 20°C 1 atmosphere), however the solubility is increasing in the presence of ferrous salts.

Therefore, it is able to move by diffusion in aqueous parts of the cell, but also in lipophilic environment such as membranes. Once produced, it can move from one cell to another or within a cell (Neill et al., 2002). However, being a reactive free radical, it has a relatively short half-life, in the order of a few seconds. Typically, in biological systems NO reacts rapidly with molecular oxygen (O_2), superoxide anion ($O_2 \cdot^-$) and transition metals. The reaction of NO with O_2 results in the generation of NO_x compounds (including $NO_2\cdot$, N_2O_3 and N_2O_4), which can either react with cellular amines and thiols, or simply hydrolyze to form the end metabolites nitrite (NO_2^-) and nitrate (NO_3^-). The reaction of NO with $O_2 \cdot^-$ yields peroxynitrite ($ONOO^-$), a powerful oxidant that mediates cellular injury. At physiological pH, $ONOO^-$ equilibrates rapidly with pernitrous acid (ONOOH), which, depending on its conformation, rapidly decomposes to NO_3^- or to the highly reactive hydroxyl radical $HO\cdot$. NO also forms complexes with the transition metals found in heme- or iron cluster-containing proteins, thus forming iron-nitrosyl complexes (Wendehenne et al., 2001). Due to these rapid reactions, the range of NO effects is limited to the cell in which it is generated, or to cells in the near neighbourhood.

1.1.2 NO Biosynthesis

Studies conducted in last years have indicated that NO is endogenously produced in plants. NO can be synthesized either by an inorganic nitrogen pathway or by enzymatic catalysis (Figure 1).

Slow and spontaneous liberation of NO occurs from nitrite at neutral pH (Yamasaki and Sakihama, 2000). Acid pH and reducing agents such as ascorbate and phenolics, which are abundant in plants, can also accelerate the rate of NO production (Yamasaki and Sakihama, 2000; Bethke et al., 2004). Recently, Bethke and colleagues have demonstrated synthesis of NO via the non-enzymatic reduction of apoplastic nitrite in seeds (Bethke et al., 2004), although it is unlikely that this route of production of NO is significant in response to pathogen attack as the apoplastic pH is likely to be too alkaline (Bolwell et al., 2002).

In plants, the first enzyme found to be implicated in NO synthesis was nitrate reductase (NR). NR catalyses the NAD(P)H-dependent reduction of nitrite to NO. This protein has a fundamental role in nitrogen assimilation and produces NO when photosynthetic activity is absent or inhibited and when nitrite, the substrate for NR-dependent NO synthesis, can be accumulated (Yamasaki and Sakihama, 2000). Genetic evidence indicates that NR-mediated NO synthesis is required for ABA signalling in *A. thaliana* (Desikan et al., 2002). In addition, since transcript and protein levels of NR are increased in potato tubers treated with

either *Phytophthora infestans* or an elicitor derived from this oomycete pathogen, NR may synthesise NO during plant defence (Yamamoto et al., 2003). However, no significant differences in NO accumulation have been observed between wild-type Arabidopsis plants and the NR double mutant nia1/nia2 in response to infection with avirulent pathogens (Zhang et al., 2003).

In addition to NR, nitrite-NO oxidoreductase (Ni-NOR) is involved in NO formation from nitrite, but exclusively in roots. Ni-NOR activity is coordinated to that of a plasma membrane-bound NR that reduces nitrate to nitrite (Stohr et al., 2001). It appears to use cytochrome *c* as an electron donor in vitro, but it has yet to be cloned and fully identified. Ni-NOR may be involved in several physiological processes in root, including development, response to anoxia, and symbiosis (Stohr and Stremlau, 2006).
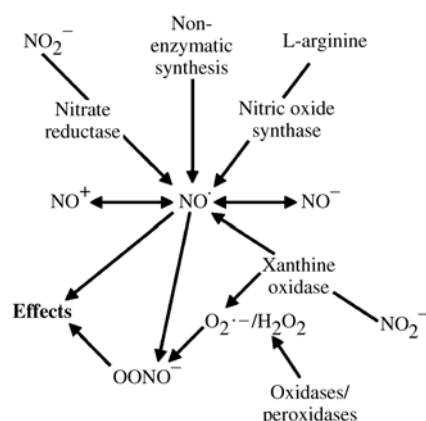
Figure 1. The production of NO (Neill et al., 2003)

There is evidence for several potential sources of NO in plants, including nitric oxide synthase (NOS), nitrate reductase (NR), xanthine oxidoreductase or non enzymatic sources. Once generated, NO can induce various effects, or react with reactive oxygen species to generate peroxynitrite. It should be noted that NO can exist in three forms, and although it is implied here that only the radical is biologically active, both the NO^+ and NO^- may have biological effects.

During the last few years, several groups have provided evidence for the existence of NOS-like activity in plants. NOS catalyses the formation of NO from L-arginine, which undergoes a five electron oxidation to L-citrulline. NADPH and molecular oxygen are essential requirements. Arginine is first converted to hydroxyarginine, a non released catalytic intermediate, with the final products being citrulline and nitric oxide (Furchgott, 1995). NOS-like activities, detected by the oxidation of arginine to citrulline or by electron paramagnetic resonance, have been identified in several plant species such as Mucuna hassjoo, Lupinus albus, tobacco, pea, maize and soybean (Neill et al., 2003). In addition, inhibition of NO production by mammalian NOS inhibitors has been observed in pea, soybean, tobacco and Taxus brevifolia (Wendehenne et al., 2001). Furthermore, confirmatory results have been obtained from immunological and immunocytochemical analysis using antibodies raised against mammalian NOS isoforms (Modolo et al., 2002). A search for the enzyme(s) that catalyze(s) these activities in Arabidopsis led to a hormone-activated NOS, AtNOS1 (Guo et

al., 2003). However, the NO producing ability of the recombinant AtNOS1 could not be confirmed in our and other laboratories (Zemojtel et al., 2006). Reflecting this, it has been suggested to change the name of the protein to *Arabidopsis thaliana* NO-associated 1 (AtNOA1) (Crawford et al., 2006). AtNOA1 is a member of the circularly permuted GTPase family (cGTPase) and specifically binds GTP and hydrolyzes it (Moreau et al., 2008). Nonetheless, this protein seems to be an important factor in NO synthesis and/or accumulation.

Other enzymes have been found in plants that can also generate NO. Animal xanthine oxidoreductase (XOR) is capable of producing NO under hypoxic conditions (Millar et al., 1998), but work with recombinant suggested that this enzyme is probably not relevant to NO signalling in plants XOR (Planchet and Kaiser, 2006). Organelle NO generation has also been reported by several groups. Planchet et al. (Planchet et al., 2005) showed reduction of nitrite to NO by tobacco mitochondria, while soy bean chloroplasts appear to use either arginine or nitrite to generate NO (Jasid et al., 2006).

1.1.3 NO Function in Plants

The unique free radical chemistry of NO, which permits either to gain or lose an electron to energetically more favourable structures, confers to NO stability and reactivity (Beligni and Lamattina, 2001). NO can interact with a variety of intracellular and extracellular targets, acting as either cytotoxic or cyto-protecting agents. High levels of NO are associated with cell death and DNA fragmentation in Taxus cultures (Pedroso et al., 2000), reduction of photosynthesis in oat (Clyde Hill and Bennett, 1970) and of respiration in carrot cell suspensions (Zottini et al., 2002). On the other hand, NO stimulates seed germination in different species and a decrease in NO levels has also been associated with fruit maturation and flower senescence, suggesting its involvement in the modulation of these physiological processes (Beligni and Lamattina, 2001). Nitric oxide has been reported to be induced rapidly by several different types of chemical, mechanical and environmental stressors in a variety of plant species, and to regulate the plant responses to the abiotic stresses (Table 1). Almost all abiotic stressors generate free radicals and other oxidants, particularly from the chloroplasts, mitochondria and peroxisomes, resulting in oxidative stress in terms of an increased level of reactive oxygen species (ROS) in plant cells (Mittler, 2002).

Introduction

Table 1. Reports of induction of NO production by abiotic stress and NO-mediated effect (Qiao and Fan, 2008)

ABA, abscisic acid; LEA, late embryogenesis abundant; ROS, reactive oxygen species.

STRESSOR	NO-MEDIATED EFFECT	SPECIES OF INDUCED NO	REFERENCE
Drought/osmotic stress	Involved in ABA signalling, stomatal closure	*Nicotiana tabacum*	Gould et al. (2003)
	Induction of ABA synthesis, LEA expression	*Pisum sativum*	Leshem and Haramaty (1996)
Salinity	Increased osmotic tolerance; induced expression of Na^+/H^+ antiporter gene	*N. tabacum maize*	Gould et al. (2003) Zhang et al. (2006b)
Heavy metal toxicity	Increased the root elongation; reduced the NOS activity	*Hibiscus moscheutos* (Al^{3+}) (Reduced NO level)	Tian et al. (2007)
Herbicide	Promoted the activity of antioxidant enzymes	*Scenedesmus obliquus*	Mallick et al. (2000)
		Chlamydomonas reinhardtii	Sakihama et al. (2002)
High temperature	Increased tolerance of seedlings; rapid NO release	*Medicago sativa*	Leshem et al. (1998)
		N. tabacum	Gould et al. (2003)
Low temperature	Decline in the ROS level	*S. obliquus*	Mallick et al. (2000)
Mechanical injury	NO burst result in cell death	*Arabidopsis thaliana*	Garces et al. (2001)
		Taxus brevifolia	Pedroso et al. (2000a)
Nutrient deficiency		*S. obliquus*	Mallick et al. (2000)
UV-B radiation	Induced the expression of CHS gene	*A. thaliana*	Mackerness et al. (2001)

ROS not only causes oxidative damage, but also exerts some signalling responses. Thus plants controlling the concentration of ROS is a survival response (Vranova et al., 2002). In fact, lower concentrations of NO eliminate the superoxide anion O_2^-, and lipid radical R^-

activates the antioxidant enzymes, particularly superoxide dismutase (SOD). The scavenging of O_2^- by NO leads to the formation of peroxyntrite ($ONOO^-$), which is strongly toxic in animal cells but not toxic for plant cells (Delledonne et al., 2001; Kopyra and Gwó d, 2004). In contrast, high concentration of NO enhances superoxide production in mitochondria by inhibiting electron flow cytochrome c oxidase (Millar and Day, 1996). The antioxidant role of NO is mainly based on its ability to maintain the cellular redox homeostasis and regulate the toxicity of ROS. Moreover, NO was also proposed to eliminate the excess of nitrite from plant cells, as high concentrations of nitrite are toxic to plant cells (Shingles et al., 1996).

Another important role of NO in abiotic stress responses relies on its properties as a signalling molecule. NO is involved in the signalling pathway downstream of jasmonic acid synthesis and upstream of H_2O_2 synthesis, and regulates the expression of some genes involved in abiotic stress tolerance (Orozco-Cardenas and Ryan, 2002; Wendehenne et al., 2004). There is a synergistic effect between NO and ROS in ABA biosynthesis (Zhao et al., 2001). Furthermore, NO influences Ca^{2+} level in response to either salinity or osmotic stress caused by sorbitol (Gould et al., 2003; Zhao et al., 2004).

1.1.4 NO Perception and Signal Transduction

Despite the proved importance of NO, little is known about signalling pathways downstream of it. It seems unlikely that specific receptors exist for NO, as NO is such a simple, small and diffusible molecule. However, cells undoubtedly do sense NO, as various cellular activities are modulated in its presence. Given the ability of NO to react with a range of target molecules it may be that there are several cellular 'NO sensor' able to act as signal transducers (Figure 2).

- **Cyclic GMP, cyclic ADP ribose and Ca^{2+} as nitric oxide mediators**

It has been shown that NO signalling during both programmed cell death and defence responses requires cyclic GMP (cGMP) and cyclic ADP-ribose, two molecules that can serve as secondary messengers (Wendehenne et al., 2001).

Soluble guanylate cyclase (sGC) is a key player in animal NO signalling. Binding of NO to its haem domain results in increased cGMP levels which in turn activates a number of downstream signalling processes. The use of pharmacological inhibitors of mammalian sGC in plants has placed cGMP downstream of both guard cell ABA and NO signalling during stomatal closure (Neill et al., 2003). NO induces raised levels of cGMP in plants (Durner et al., 1998), and both ABA and the NO donor SNP induce a transient increase in cGMP in guard-cell-enriched preparations from Arabidopsis (Neill et al., 2008). This can be prevented

by the application of the sGC inhibitor or the NO scavenger cPTIO. Thus, a similar mechanism of NO-induced cGMP synthesis and signalling may also operate in plants.
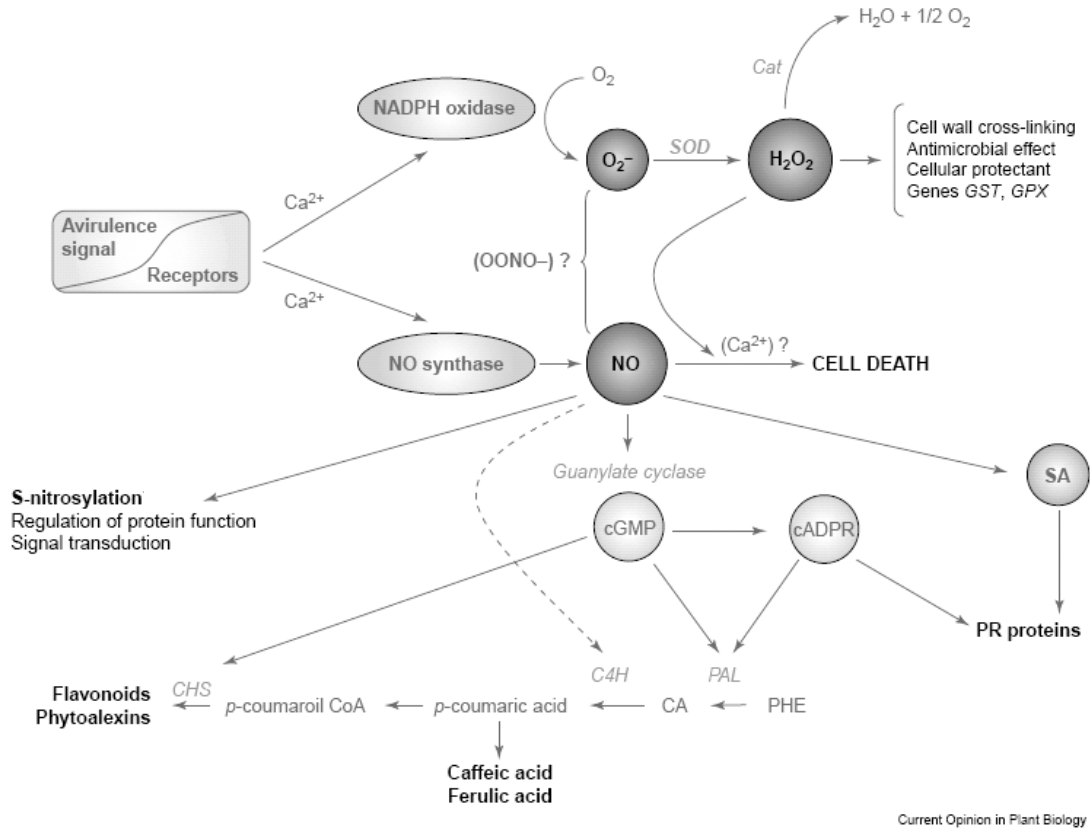
Figure 2. Representation of NO signalling functions during response to avirulent pathogens
(Delledonne, 2005)

CA: cinnamic acid; Ca^{2+}: calcium influx; cADPR: cyclic ADP ribose; Cat: catalase; C_4H: cinnamic acid-4-hydroxylase; CHS: chalcone synthase; cGMP: cyclic GMP; GPX: glutathione peroxidase; GSNO: S-nitroso-l-glutathione; GST: glutathione S-transferase; NOS: nitric oxide synthase; ONOO−: peroxynitrite; PAL: phenylalanine ammonia lyase; PHE: phenylalanine; PR: pathogenesis-related proteins; SA: salicylic acid; SOD: superoxide dismutase.

NO is known to cause increases in the level of free Ca^{2+} (Durner et al., 1998; Garcia-Mata et al., 2003), and cGMP, cADPR and Ca^{2+} have all been shown to be involved in regulating stomatal movements in response to ABA (Garcia-Mata and Lamattina, 2002; Neill et al., 2003). Removing the NO during this process effectively prevents stomatal closure and simultaneously inhibits the ABA-induced inactivation of the Ca^{2+}-dependent inward rectifying K^+ channel and activation of the outward rectifying Cl^- channel (Garcia-Mata et al., 2003). Thus, NO and Ca^{2+} are both strongly implicated in the signalling cascade that must operate.

Thus, it would seem very likely that responses to NO may be accomplished by signalling through cGMP, cADPR and Ca^{2+}.

- **MAP kinase pathways**

In common with other plant hormones, NO is also known to activate MAP kinase signalling pathways (Nakagami et al., 2005) which presumably results in altered gene expression. A MAPK has been found to be activated by NO in Arabidopsis (Clarke et al., 2000), although its function in the induction of genes involved in defence has not been clearly shown. Nevertheless, at least two MAPKs have been reported to function as regulators in the early plant defence response (Cardinale et al., 2000).

- **Tyrosine Nitration**

In animals, tyrosine nitration is classically associated with loss of protein functions and is a relevant biomarker of NO-dependent oxidative stress (Hanafy et al., 2001). However, recent studies also highlight a role for this posttranslational modification in signalling (Hanafy et al., 2001; Schopfer et al., 2003). Endogenous protein tyrosine nitration occurs in mutant tobacco plants exhibiting greatly increased NO production (Morot-Gaudry-Talarmain et al., 2002) and in the leaves of olives during salt stress (Valderrama et al., 2007). However, the extent and biological significance of protein nitration in plants remain to be seen.

- **S-Nitrosylation**

Many of the biological functions of NO arise as a direct consequence of chemical reactions between proteins and NO or NO oxides generated as NO/O_2 or NO/superoxide reaction products. NO groups can modify cysteine thiols and transition metal centres of a broad functional spectrum of proteins, as already showed for many animal proteins (Foster and Stamler, 2004; Dahm et al., 2006). S-nitrosylation, the covalent attachment of a nitrogen monoxide group to the thiol side chain of cysteine, is a labile post-translational modification with half-lives of seconds-few minutes and represents a very sensitive mechanism for regulation cellular processes (Hess et al., 2005). As most proteins possess cysteine residues, substrate specificity is a very important feature of endogenous protein S-nitrosylation. This includes structural factors that influence the susceptibility to S-nitrosylation like surrounding acidic or basic amino acids and the presence of a hydrophobic environment that enables the formation of S-nitrosylating species via the reaction between oxygen and NO (Stamler et al., 1997). An acid-base motif containing acidic (Asp, Glu) and basic (Arg, Lys, His) residues,

promotes S-nitrosylation of the NO-sensitive cysteine residues (Stamler et al., 1997). The basic amino acids support the H^+ release of the thiol group of the cysteine, whereas acidic amino acid side chains promote NO^+ donation of the NO donor (Perez-Mato et al., 1999). Recently, protein S-nitrosylation was thought to be controlled principally through the regulation of NO biosynthesis (Stamler et al., 2001). Emerging evidence, however, indicates that SNO turnover may provide an alternative regulatory mechanism. S-nitrosylation of the antioxidant tripeptide glutathione forms S-nitrosoglutathione (GSNO), which is thought to function as a mobile reservoir of NO bioactivity (Feechan et al., 2005). An enzyme has now been uncovered that metabolizes this molecule. Whereas this GSNO reductase (GSNOR) activity is highly specific for GSNO, it has been shown to control intracellular levels of both GSNO and SNO proteins in yeast and mice (Liu et al., 2001). The trans-S-nitrosylation from GSNO to proteins seems to be promoted by acidic, basic, and hydrophobic side chains neighboring the target cysteine residue (Hess et al., 2005). There are S-nitrosylation motifs that promote binding of GSNO in a way that the NO group of GSNO is positioned close to the sulfhydryl group of the reactive cysteines. By molecular modelling and data base screening Hess et al. identified the optimal positioning of GSNO, which is achieved through hydrogen bonding between the γ-glutamyl amine of GSNO and the γ-carboxylate of the acidic amino acid C-terminal of the target cysteine residues (Hess et al., 2005).

Many examples of protein S-nitrosylation and consequent modulation in activity have been reported in animal system. For example, caspase-3 zymogens are S-nitrosylated at the active site cysteine and enzyme activity inhibited, whereas during Fas-induced apoptosis they are de-nitrosylated and the function of the catalytic site is regained (Mannick and Schonhoff, 2004). Lindermayr et al. (2005) identified plant proteins sensitive to this post-translational process, in extracts of Arabidopsis cell cultures treated with the NO donor GSNO and in Arabidopsis plants treated with gaseous NO. Moreover, by using the same proteomic approach, changes in S-nitrosylated proteins in *Arabidopsis thaliana* leaves undergoing hypersensitive response (HR) were characterized (Romero-Puertas et al., 2008). Although more than 50 proteins were identified, there are experimental evidences for only few plant proteins to be regulated by S-nitrosylation. Examples are the methionine adenosyltransferases (Lindermayr et al., 2006), the peroxiredoxin II E (Romero-Puertas et al., 2007), the metacaspase (Belenghi et al., 2007) and NPR1, a master regulator of salicylic acid–mediated defence genes (Tada et al., 2008).
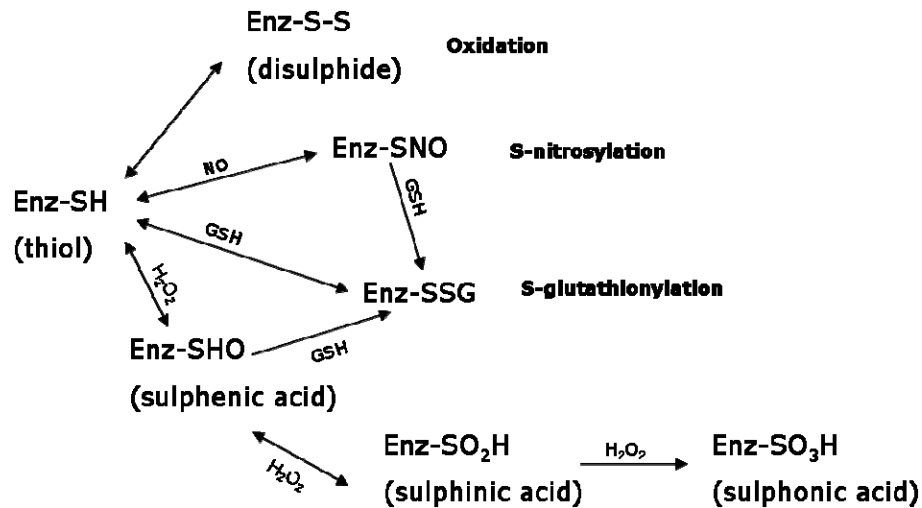
Figure 3. Competition for thiol groups

Two cysteine thiol groups within a protein may interact to form a disulphide bond. However, single thiol groups may be either reversibly (Enz-SOH and Enz-SO$_2$H) and irreversibly (Enz-SO$_3$H) oxidized by reactive oxygen species (ROS) such as H$_2$O$_2$ or may be S-nitrosylated by nitric oxide (NO). Additionally, thiol groups may react with compounds such as glutathione (GSH). Thus, there is most likely competition for thiol group availability in terms of NO signalling by S-nitrosylation. Enz: enzyme.

While ROS can directly affect NO synthesis and accumulation, they can also compete for potential NO binding sites. Thiol groups are not only potential sites for S-nitrosylation, but also subjects to competitive interaction with other ROS. Moreover, the nitrosothiol itself represents an activated form that can react with GSH leading to S-glutathionylation (Martinez-Ruiz and Lamas, 2007). Figure 3 highlights the processes that potentially occur and which may thus, attenuate or modify NO signalling.

- **Transcriptional changes in response to NO**

Besides the regulation of metabolic enzymes, NO can control physiological processes directly by encroaching upon gene transcription. Transcriptional changes in *Arabidopsis thaliana* in response to NO were analyzed using different techniques like cDNA-amplified fragment length polymorphism (Polverari et al., 2003), microarray and real-time PCR (Huang et al., 2002; Parani et al., 2004). Identified NO-modulated genes are involved in different functional processes such as signal transduction, defence and cell death, transport, basic metabolism, ROS production and degradation. An important part of these modulated genes corresponds to proteins with a regulatory role as components of signal transduction cascade or transcription factors.

The transcription of genes is regulated by transcription factors. These proteins bind to defined promoter sequences to enhance or repress gene expression by assisting or blocking RNA polymerase binding, respectively. Next to direct DNA-binding, transcription factors often interact with other proteins and bind to promoter region as multi-protein complexes. The DNA-binding affinity of transcription factors can be altered for example by phosphorylation or redox-dependent modifications, such as protein S-nitrosylation. For example, the activity of the thiol-containing transcriptional activator OxyR, whose oxidation controls the expression of genes involved in H_2O_2 detoxification, is modulated by the S-nitrosylation (Hausladen et al., 1996). The use of whole genome transcript analyses to identify co-regulated genes has been rapidly becoming a widespread approach to understand the regulation of physiological processes.

1.2 MITOCHONDRIA IN REDOX SIGNALLING

1.2.1 Mitochondrial ROS

In addition to the established role of the mitochondria in energy metabolism, regulation of cell death has emerged as a second major function of these organelles. This seems to be intimately linked to their generation of ROS (Rhoads et al., 2006). Oxidative stress is generally defined as an imbalance that favors the production of ROS over antioxidant defences; however, the precise mechanisms by which ROS produce cellular injury remain elusive. The amount of ROS produced by mitochondria and the fraction of total cellular ROS that come from mitochondria are difficult to determine, in part because ROS levels in general are difficult to measure accurately (Halliwell and Whiteman, 2004). However, it is possible to estimate that the in situ level of mitochondrial ROS evolution normally is considerably less than that of chloroplasts or peroxisomes in the light due to the operation of photosynthesis and photorespiration (Foyer et al., 2003). However, in the dark or in non-green tissues, mitochondria will be a major source of ROS (Puntarulo et al., 1988).

The majority of ROS are products of mitochondrial respiration (Figure 4). Approximately 1%–2% of the molecular oxygen consumed during normal physiological respiration is converted into superoxide radicals. The one-electron reduction of molecular oxygen produces a relatively stable intermediate, the superoxide anion ($O_2^{\cdot-}$), which can be regarded as the precursor of most ROS. The one-electron reduction of oxygen is thermodynamically favourable for most mitochondrial oxidoreductases (Turrens, 2003). The mitochondrial electron transport chain (mtETC) contains several redox centers that may leak electrons to molecular oxygen, serving as the primary source of superoxide production in

most tissues. There is growing evidence that most of the $O_2^{\cdot-}$ generated by intact mitochondria in vitro is produced by complex I and complex III (Moller, 2001).
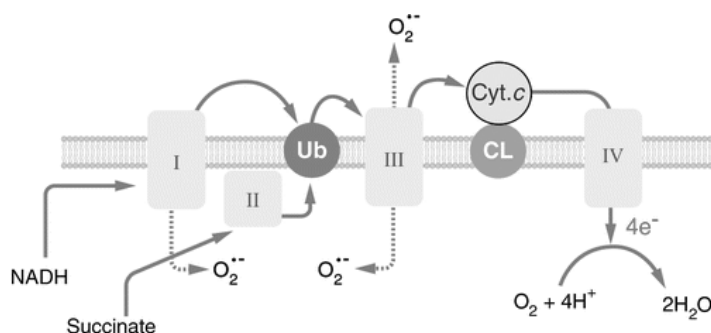
Figure 4. Formation of reactive oxygen species by the mitochondrial respiratory chain

CL: cardiolipin; Cyt. *c*: cytochrome *c*; Ub: ubiquinone.

Photorespiration is a high flux, information-rich pathway that achieves optimal rates under high light, high temperatures, and CO_2 or water deficits in C3 plants. The majority of higher plant species photosynthesize using only the C3 pathway, where photorespiration has a major impact on cellular carbon metabolism, bioenergetics, nitrogen assimilation and respiration. The photorespiratory pathway is a source of H_2O_2 in photosynthetic cells. Through H_2O_2 production and pyridine nucleotide interactions, photorespiration makes a key contribution to cellular redox homeostasis. In doing so, it influences multiple signalling pathways, particularly those that govern plant hormonal responses controlling growth, environmental and defence responses and programmed cell death. The potential influence of photorespiration on cell physiology and fate is thus complex and wide-ranging.

1.2.2 Mitochondria and NO

Mitochondria are highly membranous organelles and sequester lipophilic molecules such as NO. A growing body of evidence suggests that mitochondria play an essential role in the NO-signal transduction in plants.

Stimulation of $O_2^{\cdot-}$ and H_2O_2 production by mitochondria was demonstrated in the presence of NO. Infect, NO has been found to inhibit cellular respiration through its action at cytochrome *c* oxidase (complex IV), via binding its binuclear CuB/heme-a3 active site (Cleeter et al., 1994; Shiva et al., 2001). Moreover, Huang et al. (2002) showed that NO causes an inhibition of KCN-sensitive respiration and an activation of the alternative pathway respiration in *Arabidopsis thaliana*.

Mitochondria contain sizeable thiol pools, are abundant in transition metals, all of which are known to modulate SNO biochemistry (Foster and Stamler, 2004). Additionally, the formation the S-nitrosylating intermediate N_2O_3 is enhanced within membranes (Burwell et al., 2006). An example in the animal system is the S-nitrosylation of the catalytic site cysteine of a subset of mitochondrial caspase members. These events serve as an on/off switch regulating caspase activity during apoptosis (Mannick et al., 2001). Moreover cytochrome *c*, whose release from mitochondria into the cytoplasm plays a critical role in many forms of apoptosis by stimulating apoptosome formation and subsequent caspase activation, is nitrosylated on its heme iron during apoptosis (Schonhoff et al., 2003). Despite this evidence of mitochondria-NO interaction, no approaches were undertaken to identify the direct NO targets in plant mitochondria until now.

1.2.3 Function of Mitochondria during Plant – Pathogen Interactions

In plants, the involvement of mitochondria in pathogen induced defence responses and cell death has been demonstrated (Ryerson and Heath, 1996; Chivasa and Carr, 1998). Importantly, while an extramitochondrial trigger may initiate disruptions in mitochondrial function, it appears that loss of mitochondrial function and the concomitant mtROS signal that is generated are necessary for subsequent PCD. Several evidence are present in plant bibliography, that comes trough the use of toxins or elicitors of plant pathogens (Robson and Vanlerberghe, 2002; Yao et al., 2002; Krause and Durner, 2004).

PCD is an important part of certain plant responses to stresses and includes the HR in response to pathogens. An early cellular signal for this process is frequently an increase in tissue ROS production due to plasma membrane NADPH oxidase activity (Overmyer et al., 2003). Plant mitochondrial responses to PCD signals are similar to those of animal mitochondria. Elevated cytosolic Ca^{2+} and oxidative stress both contribute to the opening of the mitochondrial permeability transition pore (PTP), which depolarizes the mitochondria and leads to mitochondrial swelling and subsequent release of cytochrome *c* from the intermembrane space (Goldstein et al. 2000). Cytochrome *c*, when released into the cytosol, becomes a critical component of the apoptosis execution machinery, where it activates caspases (cysteine aspartate proteases) and, if ATP is available, causes apoptotic cell death (Thornberry and Lazebnik, 1998).

1.2.4 Photorespiration: Role in Stress Protection

Photorespiration results from the oxygenase reaction catalysed by ribulose-1,5-bisphosphate carboxylase/oxygenase. In this reaction glycollate-2-phosphate is produced and subsequently metabolized in the photorespiratory pathway to form the Calvin cycle intermediate glycerate-3-phosphate (Figure 5). During this metabolic process, CO_2 and NH_3 are produced and ATP and reducing equivalents are consumed, thus making photorespiration a wasteful process. However, precisely because of this inefficiency, photorespiration is also involved in stress protection. In addition, photorespiratory metabolism can generate metabolites, such as glycine, serine or one-carbon units for other processes in plants (Madore and Grodzinski, 1984). As example, by supplying glycine for the synthesis of glutathione, a component of the antioxidative system in plants (Noctor and Foyer, 1998), photorespiration may provide additional protection against oxidative damage in high light. Thus, photorespiration, in addition to being wasteful, may also be a useful process in plants. Abolishing photorespiration by engineering rubisco may therefore not necessarily lead to improved plant performance, especially under unfavourable growth conditions.

Because of the high energy requirement of photorespiratory metabolism, it has been suggested that photorespiration is important for maintaining electron flow to prevent photoinhibition under stress conditions. An impairment of the flux through the photorespiratory pathway can lead to photoinhibition by inhibiting photosynthetic CO_2 assimilation caused by an insufficient regeneration of ribulose biphosphate (RuBP) or by an accumulation of toxic metabolites (Igamberdiev et al., 2001).
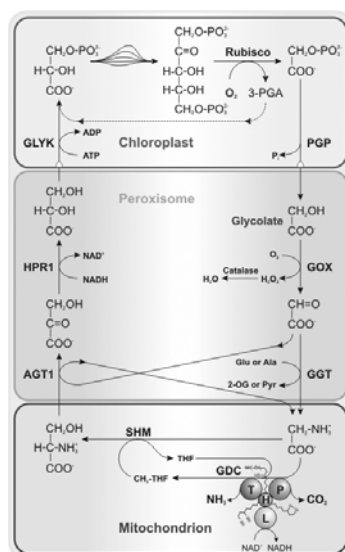
Figure 5. Photorespiratory pathway (Bauwe H.)

Plants produce oxygen as a by-product of photosynthetic light reactions. This oxygen triggers photorespiration, an ancient process inherited from the evolution of photosynthesis in bacteria. However, oxygen also binds to the same enzyme, rubisco, which is also responsible for the photosynthetic fixation of carbon dioxide. This binding of oxygen to rubisco inhibits carbon dioxide fixation and leads to the synthesis of large amounts of phosphoglycolate. In order to survive in the now 21% oxygen-containing atmosphere, plants need to convert this compound into more useful products. This is achieved by the photorespiratory cycle, which was one of the most important metabolic adaptations during the evolution of land plants.

Aim of the Study and Research Strategy

Although a lot is known about the physiological importance of NO for plant growth, development and defence, less is known about the target molecules of NO. The present work focuses on two aspects of NO signalling pathway in plants with the intention of better understanding the signalling cascade down stream of this molecule.

PART I: MODIFICATION OF MITOCHONDRIAL PROTEINS BY S-NITROSYLATION

Recent evidence points to the mitochondria as a key organelle in the regulation of cellular responses to stress. Based on the demonstrated roles of mitochondria in animal and plant apoptosis or PCD, the main emphasis of this work will be to identify NO targets in plant mitochondria using *Arabidopsis thaliana* as model system. The relation between NO and mitochondria will be investigated *via* analysing the S-nitrosylated protein pool after treating Arabidopsis mitochondria with the trans-nitrosylating agent GSNO. Furthermore, the function of protein S-nitrosylation in plant mitochondria will be analysed to get insight in signalling pathways downstream of NO as well as physiological and regulatory function of NO in plants.

PART II: NITRIC OXIDE RESPONSIVE GENES AND PROMOTERS IN *ARABIDOPSIS THALIANA*: A BIOINFORMATICS APPROACH

A further aspect of this work will be the analysis of the relation between NO and plant transcriptome from a different point of view. Transcriptional changes in *Arabidopsis thaliana* in response to NO were analyzed in the last years using different techniques like cDNA-amplified fragment length polymorphism, microarray and real-time PCR. By analysing common TFBS and promoter modules in the promoter region of NO-regulated genes, transcription factor regulated by NO will be identified. Moreover, by using this bioinformatic approach, the basis for understanding of regulatory networks involved in NO-dependent gene expression profiles will be provided.

Part I

MODIFICATION OF MITOCHONDRIAL

PROTEINS BY S-NITROSYLATION

2 Results

2.1 NITRIC OXYDE PRODUCTION IN ARABIDOPSIS MITOCHONDRIA

Although NO and its exchangeable redox activated forms are now recognized as intra- and intercellular signalling molecules (Durner et al., 1998), less is known about how NO regulates different events in plants. Mitochondria, as essential organelle for normal cellular function and as integrator for apoptotic signalling, are perfect candidates in playing a role in NO-signal cascade. Although in the last few years different publications underlined the involvement of mitochondria in pathogen/elicitor-induced defence responses and cell death in plants (Chivasa and Carr, 1998; Huang et al., 2002; Krause and Durner, 2004), a direct evidence of NO production in Arabidopsis mitochondria is still missing. To prove NO localization and production in mitochondria we used harpin, as we previously showed that this bacterial elicitor is able to induce NO production within few hours in Arabidopsis suspension cells, with a maximum accumulation of NO-dependent fluorescence after 6-8h (Krause and Durner, 2004). Using the dye diaminofluorescein diacetate (DAF-2FM DA) as NO-probe and MitoTracker Red 580 as mitochondria-specific dye, we could observe harpin dependent NO production over time (0-6h) (Figure 4). The basal fluorescence at time zero represents basal NO in untreated cells. As control, we pre-treated Arabidopsis with carboxy-2-phenyl-4,4,5,5-tetramethylimidazolinone-3-oxide-1-oxyl (cPTIO), an NO scavenger that blocks NO production as well as NO-dependent cell death (Barchowsky et al., 1999). The overlapping of the two dyes, which appears yellow, represents the co-localization of NO and mitochondria (Figure 4).

2.2 PREPARATION OF MITOCHONDRIAL FRACTION

Different mitochondria preparations were compared to obtain high amount of pure, intact mitochondria. Protocols were optimized for the isolation and purification of mitochondria from
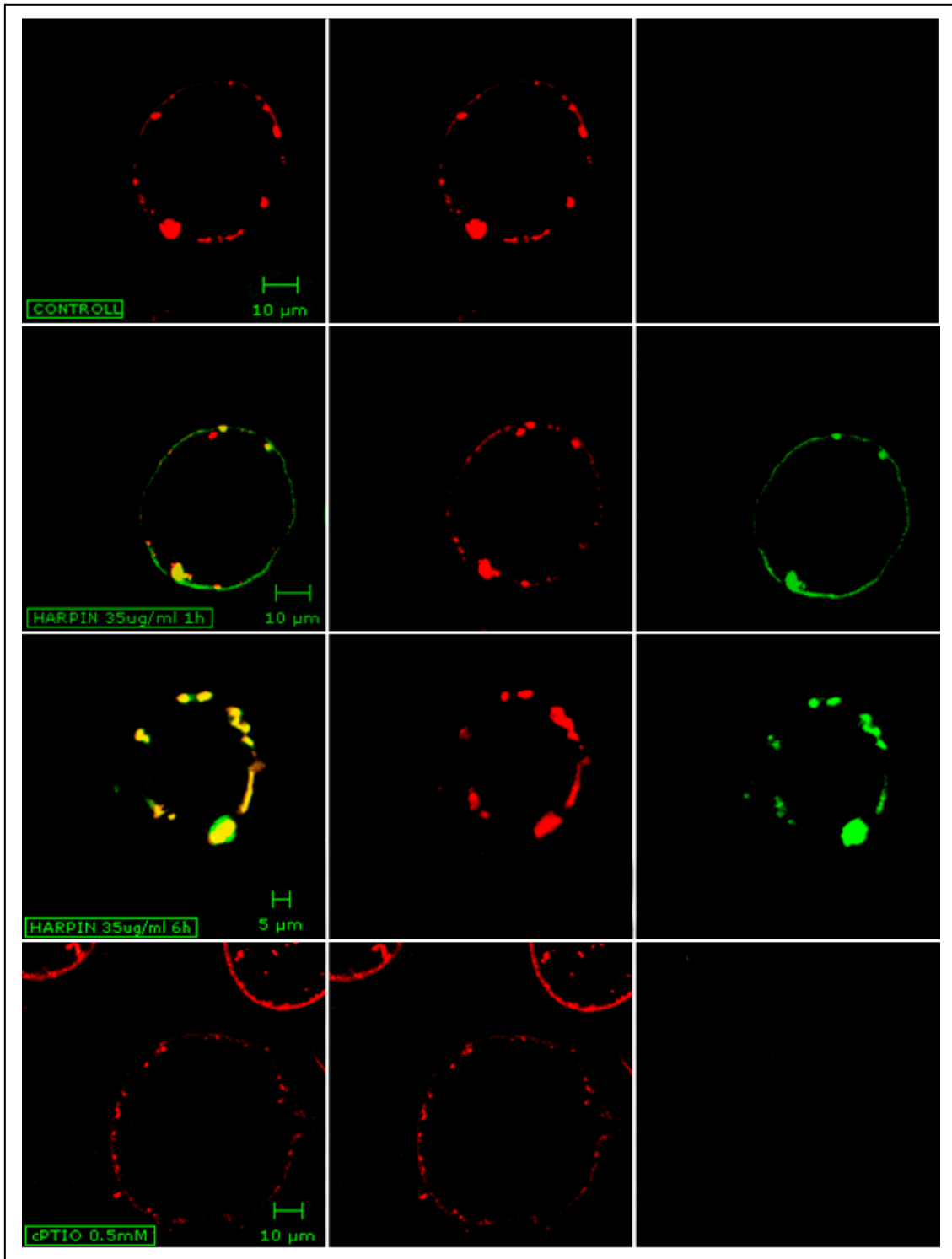
Figure 4. Harpin dependent NO production in mitochondria

Arabidopsis suspension cells were incubated with 35 μg/ml of harpin. Treated cells as well as controls were stained with MitoTracker Red 580 as mitochondria-specific dye and DAF-2FM DA as NO-probe. Stained Arabidopsis cells were observed under the fluorescent confocal microscope Zeiss LSM 510 NLO (Zeiss). Images were obtained with a 40X water lens. Mitochondria (red signal) and the produced NO (green signal) showed co-localization, which appears yellow. NO fluorescence in harpin-treated sample was completely scavenged with a pre-incubation with 0.5mM cPTIO.

Arabidopsis thaliana leaves. The high functionality was required because of the intention to study protein post-translational modification and organelles-specific enzyme activity. At the same time, the amount of mitochondrial proteins and the degree of purification from other organelles were essential prerequisites to ensure the detection of low abundant proteins. As first step of purification, crude and well-coupled mitochondria were isolated by differential centrifugation, essentially as described by Keech et al. (Keech et al., 2005). To further purify these mitochondria enriched fraction (MEF) we compared different protocols. Differential and isopycnic centrifugation using sucrose or Percoll gradients to separate organelles on the basis of size and density have been traditionally used in isolation of mitochondria from plant tissues (Neuburger et al., 1982; Millar et al., 2001). Unfortunately biological variation will always lead to a degree of overlap between different organelles or compartments. Moreover, removal of Percoll, necessary before further analysis, represented a limiting factor for many workers (Yang and Mulligan, 1996). Free-flow electrophoresis in zone electrophoresis mode (ZE-FFE) for mitochondria purification does not rely on size or density but provides separation electrophoretically by using differences in the surface charge of the organelles (Heidrich et al., 1970). ZE-FFE has successfully been employed to purify yeast and plant mitochondria (Zischka et al., 2003; Eubel et al., 2007).
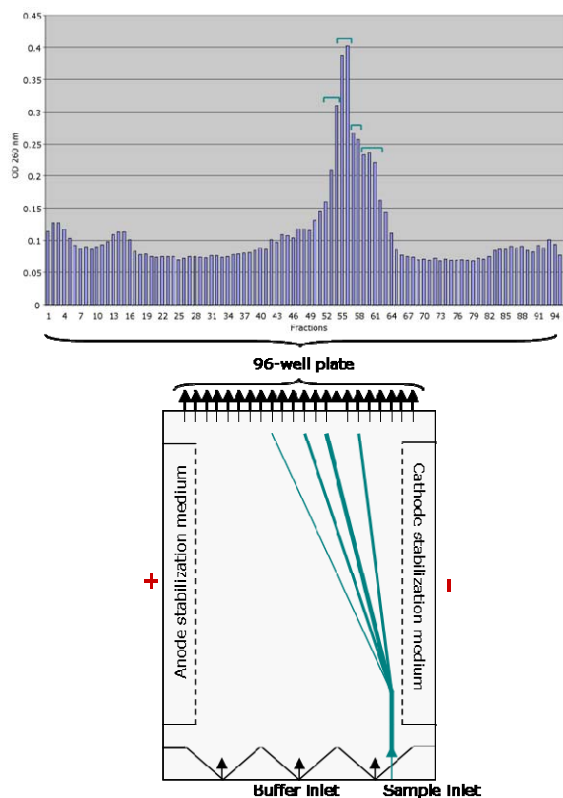
Figure 5. Purification of mitochondrial crude extract by ZE-FFE

After differential centrifugation steps mitochondria were purified by FFE to allow a second dimension of separation based on surface charge. Around 4mg of proteins at 1mg/ml were run on a FFE apparatus at 1ml/h and the fractions collected in 96-well plates. For each plate the absorbance at 260nm was measured, giving a profile of protein concentration. Following this profile, fractions were grouped and concentrated by centrifugation at 15000rcf x 15min. Precipitated mitochondria were re-suspended in washing buffer and assayed for protein concentration, organelles-specific enzymatic assays and respiration.

Therefore ZE-FFE was utilized by means of a ProTeam FFE™ free-flow electrophoresis apparatus to further purify MEF from Arabidopsis leaves. With FFE the mitochondrial enriched extract was fractionated during a laminar flow between cathode and anode, producing fractions containing in different amount functional mitochondria, depolarized mitochondria, peroxysome and chloroplast (Figure 5).
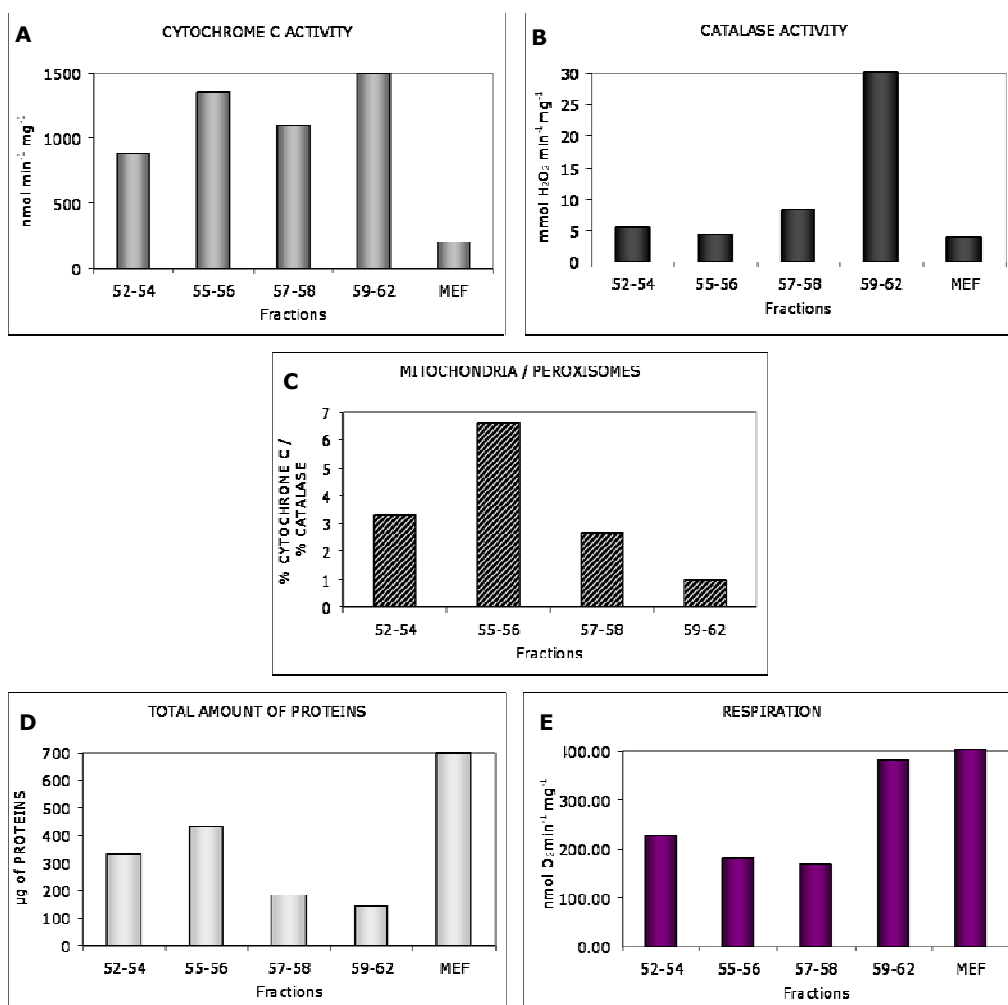
Figure 6. Analysis of mitochondrial fractions

After FFE runs the different fractions were grouped as showed in Figure 5. X and analysed for organelle-specific enzymatic assays and respiration. **A.** Quantification of mitochondrial integrity by monitoring the cytochrome c oxidase. After incubation for 15min at RT the oxidation of the ferrocytochrome c was measured as abs550/abs565 ratio of an aliquot of FFE fractions diluted 20-fold with assay buffer. **B.** Catalase activity assay to monitor the localization of peroxisomes in FFE fractions. The decomposition of hydrogen peroxide (H_2O_2) to water and oxygen via catalase was measured by colorimetric assay. The reaction kinetics was conducted at 0°C with 6mM H_2O_2 for 35min and the final reaction volume was 1ml. **C.** Mitochondria/peroxisome ratio in the different FFE fractions. The value represents the ratio between cytochrome c activity and catalase activity, calculated as percentages of the activities in the initial preparation. The most pure mitochondria were localized in the peak of the first protein curves (fractions 55-56). **D.** Protein amount in the FFE fractions. All together proteins in FFE fractions represented around 25% of starting material. **E.** Cytochrome c dependent respiration in FFE fractions. 52-54/55-56/57-58/59-62: FFE fractions as showed in Figure 5. MEF: mitochondrial enriched fraction obtained by differential centrifugations.

To compare the purification degree obtained, the different fractions were analyzed for integrity (Figure 6A), purity (Figure 6B), protein amount (Figure 6D) and respiration rate (Figure 6E). The ratio between cytochrome c activity (marker for mitochondria) and catalase activity (marker for peroxysome) gave us an overview of the enrichment of mitochondria obtained with FFE (Figure 6C). Intact mitochondria were localized in each run mostly in the left upper part of the major peak, with fractions 55-56 (top of the curve, Figure 5) containing the most pure ones (Figure 6C).

2D electrophoresis was used to verify at the qualitative level the purity of the mitochondria isolated by differential centrifugation. Overall, the general protein spot patterns were very consistent with the mitochondrial proteome profiles previously published by Eubel et al. (Eubel et al., 2007) (Figure 7).
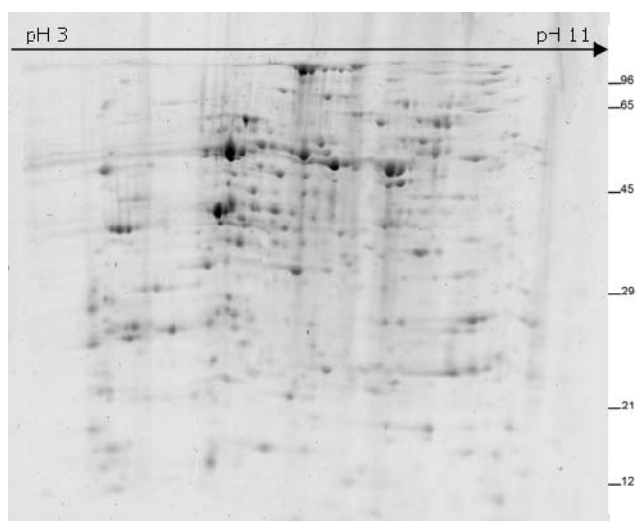
Figure 7. 2D gel analysis of MEF

300µg of mitochondria purified by differential centrifugations were desalted using a Desalting spin column (BioRad). The first dimension was performed using 18cm strip with 3 to 11 pH range (GE Healthcare). The second dimension separation was performed on a 12% polyacrylamide gel running it over night at 25mA per gel. Finally the 2D gel was stained with SYPRO® Ruby (Molecular Probes) and visualized using the Typhoon scanner with an excitation wavelength of 532nm and an emission filter for 610nm (PMT 500, normal sensitivity). The relative masses of protein standards are shown on the right (in KDa).

The efficiency of a purification step can be expressed as the ratio of the increase in purity over the loss of sample. For this reason the protein amount in different purification steps against cytochrome c activity was plotted (Figure 8B). Pure mitochondria obtained by FFE showed an 80-fold enrichment in cytochrome c activity compared to plant extract and 1.6-fold enrichment compared to MEF obtained by differential centrifugations (Figure 8A). This increase in mitochondria specific activity was accompanied by a drastic decrease in total proteins amount, passing from 4.8mg of proteins in the MEF (derived by 35g Arabidopsis leaves) to 0.4mg in the FFE-purified mitochondria (Figure 8B). Due to this high loss of proteins and taking in to account that the mitochondrial proteome of *Arabidopsis thaliana* is well established (Kruft et al., 2001; Millar et al., 2001; Eubel et al., 2007), partially purified

mitochondria were used as experimental system to study post-translational proteins modification.
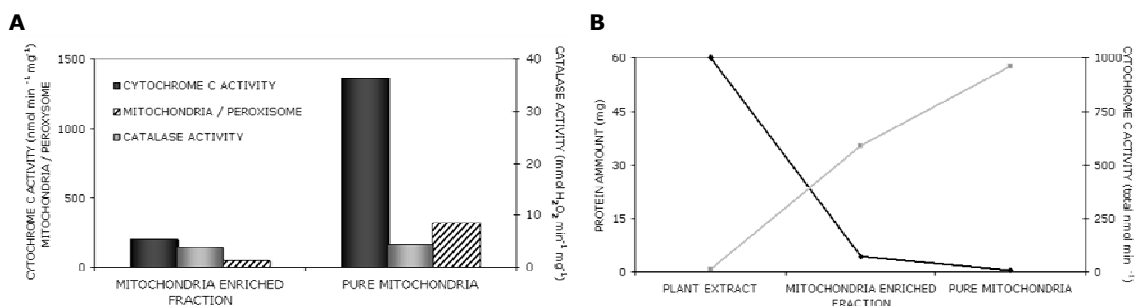
Figure 8. Mitochondria fractions purification degree

A comparison of mitochondria purification degree during different steps of isolation was performed. An aliquot of different fractions was analyzed for protein concentration and for organelle-specific enzymatic assays. **A.** Quantification of mitochondrial integrity by monitoring the cytochrome c oxidase activity (left y axis) and quantification of peroxisomes contamination by performing a catalase activity assay (right y axis). The value represents the ratio between cytochrome c activity and catalase activity. The enrichment in mitochondria in the pure fraction is of 6-fold compared with the mitochondria enriched fraction (MEF). **B.** Protein amount and total cytochrome c activity in the 3 steps of purification. Proteins in pure fraction represented around 25% of mitochondria starting material (MEF).

2.3 DETECTION OF S-NITROSYLATED PROTEINS IN ARABIDOPSIS LEAVES MITOCHONDRIA

To identify S-nitrosylated proteins in *A. thaliana* mitochondria enriched fraction, we used the biotin-switch method as described by Jaffrey and Snyder (Jaffrey and Snyder, 2001) with some modifications. This method results in the labelling of S-nitrosylated proteins with a biotin moiety specifically on S-nitrosylated cysteines and in an enrichment of biotinylated proteins by neutravidin-affinity chromatography.

After treating mitochondria proteins either with the trans-nitrosylating agent GSNO or with the reducing agents GSH (glutathione reduced) and dithiothreitol (DTT) as negative control, S-nitrosylated proteins were biotinylated, purified on a neutravidin matrix and separated by SDS-PAGE (dodecyl sodium sulphate-polyacrylamide gel electrophoresis). Several protein bands were detected in the GSNO-treated extract, whereas only a few endogenous biotinylated proteins were visible in the GSH or DTT-derived eluate and untreated extract (Figure 9).
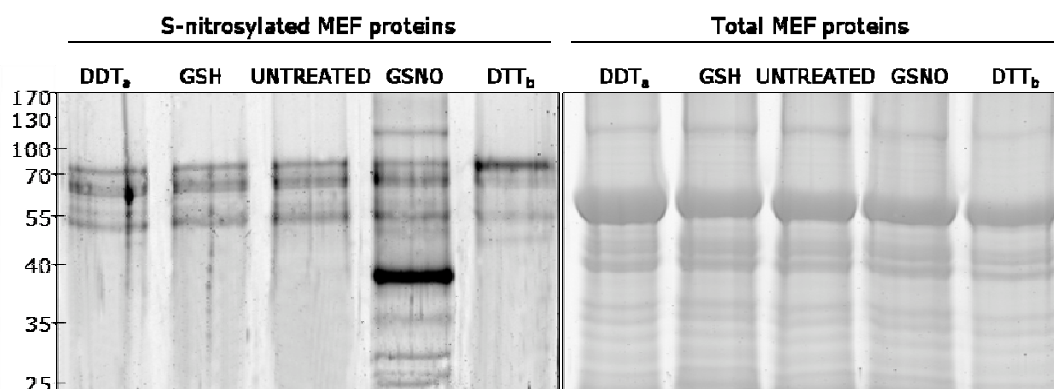
Figure 9. Biotin-switch method on mitochondrial proteome

Mitochondria extracts containing 100µg protein were treated with 1mM of GSNO, GSH or 1mM DTT and labelled with biotin using the biotin switch method. Proteins were purified by affinity-chromatography using neutravidin-agarose beads. Eluates were separated by 10% SDS-PAGE and visualized by SYPRO® Ruby staining. Additionally, aliquots of the affinity-chromatography flow through were separated on SDS-PAGE to compare the amount of total proteins in the different treatments (right gel). The relative masses of protein standards are shown on the left (in KDa). DDTa: DTT treatment before biotin switch method; Control: untreated proteins; DTTb: GSNO treated sample incubated for 10 min with DTT after biotinylation.

Six prominent protein bands derived by GSNO-treated mitochondria were excised from the gel and analyzed by peptide fingerprint by MALDI-MS/MS (Matrix assisted laser desorption/ionization time of flight mass spectrometry).

To identify low abundant S-nitrosylated proteins, 15mg mitochondrial proteins were treated with GSNO- or GSH and derived eluates were subject to liquid chromatography associated with mass spectrometry (LC-ESI-MS/MS) analysis (Figure 10). It was possible to identify 25 proteins with a significant score by the Mascot search algorithm (score>30). Five of them were contamination of chloroplast proteins and 9 of them were not listed in mitochondrial proteome (Millar et al., 2001) and did not harbour the mitochondrial targeting signal by analysis in either TargetP 1.1 or iPSORT (Table 2). Few of these proteins have previously been described as targets for S-nitrosylation, e.g. the mitochondria encoded copy of the α-subunit of ATP synthase of Arabidopsis and the rat mitochondrial catalase (Foster and Stamler, 2004; Lindermayr et al., 2005).

Figure 10. Detection of S-nitrosylated proteins in Arabidopsis mitochondria

Mitochondria extracts (MEF) containing 15mg protein were treated with 1mM of GSNO or GSH and labelled with biotin using the biotin switch method. Proteins were purified by affinity-chromatography using neutravidin-agarose beads. Elutes were separated by SDS-PAGE and visualized by SYPRO® Ruby staining. Protein bands corresponding to predominant bands of the immunoblot analysis were identified by nanoLC/MS/MS. Additionally, aliquots of the affinity-chromatography flow through were separated on SDS-gel to compare the amount of total proteins in the different treatments (right gel). The relative masses of protein standards (M) are shown on the left (in KDa).
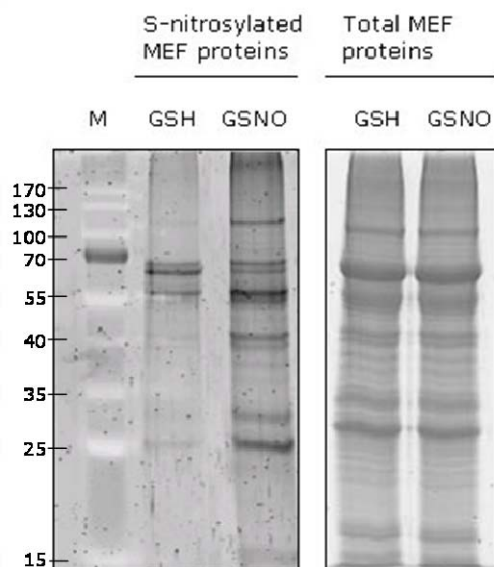
Among this pool of metabolic and stress-related mitochondrial proteins we could identify different subunits of the glycine decarboxylase complex (GDC), which is a key enzyme of the photorespiratory C2 cycle in C3 plants. During photorespiration, GDC converts two molecules of glycine to one molecule each of serine, NH_3, and CO_2 (Neuburger et al., 1986).

Table 2. Candidate proteins from Arabidopsis mitochondria for S-nitrosylation

Mitochondria extracts treated with GSNO or GSH were subjected to the biotin switch method and analyzed by LC-ESI-MS/MS after trypic digestion. The MASCOT search engine was used to parse MS data to identify proteins from primary sequence databases. The best-matching peptide identifying the protein is given. If there were further peptides found, the number of the peptides is given.

PROTEIN ID	PROTEIN NAME	MM (Da)	IDENTIFIED PEPTIDES (score)
15223217	Glycine Dehydrogenase subunit P2	18000	K.LTESPGLINSSPYEDGWMIK.V (87) +2
15221119	Aminomethyltransferase	44759	R.TGYTGEDGFEISVPDEHAVDLAK.A (80) +10
15235745	Serine Hydroxymethyltransferase	57535	K.LIVAGASAYAR.L (70) +9
15226973	Glycine Decarboxylase H1	18050	K.LTESPGLINSSPYEDGWMIK.V (87) +3
14916970	ATP Synthase subunit Alpha	55296	K.AVDSLVPIGR.G (44) +4
18394888	Catalase 3	57059	R.LGPNYLQLPVNAPK.C (54) +4
30684419	Lipoamide Dehydrogenase 2	54237	K.HIIVATGSDVK.S (47) +7
15221044	Lipoamide Dehydrogenase 1	54239	K.HIIVATGSDVK.S (47) +4
79401911	Unknown Protein *	78638	K.GSFSSVVSDK.S (42) +7
14596025	Glycine Dehydrogenase subunit P1	113852	R.EYAAFPAPWLR.S (35) +11
21537215	Unknown Protein *	32979	K.SNMSNCETSSEIQKPDYIHVR.A (28) +1

A number of studies suggest that the release of apoptotic factors from mitochondria may be a result of inhibition of respiration, mitochondrial permeability transition and formation of ROS (Saviani et al., 2002; Taylor et al., 2004; Chen and Gibson, 2008). Moreover, the GDC has already described to play a role in different biotic and abiotic stresses, i.e. induction of ROS production and apoptosis in response to the pathogen toxin Victorin in oat cells (Navarre and Wolpert, 1995; Yao et al., 2002; Tada et al., 2005).

2.4   THE GLYCINE DEHYDROGENASE P PROTEIN

2.4.1 Production of recombinant P protein

The complete GDC reaction cycle requires three different enzymes, P-, T-, and L-protein, and a small lipoylated aminomethylene carrier protein, H protein (Douce et al., 2001). Crystal structures for eukaryotic H, L, and T proteins have been obtained (Pares et al., 1994; Neuburger et al., 2000; Okamura-Ikeda et al., 2005), employing recombinant overexpression systems to obtain high amounts of purified protein. However, production of eukaryotic recombinant P protein has been not successful until now (Hasse et al., 2007). Different cloning systems, vectors and primer combinations were tried to obtain a recombinant P protein from *Arabidopsis thaliana*. Despite this, it was not possible to isolate clones carrying a non mutated P sequence. These could have been due to instability of the sequence, which is subject to a high mutation rate, or to a biological incompatibility between the encoded protein and the host.

2.4.2 Purification of the P Subunit of GDC

The isolation method described in the Materials and Methods section and based on chromatography, provides all the protein components of the glycine decarboxylase in good yield. Size exclusion chromatography (sec) on Sephacryl S-300 in the presence of 50mM-KCl and at pH 7.5 proved to be the key step in disrupting the 'multienzyme complex'. A typical elution profile is shown in Figure 11.
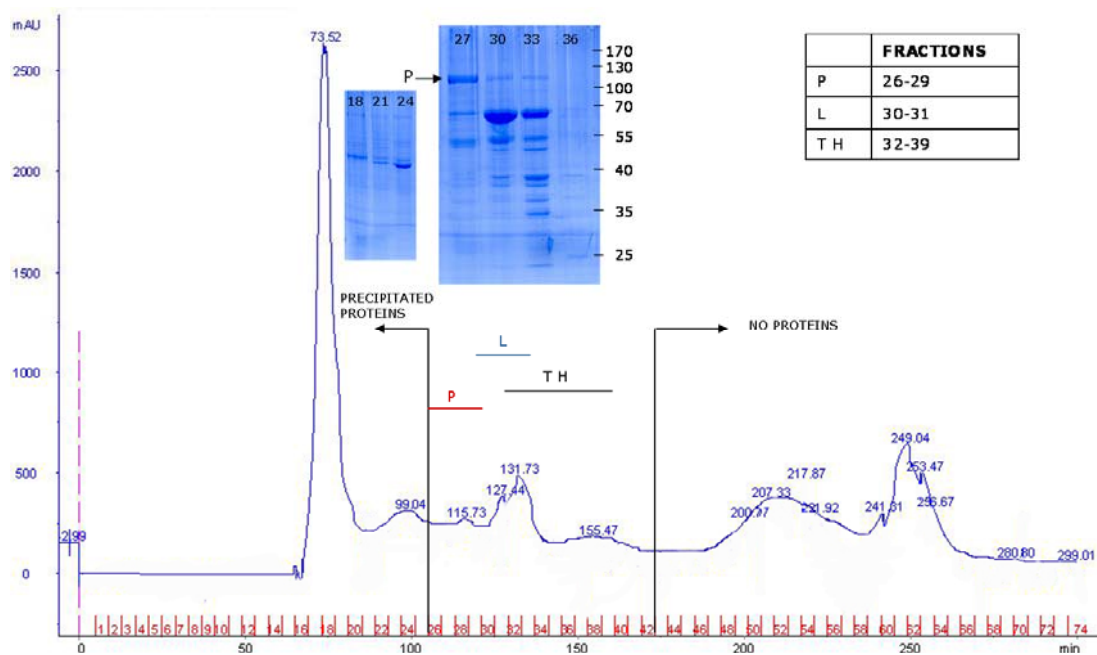
Figure 11. Size exclusion chromatography on mitochondrial proteins

The first step of purification of the P-protein was performed by separating mitochondria proteins according to differences in size. 70mg of mitochondria proteins were separated using a HiPrep 16/60 SEPHACRYL S-30 HR column (GE Healthcare) at 4°C with a flow rate of 0.5ml/min and fraction size of 2ml. The different fractions were stored at – 80°C and aliquots (20µl) analyzed by SDS-PAGE followed by Colloidal Comassie staining. The P protein was identified as a large peak in the heavy fraction, between fraction 26 and 29. T and H-protein were eluted in the light fraction (32-39) and the L-protein as a large peak with a maximum in the intermediary fraction (30-31). The numbers in the SDS-PAGE and the red ones in the x axis represent the sec fraction number.

Under these conditions, all the proteins (P, H, T and L) associated with the glycine decarboxylase were clearly resolved, with a separation of the mitochondrial matrix in heavy, intermediary and light fractions. The small subunit of Rubisco, a chloroplastic contamination of the enriched mitochondria fraction, was partially eluted in the void volume (Figure 11, precipitated proteins). After the subsequent ion exchange chromatography step (aec) on the heavy fraction of the size exclusion chromatography, P protein was almost pure. The molecular mass of P-protein was about 110kDa, as determined by SDS-gel electrophoresis (Figure 12), whereas the predominant contaminant protein appeared to be around 70kDa. Since our goal was to enrich the P subunit so that could be analyzed for S-nitrosylation by Nano-HPLC-MS[2/3], this degree of purity was considered sufficient.
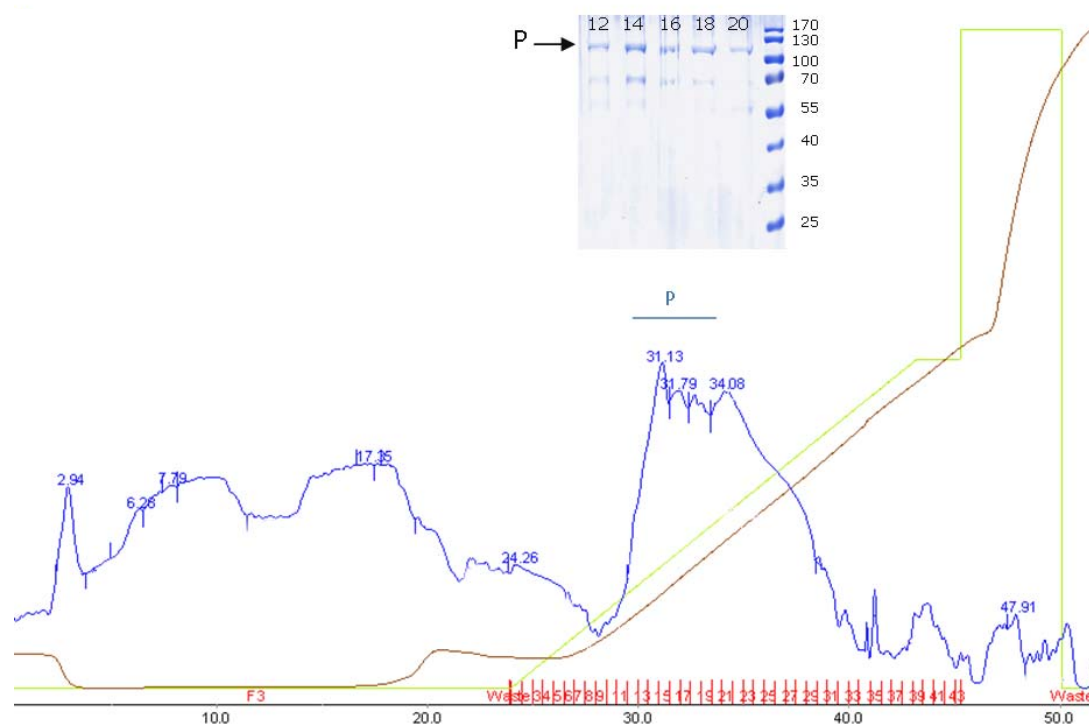
Figure 12. Anion exclusion chromatography on the sec heavy fraction

A portion of the size exclusion chromatography heavy fraction (10mg of fraction 26-29) was applied to a HiTRAP DEAE FF column (GE Healthcare) to further separate proteins according to their charge. P protein was eluted at 4°C with a continuous increasing KCl gradient (50-1000mM), emerging as a large peak in fractions 12-20. The different fractions were stored at –80°C and aliquots (20µl) analyzed by SDS-PAGE followed by Colloidal Comassie proteins staining. Blue continuous line: absorbance at 280nm; Green line: concentration of KCl; Brown line: conductivity.

2.4.3 Activity of the Partially Purified P Protein

A bicarbonate exchange reaction was used to prove the P protein folding status after the purification. The light fraction of the sec was used as source for H subunit, because of the need of a protein able to act as co-substrate during the assay. It has been shown that P protein alone is able, though slightly, to catalyse the exchange of the glycine carboxyl carbon with CO_2, but this exchange activity is greatly increased when H protein is also present (Hiraga and Kikuchi, 1982). We tested sec and aec-derived P proteins for the ability of exchange of the glycine carboxyl carbon with $^{14}CO_2$ of the sodium bicarbonate. The activity measured in both the P protein extracts in absence of the H protein was further increase by the addiction of this co-substrate (Figure 13). The addition of purified H protein fraction alone to the enzymatic assay buffer in the presence of saturating amounts of $NaH^{14}CO_2$ did not significantly change the rate of glycine oxidation (Figure 13), proving that the P protein still present in the light fraction was not sufficient to produce a detectable signal. Moreover,

the absence of the $^{14}CO_2$ donor $NaH^{14}CO_3$ or of the $^{14}CO_2$ acceptor glycine completely inhibited the activity, showing the specificity of the assay.
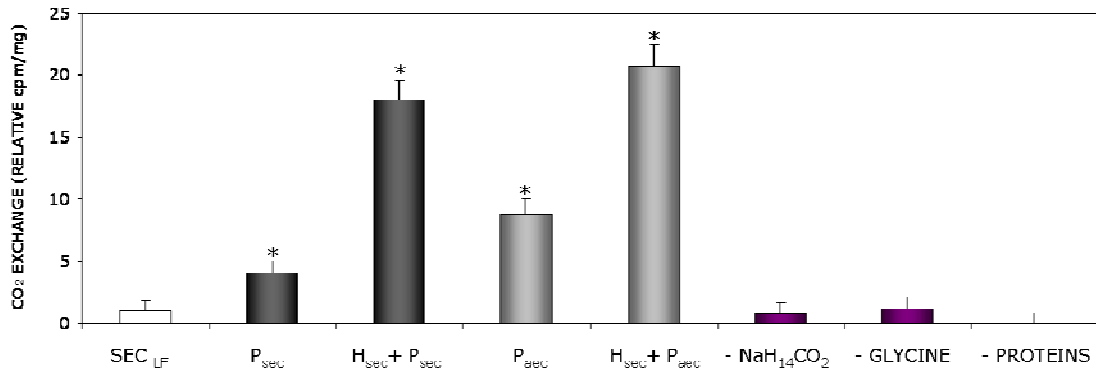
Figure 13. Bicarbonate exchange reaction with purified P protein

The activity of P protein was determined by measuring the amounts of [^{14}C]bicarbonate fixed to the carboxyl-group carbon atom of glycine in presence of saturating amount of H-protein. As source of H protein, 100µg of proteins of the light fraction of size exclusion chromatography (sec) were used. H_{sec} = fraction 31-35 sec; P_{sec} = fraction 26-29 sec; P_{aec} = fraction 12-19 anion exclusion chromatography (aec); $-NaH^{14}CO_3$ = $P_{sec/aec}$ + H_{sec} without bicarbonate; - GLYCINE = $P_{sec/aec}$ + H_{sec} without the acceptor for ^{14}C; - PROTEINS = residual $NaH^{14}CO_3$ radioactivity after acid-dependent volatilization. The asterisks indicate values statistically different from those of the H-protein alone (One-Way Anova followed by Tukey test as post hoc test, $P < 0.05$).

2.5 S-NITROSYLATION / S-GLUTATHIONYLATION OF THE P PROTEIN

Since GSNO is able to S-nitrosylate and S-glutathionylate thiol groups of cysteine residues, we investigated which kind of modifications resulted from the GSNO-treatment of the P subunit of GDC.
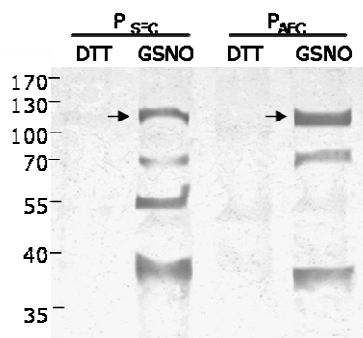
Figure 14. Biotin-switch method on partially purified P protein

30µg of P containing fraction from SEC and AEC were treated with 1mM of GSNO or 1mM DTT and labelled with biotin using the biotin switch method. For detection of biotinylated proteins by immunoblotting, proteins were first separated in a 12% SDS-PAGE. Biotinylated proteins were detected with anti-biotin mouse monoclonal antibody (AP-conjugated). The relative masses of protein standards are shown on the left (in KDa). The arrows indicate the P protein (~110kDa).

2.5.1 Biotin Switch Method on Enriched P Protein

For detection of SNO thiol groups we used the biotin switch method that specifically detects S-nitrosylated proteins. Using a specific monoclonal antibody against the biotinylated cysteine residues, we identified the partially purified P protein as S-nitrosylated after 15 min incubation with 1mM GSNO (Figure 14, band at ~110kDa). No signal was detected in the 1mM DTT-treated sample, proving the specificity of the method.

2.5.2 MS Analysis of GSNO Treated P Protein

Next to the biotin switch assay we used mass spectrometric analyses to detect GSNO-mediated modifications of the cysteine residues of P-protein, since this method allows also the detection of S-glutathionylation. We treated partially purified P_{aec} protein with 0.5mM or 1mM GSNO for 15min, digested the proteins with trypsin and analysed the cysteine containing peptides for their modifications. Post-translational modifications were searched as shift in peptide masses of 29 for S-nitrosylation and 305 for S-glutathionylation. Six cysteine residues were found to be S-glutathionylated after treatment with 1mM GSNO, whereas only 2 cysteine residues presented this modification after treatment with 0.5mM GSNO (Table 3, Appendix B). No S-nitrosylated cysteines were detected by MS analysis, probably because of the instability of this modification.

Table 3. Mass spectrometric analyses on the partially purified P_{AEC} protein

P protein (20µg) was treated with 0.5mM or 1mM GSNO for 15min. After removing the excess of GSNO, the protein was digested with trypsin and analysed as described in Material and Methods. Six peptides belonging to the P subunit (P1 protein) of the GDC showed a mass difference compared to the expected one of 305 Da, which corresponds to the addiction of one -GS group. No peptide showed a shift of 29 Da (-NO) in the mass. The asterisks indicate peptides that showed a shift in masses after both the GSNO treatments.

PEPTIDE SEQUENCE	PEPTIDE IDENTIFICATION PROBABILITY	MODIFICATIONS IDENTIFIED BY SPECTRUM	ACTUAL PEPTIDE MASS	PEPTIDE START	PEPTIDE STOP
F**C**DALISIR	95%	Glutathione (+305)	1,341.61	942	950
F**C**GFDHIDSLIDATVPK	95%	Glutathione (+305)	2181.97	97	113
TF**C**IPHGGGGPGMGPIGVK	95%	Glutathione (+305)	2085.94	775	793
DKATSNI**C**TAQALLANMAAM YAVYHGPAGLK *	95%	Glutathione (+305)	3498.65	395	425
CSDAHAIADAASK *	95%	Glutathione (+305)	1563.63	463	475
LV**C**TLLPEEEQVAAAVSA	95%	Glutathione (+305)	2147.02	1020	1037

2.5.3 S-Nitrosylation or S-Glutathionylation?

Since it was not possible to prove *via* MS analysis that GSNO is able to S-nitrosylate cysteines residues of the P protein, we tested the ability of NO to affect P protein activity *in vitro*. We tested aec-derived P subunit for the ability of exchange of the glycine carboxyl carbon with $^{14}CO_2$ of the sodium bicarbonate (Figure 15). The partially purified subunit was treated with the NO donor sodium nitroprusside (SNP), which is not able to S-glutathionilate cysteine residues. As showed in figure 16, 250µM SNP was able to inhibit the CO_2 exchange reaction, while the NO scavenger cPTIO (500µM) was able to almost completely restore it.
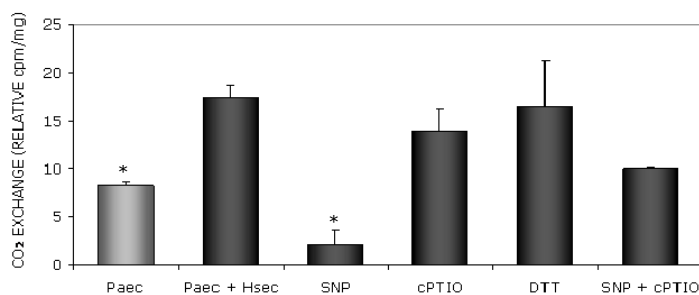
Figure 15. CO$_2$ exchange reaction modulation by NO

The activity of P protein was determined by measuring the amounts of [^{14}C]bicarbonate fixed to the carboxyl-group carbon atom of glycine in presence of saturating amount of H-protein. Proteins were treated with 1mM DTT, 250µM SNP and/or 500µM cPTIO for 10min and the activity measured 30 min after the addiction of bicarbonate. Black: H + P proteins; Grey: P protein alone; H$_{sec}$: 100µg; P$_{aec}$: 30µg. Each value represents the mean of at least 3 technical replicates. The asterisks indicate values statistically different from those of the sample with P and H protein together (P <0.05).

2.6 INHIBITION OF GDC BY NO

The glycine-serine interconversion catalyzed by the GDC is an essential reaction in plants by providing one-carbon units for many biosynthetic reactions and being an integral part of photorespiratory metabolic pathway in mitochondria (Douce et al., 2001).

2.6.1 Modulation of GDC Activity by GSNO in Mitochondria

To elucidate effects of GSNO on GDC enzyme activity and protein structure, we treated enriched mitochondria with different concentration of GSNO (50µM-1mM) and we monitored the glycine decarboxylase activity in vitro (Walker et al., 1982; Walker and Oliver, 1986). Following the $^{14}CO_2$ release from [1-^{14}C]glycine, i.e. the activity of P and H-subunits, we could observe a significant reduction of decarboxylation dependent on GSNO-concentration (Figure 16). After 30min, the GDC activity of mitochondria incubated with 0.25mM GSNO showed an inhibition of 60% compared to the GDC activity of untreated organelles.

Treatment with 1mM GSNO further decreased the decarboxylation to about 30%, similar to the inhibition obtained with the GDC specific inhibitor aminoacetonitrile (AAN 10mM). The incubation of mitochondria with the reducing agents DTT and GSH increased decarboxylation activity to 176% and 115% in vitro, suggesting a change in the mitochondria redox-status during purification.
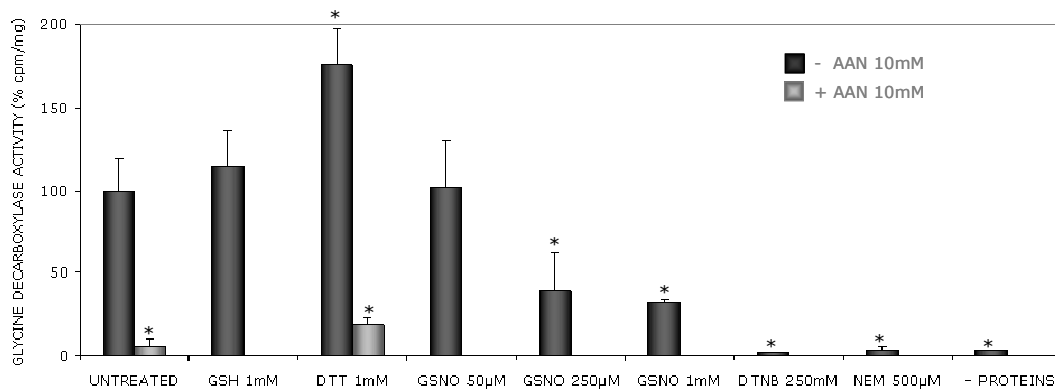
Figure 16. Modulation of glycine decarboxylase activity
Enriched mitochondria fractions were pre-incubated with the indicated amounts of GSNO or SH-modifying agents for 20 min at room temperature in the dark, and enzyme activity was determined subsequently. The activity of the control (untreated) was set to 100% and used to normalize other values. The untreated and DTT (1mM) treated samples were also incubated with a specific GDC inhibitor aminoacetonitrile (AAN 10mM). Each value represents the mean of at least 3 biological and technical replicates. The asterisks indicate values statistically different from those of the untreated proteins (P <0.05). – PROTEIN: signal due to the auto decomposition of [^{14}C]glycine.

To further characterize the mechanism of GSNO-mediated inhibition of GDC, we tested two cysteine-modifying agents on the GDC activity: N-ethylmaleimide (NEM), a highly reactive agent that covalently and irreversibly alkylates free cysteine thiol groups and 5,5-dithiobis-2-nitrobenzoicacid (DTNB) an oxidizing reagent that acts by formation of a disulfide bond between itself and free cysteine thiol groups. Both treatments resulted in a complete inhibition of P/H-proteins activity within the 30min (Figure 16).

2.6.2 Modulation of GDC Activity by GSNO in Arabidopsis Leaves

The modulation of activity by S-nitrosylation was confirmed using Arabidopsis thaliana leaves slices as described by Navarre and Wolpert, 1995. Twenty minutes incubation with 1mM GSNO resulted in an inhibition of GDC activity of 75%, which could be restored by 1mM DTT (Figure 17).
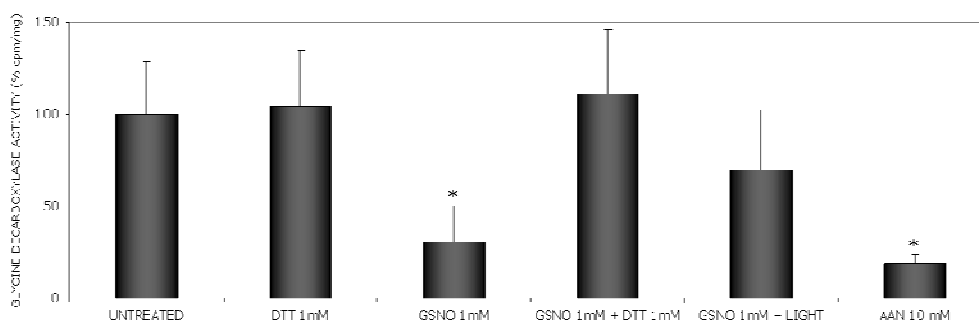
Figure 17. GDC in Arabidopsis leaves after S-nitrosylation

Leaf slices were treated for 20min with 1mM GSNO at room temperature after equilibration in a MOPS buffer for 1h at 30°C. For restoring GDC activity, 1mM DTT was added to the inhibited enzymes and incubated for additional 10min or samples were exposed for few seconds to UV light. A control treatment with the specific GDC inhibitor AAN was added. Additionally a UNTREATED + LIGHT sample was performed showing no difference with the activity of the UNTREATED sample (data not show). The glycine decarboxylase activity in untreated control was set at 100%.

Moreover, to prove that the GSNO-dependent modulation of GDC activity was due to a direct effect on the photorespiratory system, Arabidopsis leaf slices were incubated with inhibitors of the complex I of the mitochondrial respiration (rotenone) and of the alternative oxidase (SHAM) (Figure 18). In animal system, complex I has already been shown to be regulated by S-nitrosylation and to be involved in reversible ROS production (Borutaite and Brown, 2006; Burwell et al., 2006). Moreover, in plants it was proved that the NO-induced AOX is scavenging the ROS production and cell death induced by KCN-sensitive respiration inhibition (Huang et al., 2002). The GSNO-dependent modulation of GDC activity could have been an indirect effect of the ROS produced by complex I inhibition. On the contrary, blocking the complex I in mitochondria via rotenone was not able to influence GDC activity within 30min reaction (Figure 18). Also the increase of ROS level in GSNO-treated mitochondria by AOX inhibition or the scavenger effect on H_2O_2 by catalase did not influence the modulation of GDC activity, confirming that this was due to a direct S-nitrosylation/S-glutathionylation of one or more glycine decarboxylase subunits (Figure 18).
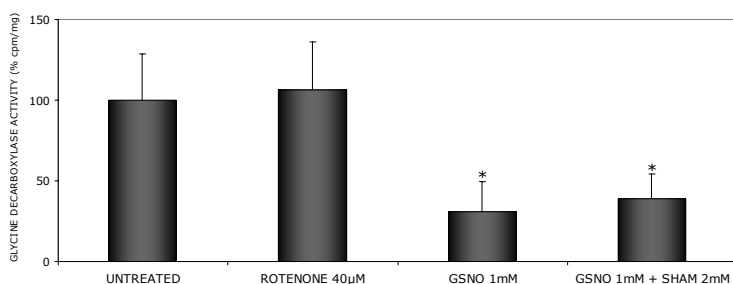
Figure 18. GDC modulation by respiratory inhibitors

To prove that the GSNO-dependent modulation of GDC activity was due to a direct effect on the photorespiratory system, Arabidopsis leaves were incubated with inhibitors of the cytochrome *c* respiration (rotenone), of the alternative oxidase (SHAM) and with a H_2O_2 scavenger (catalase). Leaf slices were treated for 20min at room temperature after equilibration in a MOPS buffer for 1h at 30°C.

2.7 ROLE OF GDC IN PLANT RESPONSE TO HARPIN

Since S-nitrosylation is emerging as a specific and fundamental signal for the transduction of NO pathway, i.e. during plant-pathogen interaction (Romero-Puertas et al., 2004), we tested the involvement of GDC inhibition in stress-related response. Harpin is a well-known proteinaceous bacterial elicitor of Erwinia, Pseudomonas, and Xanthomonas strains that can induce an oxidative burst and programmed cell death in various host plants. Recently, it was shown that harpin induced a decrease of ATP-pool size in tobacco cell cultures (Xie and Chen, 2000). Moreover, harpin induces accumulation of NO and mitochondrial ROS, membrane depolarization, cytochrome *c* release, and induction of redox-protecting components, all defence responses often associated with apoptotic events in animals and plants (Krause and Durner, 2004; Livaja et al., 2008). Using recombinant harpin protein from *Pseudomonas syringae* we investigated the role of GDC during plant defence responses or cell death *in vitro* and *in vivo*.

2.7.1 Effect of Harpin on GDC in Arabidopsis Leaves

Leaf slices were incubated at room temperature with 35µg/ml of recombinant harpin protein or with a not transformed E. coli DH5α extract as control and the GDC activity was followed over 4h by monitoring the $^{14}CO_2$ release from $[1-^{14}C]$glycine. A visible inhibition of the decarboxylase activity in harpin-treated samples was visible after 30min and increased after 4h to 61% in comparison with untreated and E. coli-treated samples (Figure 19). The specific inhibitor AAN was used as positive control. Moreover, no effects on the GDC activity were visible in untreated Arabidopsis leaves 4h after incubation in MOPS buffer at 30°C.

Figure 19. Effect of harpin on glycine decarboxylase activity

Leaf slices were treated with 35µg/ml of harpin recombinant protein or with a not induced E. coli extract (as control) at room temperature after equilibration in a MOPS buffer for 1h at 30°C. Treatment with the specific GDC inhibitor AAN was used as control. The glycine decarboxylase activity in untreated control was set at 100%. Each value represents the mean of at least 3 replicates. The asterisks indicate values statistically different from those of the untreated proteins (P <0.05).
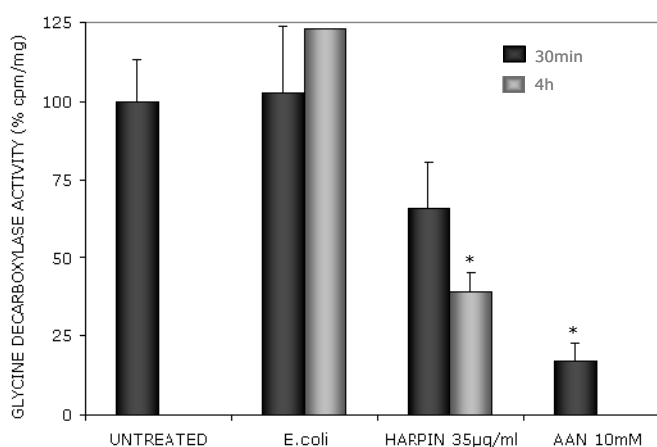
2.7.2 Effect of Harpin on Photorespiratory Rate

The glycine-serine interconversion, catalyzed by GDC in conjunction with the serine hydroxymethiltransferase, is an integral part of the photorespiratory metabolic pathway (Douce et al., 2001; Bauwe and Kolukisaoglu, 2003). Therefore, we investigated the role of GDC during plant defence responses in vivo monitoring the photorespiration rate and the leaf amino acid content in *Arabidopsis thaliana* leaves.

The exact determination of photorespiration rates in vivo in photosynthesizing leaves in the light is a complicated task requiring discrimination between opposite CO_2 fluxes: CO_2 uptake and re-fixation in the Calvin cycle, CO_2 release from mitochondrial photorespiration and residual "dark" respiration in the light. Moreover photorespiratory O_2 uptake is strictly dependent to the photosynthetic O_2 evolution and to the O_2 consumption during mitochondrial respiration and other metabolic processes (Parnik et al., 2007). A reliable technique is to measure the response of the rate of net CO_2 assimilation (A) to the intracellular partial pressure of CO_2 at different irradiance (Brooks and Farquhar, 1985). Using an Infrared Gas Analyzer (IRGA) system (LICOR 6400, Licor Bioscience) A was measured at several intracellular CO_2 concentrations (Ci) to eliminate effects of boundary layer and stomata aperture. Extrapolation to zero CO_2 yielded the rate of CO_2 release from the leaf, i.e. the sum of photorespiration and respiration in the light (CO_2 compensation point, Γ) (Figure 20A). This response of A to C_i was measured at three different irradiance to find the curves-intersection point where A is the same at all irradiance (Figure 20B).
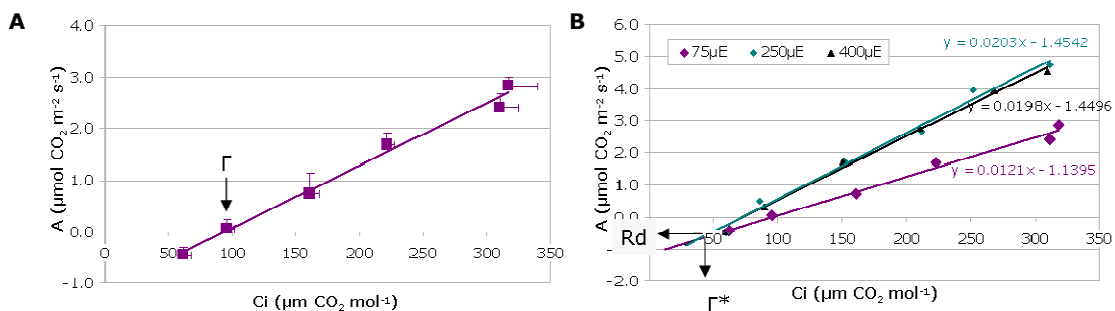
Figure 20. Gas exchange measurements

The photorespiration rate *in vivo* was monitor following the response of the photosynthesis (A) to intracellular CO_2 mole fraction (Ci) with an Infrared Gas Analyzer (IRGA) system (LICOR 6400, Licor Bioscience). **A.** Apparent CO_2 exchange rates (A) were measured at 6 different CO_2 concentrations (400, 300, 200, 100, 50, 400ppmol). Extrapolation to zero yields the rate of CO_2 released from the leaf, the sum of photorespiration and respiration in the light (compensation point Γ). Each point represents the mean of at least 3 independent replications. **B.** Photorespiration rate was calculated as photosynthetic CO_2 compensation point in absence of respiration in the light (Γ^*). It was defined as the interception point of different curves measured at different light intensities (75, 250, 400µE). The y coordinate of this point gave the respiration in the light (-Rd). Each curve represents the mean of at least 3 independent replications.

This approach allows the determination of the in vivo Rubisco oxygenation rate, thereby allowing the separation of contributions from respiration in the light to total CO_2 efflux (Farquhar, 1979; Farquhar et al., 1980). It allows to determine the chloroplastic CO_2 concentration where the rate of RubP carboxylation equals the rate of photorespiratory CO_2 release. This CO_2 concentration is defined as the photosynthetic CO_2 compensation point in absence of respiration in the light ($\Gamma*$), and correspond to the curves-intersection point determined by using different light intensity (Figure 20B, Appendix C).

Arabidopsis plants were infiltrated with either 35µg/ml of recombinant harpin protein or with a not induced E. coli extract and stored in grow-chamber for 4h. E. coli-treated control plants showed a non-significant decrease in photorespiration rate, probably due to a stress caused by the infiltration (Figure 21A). On the contrary, harpin treatment completely suppress photorespiration rate within 30min, confirming the results obtained with in vitro experiment (Figure 21A). The concentration of harpin used was able to cause cell death after 24h when infiltrated in Arabidopsis leaves, whereas no induction of cell death was observed when leaf slices were incubated for 30min with harpin solution. The harpin treatment caused in 4h also a decrease in photosynthetic rate, supporting the idea that a redox stress produced in mitochondria by inhibiting GDC can cause a redox perturbation in chloroplast (Igamberdiev et al., 2001) (Figure 22).
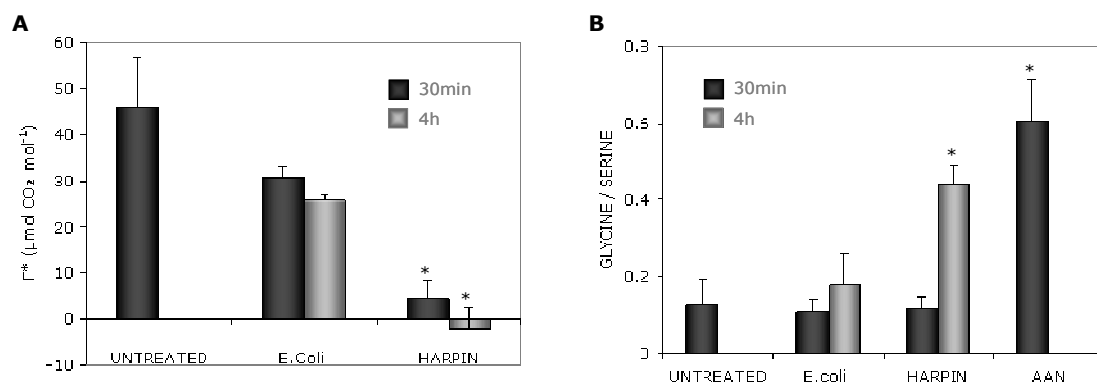
Figure 21. CO_2 compensation point* and glycine-serine ratio

The photorespiratory rate in vivo after treatment with 35µg/ml of harpin recombinant protein or with a not induced E. coli extract (as control), was analyzed measuring the CO_2 compensation point in absence of respiration in the light ($\Gamma*$) and the glycine/serine ratio. Arabidopsis plants were infiltrated and stored in the grow-chamber until measurements. **A.** $\Gamma*$ point represents the mean of 2 independent measurements with 3 biological replicates each. **B.** The inhibition of the activity of GDC was monitored following the increase in glycine / serine ratio in Arabidopsis leaves (µmol/g FW). Amino acid content analysis was performed using 100mg of fresh tissue and a HPLC system. The GDC specific inhibitor AAN was used as control. The asterisks indicate values statistically different from those of the untreated proteins (P <0.05).

2.7.3 Effect of Harpin on Glycine and Serine Content

A more direct technique to monitor the GDC activity in vivo was to determine the quantitative impact of harpin on leaf amino acid contents (Blackwell et al., 1990; Heineke et al., 2001). The inhibition of GDC activity observed after harpin-treatment led to an increase in glycine/serine ratio in Arabidopsis leaves after 4h, while the small effect of E. coli did not correspond to a change in this amino acid content (Figure 21B). As control, leaves were infiltrated with the specific GDC inhibitor AAN, which resulted in a fast increase in glycine/serine within 30min (Figure 21B).
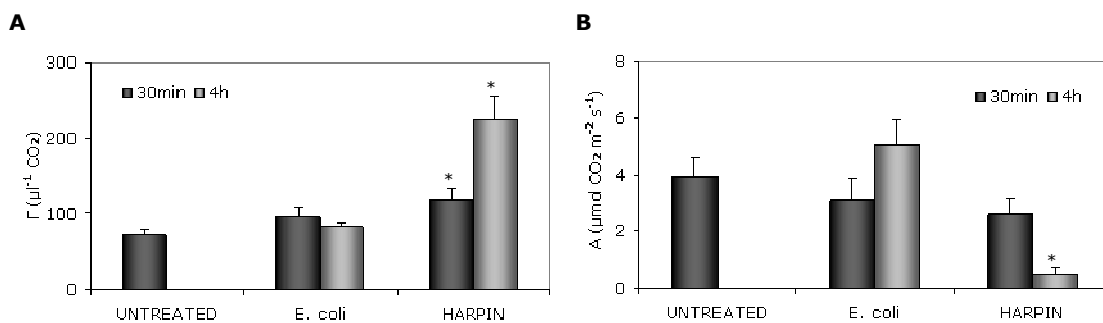
Figure 22. CO_2 compensation point and photosynthesis rate at 250µE

Five weeks old Arabidopsis plants were infiltrated with a suspension of 35µg of harpin recombinant protein or with a not induced E. coli extract (as control) and stored in the growing chamber until the measurements. The measurement was performed using LICOR 6400 IRGA system. **A.** CO_2 compensation point at 250µE and 400ppmol of CO_2. **B.** Photosynthesis rate at 250µE and 400ppmol of CO_2.

2.8 MITOCHONDRIAL AND CELLULAR RESPONSE TO GDC INHIBITION

To confirm the role of GDC in harpin-induced plant defence response, Arabidopsis plant and cell culture were treated with the specific GDC inhibitor AAN, which has no side effect on dark respiration and on CO_2 fixation (Usuda and Edwards, 1980; Creach and Stewart, 1982). Yao et al., already described AAN to be able to mimic the toxin victorin-induced mitochondrial oxidative burst in oat cells (Yao et al., 2002).
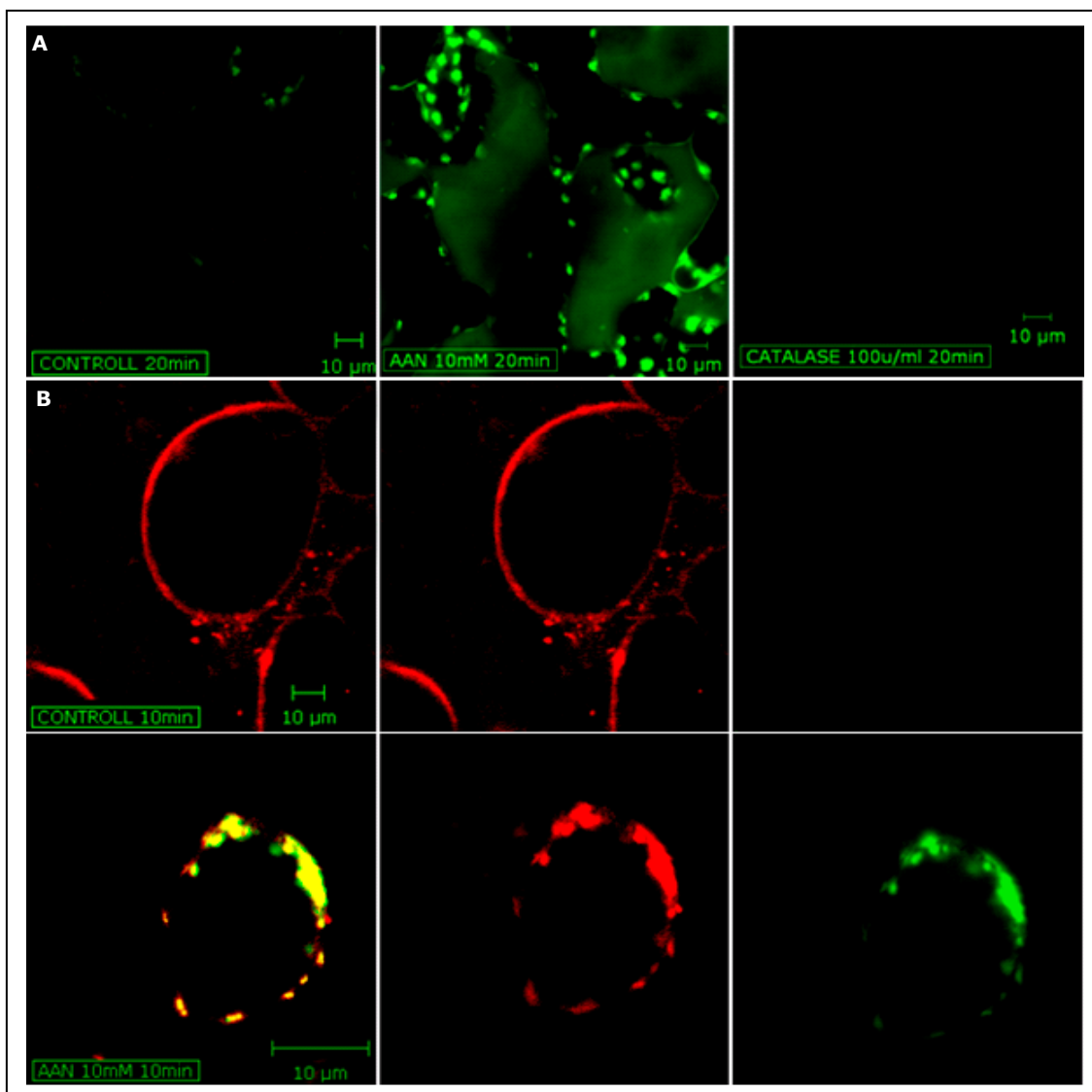
Figure 23. AAN-dependent ROS production in Arabidopsis cell culture

Confocal microscopy images were obtained using Zeiss LSM 510 NLO (Zeiss) with a 40X water lens. **A.** Arabidopsis leaves were stained with the ROS detecting dye $H_2DCF-DA$ for 20min, followed by treatment with 10mM AAN for 20min. A pre-incubation with 100units/ml of catalase for 20min scavenged the AAN-induced H_2O_2 dependent fluorescence. **B.** After labelling Arabidopsis cells for 20min in the dark with MitoTracker Red 580 as specific mitochondrial marker, cells were stained with the ROS detecting dye $H_2DCF-DA$ (10µM). For each image are given pictures with red fluorescence (mitochondria), green fluorescence (ROS) and the mitochondria-ROS co-localization, which appears yellow.

2.8.1 Generation of Mitochondrial ROS

Stress-induced ROS generation has been reported as essential signal for activation of resistance in several plants (Desikan et al., 1998; Delledonne et al., 2001; Krause and Durner, 2004). Photometrical determination of H_2O_2 was performed using a ROS-specific fluorescence dye, the dichlorofluorescein ($H_2DCF-DA$). ROS production over the time was

monitored with a fluorescence plate reader (Tecan GENios, Figure 24A), whereas the localization of ROS production in Arabidopsis cells was analyzed with a confocal microscope (Zeiss, LSM510 NLO, Figure 23).

H$_2$DCF-DA has already been used to visualize oxidative processes in plants and animals in response to various stresses (Allan and Fluhr, 1997; Yao et al., 2002). As shown in Figure 24A, the DCF signal increased already 10min after the addiction of AAN to 1week-old cell cultures, whereas untreated cells had almost no fluorescence even after 60min. Catalase was able to scavenge completely the AAN-dependent H$_2$O$_2$ production in the assay showing the specificity of the DCF signal, whereas the pre-treatment with the AOX inhibitor SHAM increased the 60min-DCF fluorescence in Arabidopsis cells treated with AAN (Figure 24A). This data proved that the inhibition of the GDC brings to an activation of alternative oxidase respiration, as previously shown after NO-dependent cytochrome c respiration inhibition (Huang et al., 2002), and confirmed a connection between GDC and AOX (Igamberdiev et al., 2001) (Figure 24B).
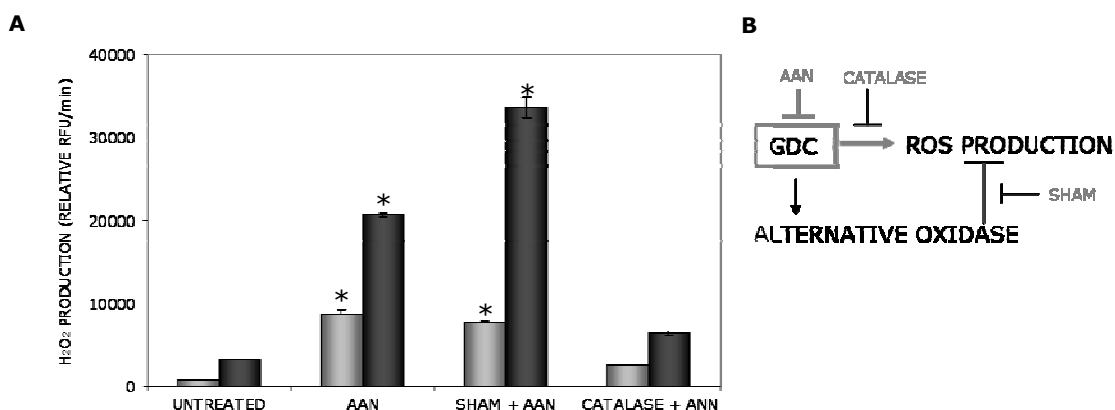
Figure 24. AAN-dependent ROS production in Arabidopsis suspension cells and leaves
The specific inhibitor of the GDC (AAN) was used to study the effect of GDC inhibition in Arabidopsis cell culture. The ROS dependent fluorescence of the cH$_2$DF-DA dye was monitored with a TECAN GENios fluorescence plate reader (TECAN). 250µl of 1week-old cell cultures were co-incubated for 30min with the different inhibitors and the dye in a 96well plate in the grow-chamber. After removing excess of dye, AAN was added and the measurement was started. **A.** Relative fluorescence, 10 and 60min after AAN addiction. Catalase was used to scavenge H$_2$O$_2$ production in the assay and its RFU value, corresponding to the dye background, was subtracted from other samples. SHAM: 2mM, AOX inhibitor; Catalase: 100units/ml, ROS scavenger. **B.** Model proposed to explain the relation between GDC and AOX in modulating ROS production.

H$_2$O$_2$ production after inhibition of the glycine decarboxylase was further confirmed in Arabidopsis leaf using H$_2$DCF-DA and confocal microscopy (Figure 23). To prove that mitochondria were the site of ROS production, Arabidopsis cells were double stained with H$_2$DCF-DA and Mitotracker Red 580 (Yao et al., 2002; Krause and Durner, 2004). The intracellular localization of DCF signal in the ANN-treated samples matched that of

mitochondria-staining dye, as a overlapping of the two signal revealed a yellow signal (Figure 23).

2.8.2 Mitochondrial Transmembrane Potential

Plant mitochondrial responses to stress signals are similar to those of animal mitochondria and include a collapse of the transmembrane potential ($\Delta\Psi_m$), release of cytochrome c and decrease in ATP production (Saviani et al., 2002; Tiwari et al., 2002; Krause and Durner, 2004). Normally, the mitochondria H_2O_2 burst appears to precede the breakdown in the $\Delta\Psi_m$, probably as result of the perturbation of the mtETC (Pellinen et al., 1999; Yao et al., 2002). JC-1 was used as dye to probe mitochondrial membrane potential in AAN-treated Arabidopsis cell culture, since this dye is not affected by other factors such as size, shape or density of mitochondria. High mitochondrial $\Delta\Psi_m$ leads to J-aggregates of the dye, which exhibits red fluorescence (Petit et al., 1995). The depolarization is indicated by a decrease in the ratio of red/green fluorescence intensities.
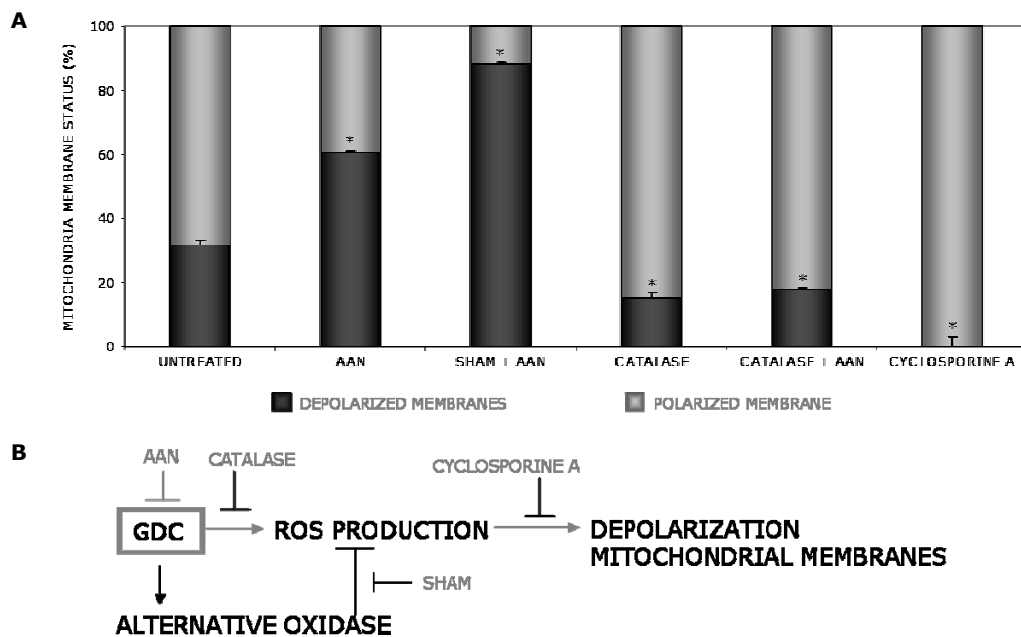
Figure 25. AAN-induced depolarization of mitochondrial membranes
AAN was used to study the effect of GDC inhibition in Arabidopsis. **A.** One week old cell cultures were treated for 30min with different inhibitors in the 96well plate in the grow-chamber. Afterwards JC1 dye (5µg/ml), to probe the mitochondrial membrane potential, and 10mM AAN were added and the measurement started. The mitochondrial depolarization was indicated by a decrease in the red/green fluorescence intensity ratio. The data represents the status of mitochondrial membrane 30min after AAN treatment. SHAM: 2mM, inhibitor of AOX; catalase: 100units/ml, ROS scavenger; cyclosporine A: 50µM, inhibitor of the mitochondrial PTP. **B.** Model proposed to explain the relation between GDC and AOX in modulating depolarization mitochondrial membranes.

Using a plate reader equipped with excitation and emission filters for green and red fluorescence (Tecan GENios), we monitored changes over time. Thirty minutes after treatment with AAN, approximately 50% of cells showed a decrease in $\Delta\Psi_m$ compared to 30% of the control cells (Figure 25A). The depolarization observed in the control was most likely due to a stress condition of cells in the plate reader, and was completely suppressed pre-treating them with an inhibitor of the mitochondrial transition pore, cyclosporine A (Saviani et al., 2002). In addition the ROS-scavenger catalase was able to reduce the $\Delta\Psi_m$ in untreated or AAN-treated cells, confirming that the oxidative burst is essential for the breakdown of mitochondrial membrane potential (Figure 25A). Furthermore, blocking the ROS-scavenging ability of AOX (via SHAM) resulted in increased loss of red fluorescence, with approximately 90% of depolarized mitochondrial membranes (Figure 25B). In figure 26, the depolarization of mitochondrial membranes over the time is presented. Harpin treatment was used as positive control (Krause and Durner, 2004), showing a mostly identical effect as 10 and 50mM AAN. One hundred minutes after treatment, 40% of mitochondrial membranes were depolarized in Arabidopsis cells, whereas untreated cells did not show almost any shift in red/green fluorescence (Figure 26).
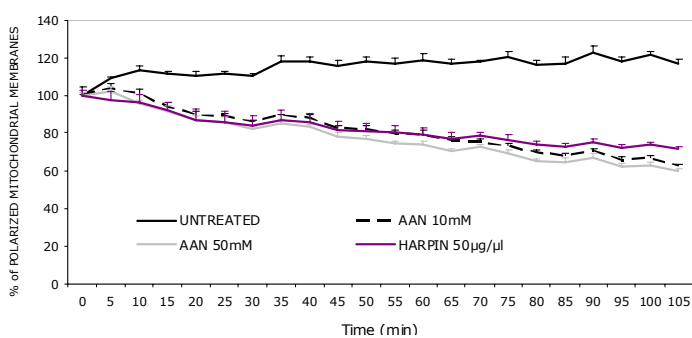
Figure 26. Implication of GDC inhibition on $\Delta\Psi_m$

The graph illustrates the depolarizing effect of AAN on mitochondrial membrane in Arabidopsis suspension cells in comparison with untreated control cells. JC-1 labelled cells were treated with different concentration of AAN or with 50µg/µl of harpin (as positive control), followed by measuring of red and green fluorescence intensity. The mitochondrial depolarization is indicated by a decrease in the red/green fluorescence intensity ratio over 105min.

2.8.3 Induction of cell death

Using toxins of plant pathogens or mutant of mitochondrial protein, it appears that loss of mitochondrial function and concomitant mitochondrial ROS formation and signalling is necessary for subsequent cell death (Robson and Vanlerberghe, 2002; Vanlerberghe et al., 2002; Yao et al., 2002; Krause and Durner, 2004).

To monitor the AAN-induced cell death, we measured the loss of plasma membrane integrity double-staining Arabidopsis suspension cells with Evans blue and fluorescein diacetate

(Huang et al., 2002). Despite Evans blue is widely used to assay cell death, cells at a late stage of dying are frequently not stained. Therefore, we also performed a counterstain with fluorescein diacetate, staining live cells only, and the fluorescence visualized by confocal microscopy (Zeiss LSM510 NLO, Zeiss). Untreated cells showed high green fluorescence, while 15 to 30min after treatment with AAN could be observed a decrease in fluorescein signal and an increase in red fluorescence (Figure 27).
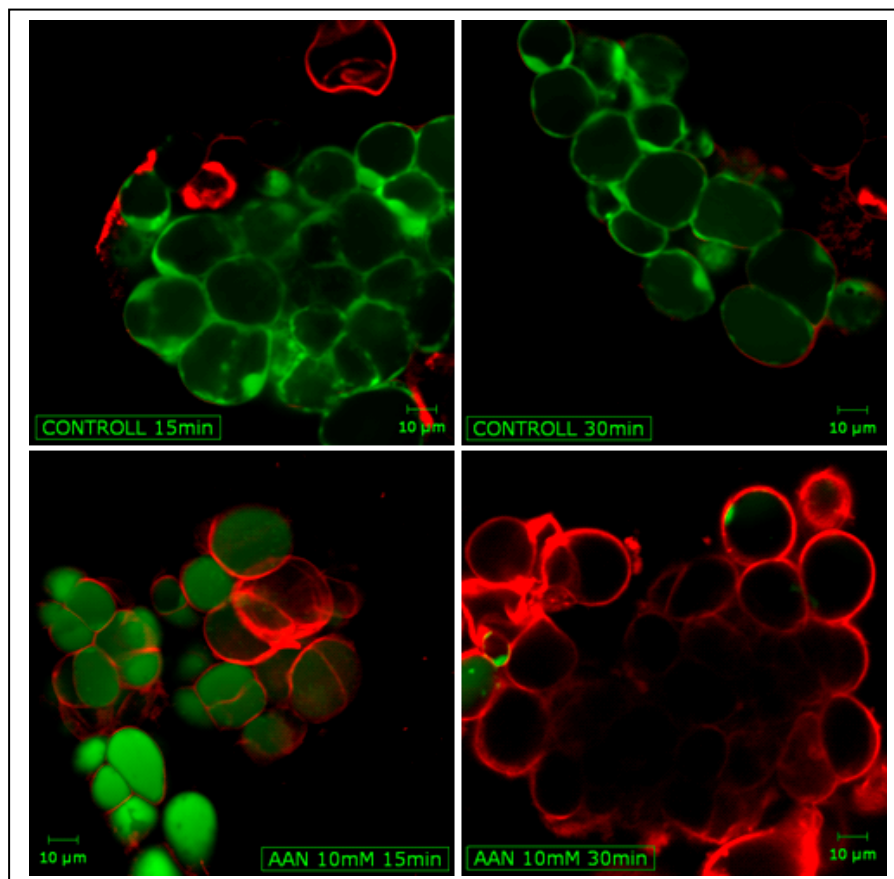
Figure 27. Visualization of AAN-induced cell death in Arabidopsis cell cultures
Confocal microscopy images were obtained using Zeiss LSM 510 NLO (Zeiss) with a 40X water lens. Cell death, measured as loss of plasma membrane integrity, was detected by double staining with Evans blue (red fluorescence, dead cell), and fluorescein diacetate (green fluorescence, living cells). After incubation with the dyes for 5min, to analyse the effect of GDC inhibition on Arabidopsis cells, 10mM AAN was added and the fluorescence visualized.

3 Discussion

The programmed cell death (PCD) observed in the HR in several plant-pathogen interactions exhibits similarities to that seen in animal apoptosis, including chromatin condensation and fragmentation (Mur et al., 2008) and caspase-like proteolytic activity (Lam and del Pozo, 2000). Furthermore, it has been shown that NO and ROS play a major regulatory and antimicrobial role in plant defence response (Delledonne et al., 2001). It was postulated that ROS act as a trigger for PCD locally and as diffusible signal for the induction of cell defences in neighbouring cells (Vranova et al., 2002). ROS may possess direct antimicrobial activity and function in cell wall reinforcing processes. Plants response to ROS in a dose-dependent manner - high doses trigger HR-related PCD, whereas low doses induce antioxidant enzymes. NO acts synergistically with ROS to increase host cell death of soybean suspension cells and inhibitors of NO compromise HR in *Arabidopsis thaliana* and tobacco (Delledonne et al., 2001). Produced NO/ROS activate the transcription of defence genes, are able to damage proteins, lipids and nucleic acids and induce PCD to prevent the spread of the pathogen from the site of infection (Durner and Klessig, 1999; Romero-Puertas and Delledonne, 2003). In animal cells, mitochondria are major sites of redox compound formation and major targets of NO/ROS-induced damage (Skulachev, 1996). In plant cells large quantities of reactive species are produced in plastids and peroxisomes, especially in photosynthetic cells. Additionally, plant mitochondria are also responsible of this accumulation and are an essential site of oxidative damage (Taylor et al., 2002).

3.1 MITOCHONDRIA AND NO

It was already demonstrated that NO is able to affect mitochondrial respiration (KCN-sensitive) leading to an induction of an alternative pathway (AOX) (Huang et al., 2002). AOX catalyses the oxidation of ubiquinol and the reduction of oxygen to water, bypassing the final steps of the cytochrome c pathway. Unlike the cytochrome c pathway, which is coupled to proton translocation, electron transport from ubiquinol to AOX is non-phosphorylating and releases energy as heat. Strikingly, AOX is not affected by NO. Despite the recovering action of AOX, the production of mitochondrial ROS will increase in this situation, because the rate

of electrons leaving the mtETC through the terminal oxidases is slowed or the rate of electron input increases in excess (Moller, 2001). Other hints to the capability of NO to modulate essential mitochondrial function emerged during the study of plants reaction to the bacteria elicitor harpin (Krause and Durner, 2004). Indeed, harpin induced mitochondrial oxidative damages, e.g. NO and ROS production, depolarization of membranes and release of cytochrome c, are essential steps for the perturbation of the entire cell and induction of cell-death (Krause and Durner, 2004). However, until now demonstration of mitochondria dependent NO localization during plant response to stresses is still missing.

Using the NO-sensitive fluorescein derivate DAF-2FM DA and Mitotracker Red, NO accumulation in mitochondria was detected in harpin-treated *Arabidopsis thaliana* cell cultures (Figure 4). This data offer support to the idea that NO and NO oxides interact directly with mitochondrial proteins, lipids and nucleic acids and alter mitochondrial functions. NO production after harpin treatment was much slower compared with an elicitor-induced NO burst in tobacco or mechanical stress of various gymnosperms (Foissner et al., 2000; Pedroso et al., 2000). However, induction of NO was consistent on one side with the published data on Arabidopsis response to harpin and on the other side with the simultaneous ROS production, both starting within a few minutes after addition of harpin (Krause and Durner, 2004). The source of this NO burst in mitochondria remains still to be clarified. Mammalian mitochondria reduce nitrite to NO (Kozlov et al., 1999) and in the unicellular green alga *Chlorella sorokiniana*, mitochondria contribute to NO production (Tischner et al., 2004). Recently, Planchet and associates identified the mitochondrial electron transport chain as a major source for reduction of nitrite to NO in addition to nitrate reductases in *Nicotiana tabacum* using inhibitors and purified mitochondria (Planchet et al., 2005). Moreover, the sensitivity of NO production to the complex III inhibitor myxothiazol and to the AOX inhibitor SHAM in mitochondria purified from tobacco suspension cells and Arabidopsis root, suggests that both terminal oxidases may participate in NO production (Tischner et al., 2004; Gupta et al., 2005; Planchet et al., 2005). AtNOS1 was previously identified as mitochondria-located NO synthase (Guo et al., 2003). However, the NO producing function of this enzyme could not be verified, resulting in renaming of this protein to NO associated protein (AtNOA1) (Zemojtel et al., 2006). Summing up, whether an additional nitrite-NO reductase or a NOS-like protein is involved in mitochondrial NO production or whether this is inherent to the mitochondrial terminal oxidases, has to be clarified.

3.2 S-NITROSYLATION OF MITOCHONDRIAL PROTEINS

NO features an unmatched diversity of physiological functions. Under pathological conditions, high concentrations of NO can either be beneficial - e.g. it activates defence responses or, together with ROS, it directly kills the pathogen - or detrimental. Among the deleterious effects are lipid peroxidation, nitration of tyrosine as well as S-nitrosylation. S-nitrosylation is an important mechanism how NO can affect protein activity/function by modifying sulfhydryl groups of cysteine residues (Hess et al., 2005). Many examples for protein S-nitrosylation and consequently modulation of protein function have been reported in the animal system. NO's interaction with cytochrome *c* oxidase – *via* binding cysteine residues in the active site - has dramatic biological consequences such as the induction of apoptosis (Brunori et al., 1999). Moreover, caspase-3 zymogens are S-nitrosylated at the active site cysteine residues resulting in inhibition of enzyme activity. Interestingly, during Fas-induced apoptosis the modified residues are de-nitrosylated and the function of the enzyme is regained (Mannick and Schonhoff, 2004). But S-nitrosylation is also an important mechanism to regulate the activity of proteins in plant. GSNOR is a potentially significant player in the modulation of cellular NO status because it effectively decompose GSNO, a compound with NO-releasing and thiol-nitrosylating potential, from the cellular pool. Although GSNOR does not directly act on S-nitrosylated protein substrates, GSNOR knockout mice, Arabidopsis, and yeast cells all showed increased SNO levels (Liu et al., 2001; Feechan et al., 2005; Rusterucci et al., 2007). By analyzing both missense and null mutations of the gene encoding GSNOR, it has been demonstrated that GSNOR function is required for acclimation to high temperature and for normal plant growth and fertility (Lee et al., 2008), empathizing the importance of nitrosothiols in regulating plant reactions. Moreover, plant immunity requires conformational changes of NPR1 - a master regulator of salicylic acid-mediated defence genes – via S-nitrosylation. In unchallenged plant, NPR1 is sequestered in the cytoplasm as an oligomer through intermolecular disulfide bonds. S-nitrosylation of NPR1 by S-nitrosoglutathione (GSNO) facilitates its oligomerization, which maintains protein homeostasis upon SA induction. Upon pathogen challenge, reduction of the NPR1 oligomer releases monomer that translocates to the nucleus where it activates the expression of a battery of pathogenesis-related (PR) genes (Tada et al., 2008).

Furthermore, S-nitrosylation is important for regulation of mitochondrial functions. In fact, mitochondria contain a sizeable pool of thiols and transition metals, all of which are known to modulate SNO biochemistry (Foster and Stamler, 2004). In addition mitochondria are highly membranous and sequester lipophilic molecules such as NO. Moreover, the formation of the putative S-nitrosylating intermediate N_2O_3 is enhanced within membranes.

Several mitochondrial proteins were found to be candidates for S-nitrosylation in *Arabidopsis thaliana* (Lindermayr et al., 2005; Romero-Puertas et al., 2008). Mitochondrial malate dehydrogenase for example - already described as S-nitrosylated in the animal field by Foster and Stamler (2004) - was isolated as candidate for S-nitrosylation after NO treatment of Arabidopsis plant, GSNO treatment of Arabidopsis cell culture (Lindermayr et al., 2005) and during Arabidopsis-Pseudomonas interaction (Romero-Puertas et al., 2008). However, there were no experimental evidences available that plant mitochondrial proteins are regulated through S-nitrosylation so far.

Applying the biotin-switch method to partially purified mitochondria, 11 new mitochondrial candidates for S-nitrosylation and 9 proteins with a not defined localization in plant cells were identified (Figure 9 and 10, Table 2). Among them, the mitochondrial α subunit of ATP synthase, which is the mitochondria encoded homolog of the nuclear ATP synthase. The latter one was already identified as candidate for S-nitrosylation in NO-treated Arabidopsis (ATP synthase CF1 α-chain) (Lindermayr et al., 2005) and in the rat kidneys mitochondria subjected to ischemia and reperfusion (Eaton et al., 2003). Additionally, the catalase 3 which has been already showed to be S-nitrosylated in rat liver mitochondria (Foster and Stamler, 2004) was isolated. Although this protein is typically localized in peroxysome (Fukao et al., 2002), there are several hints that at least low amounts of catalase are present in mitochondria (Heazlewood et al., 2004), suggesting that this protein is dual-targeted in plants (Peeters and Small, 2001).

Interestingly, among the identified candidates for S-nitrosylation there were different subunits of the mitochondrial glycine decarboxylase complex (GDC), a key enzyme of the photorespiratory C2 cycle in C3 plants. GDC consists of 4 subunits named P, H, T and L protein. The H-protein undergoes a cycle of reductive methylamination (catalysed by the P-protein), methylamine transfer (catalysed by the T-protein) and electron transfer (catalysed by the L-protein) (Douce et al., 2001) (Figure 28). Low activity of the mitochondrial photorespiratory GDC, *via* antisense reduction of the P-protein, affects photosynthetic performance and redox homeostasis in potato and barley (Heineke et al., 2001; Igamberdiev et al., 2001). Moreover, GDC subunits H and P have been already described to be involved in plants response to pathogens (Yao et al., 2002). Considering all these data and because of the pivotal role of this enzyme in mitochondria metabolism, the attention was focused on the decarboxylating subunit of the GDC, the P protein (Wingler et al., 2000; Yao et al., 2002).

To investigate the ability of GSNO in causing conformational change of P protein, the cysteine residues of pure P protein were analyzed for S-nitrosylation by biotin-switch method. Although crystal structures for eukaryotic H, L, and T proteins have been obtained employing recombinant overexpression systems (Pares et al., 1994; Neuburger et al., 2000;

Okamura-Ikeda et al., 2005), such data are not yet available for the P subunit from eukaryotic sources. A crystal structure is only available for the P protein of the eubacterium *Thermus thermophilus* (Nakai et al., 2005). It is hypothesized that this prokaryotic $(\alpha^N \beta^C)_2$-tetrameric P protein and the eukaryotic α_2-type dimeric P protein share a similar three-dimensional structure; however, for unclear reasons, recombinant overexpression of eukaryotic P protein is difficult to achieve (personal communication, unpublished data from Prof. Dr. Herman Bauwe). In *Arabidopsis thaliana* there are 2 genes codifying for the P subunit (At4g33010, At2g26080) and the 2 proteins share the 95% homology. Since different expression systems failed to produce native form of both Arabidopsis P homologues partial purification was performed by size exclusion chromatography combined with ion exchange chromatography (Figure 11-13). Using the biotin-switch method, S-nitrosylated thiol groups of the P protein could be detected (Figure 14), confirming the data obtained with the mitochondrial extract.

.

3.3   EFFECT OF NO ON THE GLYCINE DECARBOXYLASE

The GDC, together with the serine hydroxymethyltransferase (SHMT), is responsible for the conversion of glycine to serine in mitochondria (Figure 28). During this metabolic process, CO_2 and NH_3 are produced and ATP and reducing equivalents are consumed, thus making photorespiration a wasteful process (Wingler et al., 2000).
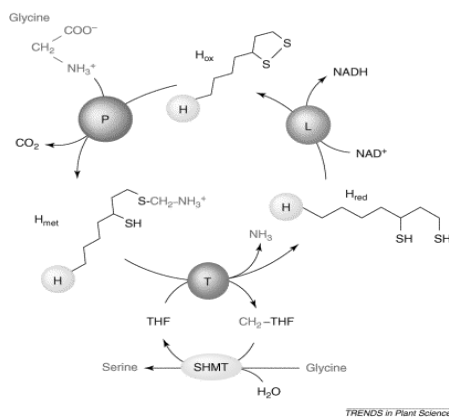
Figure 28. Glycine decarboxylase complex (Douce et al., 2001)

Outline of the reactions involved in oxidative decarboxylation and deamination of glycine in plant mitochondria. P-, H-, T- and L- are the protein components of the GDC. H-protein undergoes a cycle of reductive methylamination (catalysed by the P-protein), methylamine transfer (catalysed by the T-protein) and electron transfer (catalysed by the L-protein). SHMT: serine hydroxymethyltransferase involved in the conversion of CH_2–THF to THF at the expense of a second molecule of glycine. H_{met}, H_{red} and H_{ox}: methylaminated, reduced and oxidized forms of the H protein, respectively.

Precisely because of this inefficiency, it was proposed that the photorespiration could serve as an energy sink preventing the over-reduction of the photosynthetic mtETC and photoinhibition, especially under stress conditions (Wingler et al., 2000). Furthermore,

photorespiration provides compounds for other metabolic processes, e.g. glycine for the synthesis of glutathione, which is also involved in stress protection (Blackwell et al., 1990). Barley GDC mutant - exhibiting very low amount of P and H subunits - shows a very low amount of the AOX protein and, under photorespiratory conditions, an over-reduction and over-energization of the cell can be observed (Igamberdiev et al., 2001). Oat GDC was described to be involved in the response to the toxin victorin produced by the fungus *Cochliobolus victoriae* (Navarre and Wolpert, 1995; Yao et al., 2002). The P subunit of the GDC was found to bind victorin *in vivo* only in susceptible genotypes, while the H subunit was binding victorin *in vivo* in both susceptible and resistant genotypes (Navarre and Wolpert, 1995). In addition, the application of the GDC inhibitor AAN resulted in apoptosis-like cell death and disease symptoms similar to those induced by native victorin (Yao et al. 2002). Although it was recently shown that the inhibition of GDC activity by victorin plays just a partial role in the onset of cell death and defence responses, it may contribute to symptom development and provide subsequent benefit for the pathogen in terms of feeding nutrients and colonizing host plants (Tada et al., 2005). Considering these findings, the role of GDC in redox stress in Arabidopsis mitochondria was investigated. Following the $^{14}CO_2$ release from [1-^{14}C]glycine, i.e. the activity of P and H-subunits, a clear modulation of the GDC activity by redox agents was observed in both intact mitochondria and plant leaves. The decarboxylation activity significantly decreased in presence of GSNO or after blocking the free cysteines with cysteine-modifying agents. In contrast, reducing agents such as DTT and GSH promoted GDC activity (Figure 16, 17). The requirement of a reduced environment for both the CO_2 exchange reaction and the decarboxylase activity of GDC *in vitro* has been already described, but the function of the reducing agent has not been characterized (Hiraga and Kikuchi, 1980; Walker and Oliver, 1986). The inactivation of GDC after treating mitochondria with NEM or DTNB provided a further hint to the importance of cysteine residues for the enzyme activity.

In the animal system, the toxicity of NO is a result of inhibition of cellular respiration (Clementi et al., 1998). NO's interaction with cytochrome *c* oxidase (complex I) has dramatic biological consequences, such as the increase in mitochondrial ROS level and the induction of apoptosis (Brunori et al., 1999). In this situation, the reason for NO toxicity is not a shut down of respiration *per se*, but is due to an over-reduction of the ubiquinone pool. This inhibitory effect of NO on cytochrome *c* oxidase has been described also for soybean and mung bean mitochondria (Millar and Day, 1996; Yamasaki et al., 2001). Consequently, the modulation of GDC activity observed after GSNO treatment could be a secondary effect due to inhibition of the respiration and subsequent accumulation of ROS in mitochondria. In contrast, specifically blocking the mitochondrial complex I *via* rotenone did not influence GDC

activity within the 30min reaction (Figure 18). Also the increase of ROS level by eliminating the ROS-scavenger effect of the alternative oxidase did not influence the GSNO-dependent inhibition of GDC activity, proving that a direct action of GSNO on the GDC is responsible for the decreased activity (Figure 18).

GSNO is able to S-nitrosylate or S-glutathionylate cysteine residues and both modifications can have different effect on proteins conformation and activity. To investigate which post-tranlational modification cause GDC activity inhibition, the partially purified P protein was analyzed by Nano-HPLC-MS[2/3]. Interestingly only S-glutathionylated cysteines residues could be identified by MS analysis (Table 3, Appendix E). The alignment of Arabidopsis P proteins with orthologs proteins revealed that all modified cysteine residues are uniquely present in *Arabidopsis thaliana*. No SNO modified cysteine residues were identified in P proteins by MS analysis. This result questioned if cysteine residues of the P protein are S-glutathionylated and not S-nitrosylated. To verify the ability of NO to affect P protein activity, the NO donor SNP – which is exclusively able to S-nitrosylate cysteines residues - was used. The inhibition of the GDC activity by SNP, demonstrated that NO is able to inhibit GDC activity *per se* and confirmed the strict connection between these two posttranslational modifications (Figure 3). Probably cysteine residues of the P protein are preferentially S-glutathionylated or the S-nitrosylation could not be detected by MS because of the liability of this modification. Moreover, the nitrosothiol itself was proved to be an activated form that can lead, upon reaction with the reduced form of glutathione (GSH), to S-glutathionylation (Martinez-Ruiz and Lamas, 2007).

The modulation of a key enzyme of the photorespiratory system via S-nitrosylation/ S-glutathionylation suggests a direct role of this metabolic pathway for regulating the redox state of the cell. Together with the fact that GDC was found in root and etiolated tissue of different plants, in C4 plants and in a wide range of organisms from bacteria to humans, suggests a non-photorespiratory role of this complex (Navarre and Wolpert, 1995). For this reason, the state of the GDC during a plant stress-response was analyzed, using Arabidopsis-harpin as model system (Xie and Chen, 2000; Krause and Durner, 2004; Livaja et al., 2008). Harpin induces mitochondrial disorders and defence responses normally associated with apoptotic events in animals and plants (Krause and Durner, 2004; Livaja et al., 2008). Because of contradictory data concerning studies on harpin-treated isolated mitochondria (Xie and Chen, 2000; Krause and Durner, 2004), GDC activity was monitored in Arabidopsis leaves *in vivo* and *in vitro* (Figure 21, 22). An inhibition of GDC activity occurred already 30min after harpin treatment of Arabidopsis leaf slices, which increased to 70% inhibition 4h after treatment (Figure 19). Moreover, a decrease in photorespiratory rate, measured as CO_2 compensation point in absence of respiration in the light (Γ^*), and an increase in

glycine/serine ratio were observed (Figure 21, 22). Although a difference in timing and severity of the response, these data confirmed the *in vitro* experiments and underlined the pivotal role of GDC in photorespiratory pathway. Thus, these data demonstrate that harpin inhibits not only the cytochrome *c* dependent respiration (Xie and Chen, 2000; Livaja et al., 2008) but also the photorespiratory system in Arabidopsis plants. This situation reduces the cellular capacity of ATP synthesis and increases the accumulation of ROS, leading to an over-reduction and over-energization of the entire cell.

3.4 RESPONSE TO GDC INHIBITION

The role of GDC modulation during plant stress responses has already been investigated in oat after victorin treatment. In this system the application of the GDC specific inhibitor AAN resulted in disease symptoms similar to those induced by victorin and in apoptosis-like cell death (Yao et al., 2002). To monitor just the effect of GDC inhibition on Arabidopsis mitochondria, plants and cell culture were tested with the specific GDC inhibitor AAN, which has no side effect on dark respiration and on CO_2 fixation (Usuda and Edwards, 1980; Creach and Stewart, 1982).

In animals, a variety of key events in apoptosis focus on ROS-mediated events in mitochondria, including the release of caspase activators such as cytochrome *c*, changes in electron transport, loss of mitochondrial transmembrane potential, altered cellular oxidation reduction, and participation of pro- and anti-apoptotic Bcl-2 family proteins (Green and Reed, 1998). Such events were also described to take place in plants, e.g. during Arabidopsis response to the bacterial elicitor harpin (Krause and Durner, 2004). Here, it was shown that AAN alone was able to induce an oxidative burst in Arabidopsis cell culture and leaves (Figure 23, 24). A ROS dependent fluorescence burst was visible in both Arabidopsis plants and cell cultures treated with AAN (Figure 23). While catalase was able to scavenge the AAN-induced ROS accumulation, the inhibitor of AOX (SHAM) further increased the signal 1h after incubation (Figure 23A, 24A). These data showed that GDC inhibition results not only in the activation of a general stress-response pathway, but also in the activation of the NO-insensitive AOX pathway. AOX frequently is induced during plant-pathogen interactions and plant defence, and seems to play a role in containment of lesions and control of initial plant defence reaction (Lennon et al., 1997; Chivasa and Carr, 1998). Furthermore, these results confirm the role played by AOX pathway as direct ROS detoxifier in plant (Huang et al., 2002; Rhoads et al., 2006) and demonstrate a connection between GDC and AOX (Igamberdiev et al., 2001) (Figure 24B). Although plant mitochondria are known to produce high amounts of ROS (Moller, 2001), they frequently have been overlooked as a source of

Discussion

ROS in the context of defence responses. Here the use of the mitochondrial specific dye Mitotracker Red allowed us to localize the ROS-burst in Arabidopsis mitochondria (Figure 23B). Thereby it has to be noted that the obtained Mitotracker Red signals require intact membrane potential, ruling out the possibility that destroyed or non-functional mitochondria contribute to the ROS stain. However, co-localization of mitochondria and ROS formation does not necessarily implicate a key role for mitochondrial ROS during early stages of apoptotic response.

Mitochondria are organelles with two well-defined compartments: the matrix, surrounded by the inner membrane, and the intermembrane space surrounded by the outer membrane. The inner membrane is folded into numerous christae, which contains the protein complexes from the electron transport chain, and the ATP synthase. To function properly, it is almost impermeable in physiological, thereby allowing the respiratory chain to create an electrochemical gradient ($\Delta\Psi_m$). The mitochondrial transmembrane potential $\Delta\Psi_m$ is indispensable for driving the ATP synthase which phosphorylates ADP to ATP. ATP generated on the matrix side of the inner membrane is then exported in exchange for ADP by ADP/ATP carrier (Siedow and Umbach, 1995). In animal cells the increase of mitochondrial ROS together with an elevation of cytosolic Ca^{2+}, contribute to the opening of the mitochondrial permeability transition pore (PTP), which depolarizes the mitochondria and leads to mitochondrial swelling and subsequent release of cytochrome *c* from the intermembrane space (Goldstein et al., 2000). Moreover, the participation of the mitochondrial PTP in NO-induced plant cell death was demonstrated (Saviani et al., 2002). Treatment of Arabidopsis cells with the GDC inhibitor AAN resulted in loss of 60% of membrane potential. This decrease in membrane potential was limited by the action of the alternative respiratory pathway, as proved by the addiction of the AOX inhibitor SHAM (Figure 25A, 26). Moreover the scavenging effect of catalase proves the direct involvement of ROS in activating the depolarization of mitochondrial membranes in plants (Figure 25B).

Proteins released from mitochondria after depolarization of the mitochondrial membrane includes not only cytochrome *c* but also apoptosis-inducing factor. This protein moves directly to the nucleus where it causes chromatin condensation and nuclear fragmentation. Furthermore, cytochrome *c* activates a caspase signalling cascade that selectively cleaves vital substrates in the cell, including the nuclease responsible for DNA fragmentation (Green and Reed, 1998). In agreement with this scheme of actions, inhibition of Arabidopsis GDC by AAN resulted in loss of plasma membrane integrity and cell death (Figure 27).

3.5 CONCLUSION

This section of the work proved the ability of NO to modulate Arabidopsis mitochondrial metabolism *via* affecting the photorespiratory pathway by thiol modification of the P subunit of the GDC. Moreover it was observed that this modulation, together with the inhibition of dark respiration and activation of the alternative oxidase pathway, is part of the stress-related response of Arabidopsis to the bacterial elicitor harpin. These data confirmed the finding that GDC is essential for the redox balance of plant mitochondria and participated to stress responses, as it has been already described for oat cells response to the toxin victorine.

In summary, the inhibition of the photorespiratory pathway *via* S-nitrosylation/S-glutathionylation of the P subunit of glycine decarboxylase complex induces a fast ROS production in Arabidopsis mitochondria (Figure 29). This perturbation of mitochondrial redox state is counterbalanced by the activity of the alternative respiration - not affected by NO -, which acts as direct ROS detoxifier in plant. Despite the recovering action of AOX, the production of mitochondrial ROS will increase and will be followed by mitochondrial membranes depolarization, release of cytochrome *c* in the cytoplasm and induction of cell death.
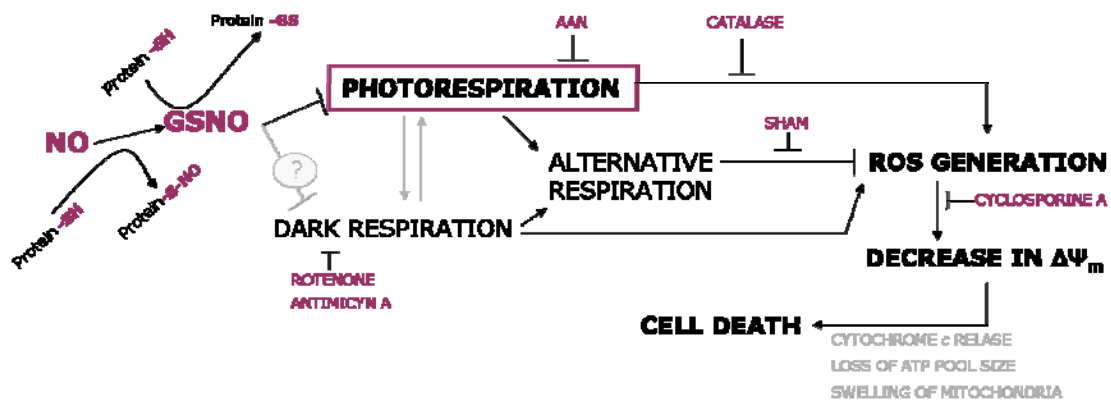
Figure 29. Overview of mitochondrial events after GDC inhibition

The inhibition of the photorespiratory pathway *via* S-nitrosylation or S-glutathionylation of the P subunit of glycine decarboxylase complex induces a fast ROS production in Arabidopsis mitochondria and a perturbation of the entire cell. The dark respiration plays a pivotal role in this response, but the way NO modulates this complex as to be further investigated. AAN: specific inhibitor of glycine decarboxylase complex of the photorespiration; rotenone: specific inhibitor of the cytochrome *c* respiration; SHAM: specific inhibitor of the alternative oxidase; catalase: H_2O_2 scavenger; cyclosporine A: inhibitor of the mitochondrial PTP.

4 Materials and Methods

4.1 PLANT MATERIAL and TREATMENTS

4.1.1 *Arabidopsis thaliana* **Suspension Culture**

Suspension cells were grown in the dark on a rotary shaker at 120rpm and 27°C. Every week two gram cells were sub-cultured with a sifter in 40ml fresh growth medium modified after Murashige & Skoog (Toshio Murashige, 1962) in a 200ml cell culture flask.

All experiments were performed using cells in the logarithmic growth phase, 5-6 days after sub-culturing.

4.1.2 *Arabidopsis thaliana* **Plants**

For plant breeding, soil was mixed with silica sand in a ratio of 4:1 and poured in 6-well plant pots. Soil was wetted with water; *Arabidopsis* seeds were sowed with a toothpick and incubated at 4°C for 3 days in the dark to synchronize germination. Plant growth chambers were provided with a 14 hours light (20°C) / 10 hours dark (18°C) cycle, relative humidity was adjusted to 70%.

Five to six weeks-old plants were used for experimentation. Leaf slices were used for the *in vivo* assay of the glycine decarboxylation and confocal microscopy. The apical section (approximately 0.2cm) and basal section (approximately 0.2cm) were removed from the blades, and the remaining leaf segment was used for sectioning. The leaf segments were sliced into 2x7mm slices with exciser, allowing slices to fall directly into distilled water. Ten leaf slices per replicate (30 per each sample) were aliquot into glass vials containing 10mM MOPS pH 7.2, and allowed to equilibrate for 1h with gentle shaking inside a 30°C water bath incubator. The elicitors/inhibitors were added and vials were incubated for requested time points. For photorespiration measurement with LICOR6400, elicitors/inhibitors were applied by pressure infiltrating Arabidopsis leaves using a 1ml needleless syringe from the abaxial side.

4.2 ISOLATION OF MITOCHONDRIA

4.2.1 Crude Mitochondria Extract

Crude, well-coupled mitochondria were isolated and purified by differential centrifugation (Keech et al., 2005). All procedures were carried out at 4°C in detergent-free vessels. About 15g of leaves were cut up with scissors and placed in a mortar. They were then ground, using a pestle, in 20ml of grinding buffer with a small amount (about 0.5g) of quartz (fine granular, washed and calcined GR from Merck). The extract was filtered through a 20µm nylon mesh and centrifuged at 2500rcf for 5min to remove most of the intact chloroplasts and thylakoid membranes. The supernatant was transferred to a new tube and centrifuged at 15000rcf for 15min. The pellet obtained was suspended in wash buffer and centrifuged at 15000rcf for 15min. The resulting supernatant was discarded and the pellet containing the crude mitochondria was re-suspended in 0.5ml of wash buffer or a specific assay buffer. The re-suspended pellet defined as mitochondria enriched fraction (MEF) was further purified by free-flow electrophoresis.

Solutions Mitochondria Grinding Buffer: 0.3 M sucrose, 60mM N-tris [hydroxymethyl]-methyl-2-aminoethanesulphonic acid (TES), 10mM ethylene diamine tetra-acetic acid (EDTA), 10mM KH_2PO_4, 25mM tetrasodium pyrophosphate, 1% (w/v) polyvinylpyrrolidone-40, 0.5%(w/v) defatted bovine serum albumin (BSA), pH-(KOH) 8.0, 1mM Phenylmethylsulfonylfluorid (PMSF), 1µM leupeptin and 1µM pepstatin added just prior to grinding. Mitochondria Wash Buffer: 0.3M sucrose, 10mM TES, 10mM KH_2PO_4, pH-(KOH) 7.5 and one tablet of 'Complete' Protease Inhibitor Cocktail for each 10ml of solution (Roche Applied Science).

4.2.2 Pure Mitochondria: Free Flow Electrophoresis

A zone electrophoretic separation (ZE) was utilized by means of a ProTeam FFE™ free-flow electrophoresis apparatus (Tecan) to further purify MEF as described by Heidrich et al. (Heidrich et al., 1970). In short, according to their surface charge, particles are deflected differently in an electric field and are separated through a buffer flow perpendicular to the electric field. Prior to the FFE fractionation, the MEF (2-4mg total protein) was diluted 1:4 in Separation Medium to reach 1mg/ml protein dilution. Electrophoresis was performed in horizontal mode at 5°C with a total flow rate of 280ml/h within the separation chamber at 750V (~135mA). All buffers were cooled on ice during separation to avoid thermal gradients. The samples were applied to the separation chamber with a flow rate of 1ml/h *via* the cathodic inlet. Fractions were collected in 96-well plates and the distribution of separated particles was monitored at a wavelength of 260nm with a Synergy™ HT microplate reader (Bio-Tek Instruments). Subsequently, FFE fractions showing increased light scattering value

were concentrated by centrifugation at 4°C with 15000rcf for 15min. The pellets were then re-suspended in Mitochondria Wash Buffer and frozen in liquid nitrogen.

Solutions Separation Medium: 100mM triethanolamine, 100mM acetic acid, pH 7 .4 (2 N NaOH).

4.2.3 Treatments of Arabidopsis Mitochondria

All activity assays were performed using freshly purified MEF. When necessary, the Mitochondria Wash Buffer was exchanged with the assay buffer with an acetone precipitation (10 volumes, -20°C, 2h) followed by centrifugation (10000rcf, 20min) or by centrifugation at 15000rcf for 15min.

4.3   ANALYSIS OF MITOCHONDRIA PURITY

To estimate the purity of the mitochondria containing fractions the specific activities of marker enzymes were determined: mitochondrial cytochrome c oxidase (Neuburger et al., 1985), peroxisomal catalase (Cohen et al., 1996) and cytochrome c dependent respiration. Enzyme activities were measured in the initial crude extract, in enriched (MEF) and purified mitochondrial fraction. Additionally a proteomic analysis was performed on the enriched fraction. Total protein concentrations were estimated according Bradford et al. (Bradford, 1976).

4.3.1 Cytochrome c Oxidase Assay

Cytochrome c oxidase is the principle terminal oxidase of high affinity oxygen in the aerobic metabolism of all animals, plants, yeasts, and some bacteria. This enzyme is located on the inner mitochondrial membrane that divides the mitochondrial matrix from the intermembrane space and it has been used for many years as a marker for this membrane integrity. The colorimetric assay for cytochrome c oxidase (Cytocrome c oxidase assay kit, Sigma) is based on observation of the decrease in absorbance at 550nm of ferrocytochrome c caused by its oxidation to ferricytochrome c by cytochrome c oxidase. The ferrocytochrome c substrate solution was made by dissolving 2.7mg cytochrome c in 1ml water, followed by addition of DTT to a final concentration of 0.5mM in order to reduce the protein. After incubation for 15min at room temperature the abs_{550}/abs_{565} ratio of an aliquot diluted 20-fold with assay buffer was determined using an Ultraspec 310pro spectrophotometer (Amersham Biosciences). An abs_{550}/abs_{565} ratio between 10 and 20 ensure that the substrate has been

71

sufficiently reduced. The reaction kinetics were conducted at 25°C, the final reaction volume was 1.1ml. The mitochondria containing fraction (50µl) was added to cuvettes containing 950 µl assay buffer and 50µl enzyme dilution buffer. After mixing by inversion the reaction was started by the addition of 50µl of ferrocytochrome c substrate. The decrease in absorption was measured in the first 45 seconds of reaction using a kinetic program: 5 seconds delay; 10 seconds interval; 6 readings. The enzyme activity of samples was calculated as follows:

$$\text{Units/ml} = \frac{\Delta A/\text{min x dil x } 1.1}{(\text{vol of enzyme}) \times 21.84}$$

Where: ΔA/min = A/minute (sample) - A/minute (blank)

dil = dilution factor of enzyme or sample

1.1 = reaction volume in ml

vol of enzyme = volume of enzyme or sample in ml

21.84 = $\Delta\varepsilon^{mM}$ between ferrocytochrome c and ferricytochrome c at 550 nm

4.3.2 Catalase Assay

Catalase catalyses the decomposition of hydrogen peroxide (H_2O_2) to water and oxygen. This assay is based on the measurement of the hydrogen peroxide substrate remaining after the action of catalase. First, the catalase converts hydrogen peroxide to water and oxygen (catalatic pathway) and then this enzymatic reaction is stopped with sodium azide. An aliquot of the reaction mix is then assayed for the amount of hydrogen peroxide remaining by a colorimetric method. Reagents and buffers for the catalase assay were stored at 0°C in an ice-water bath, except for the 0.6N H_2SO_4 which was held at room temperature. The reactions kinetic were conducted at 0°C with 6mM H_2O_2, the final reaction volume was 1ml. The mitochondria containing fraction (50µl) was added to tubes containing 800µl phosphate buffer (1M KPO_4, pH 7.0). Sodium azide (50µl, 0.5mM final concentration) was used to distinguish catalase activity from other factors that might induce loss of H_2O_2; matched controls received an equal volume of water. The reaction was started by the addition of 100µl of 60mM H_2O_2, followed by gentle mixing. At fixed time intervals, duplicate 100µl aliquots were removed and quenched by addition to a mixture of 4.0ml of 0.6N H_2SO_4 plus

1ml of 10mM $FeSO_4$ at room temperature. After all samples were collected, the colour was developed by addition of 400µl of 2.5M KSCN. Subsequently, the samples were covered with aluminium foil to protect them from light. An Ultraspec 310*pro* spectrophotometer (Amersham Biosciences) was used to measure the red colour of ferrithiocyanate. The concentration of hydrogen peroxide used in this assay (50mM) provides a measurable signal, but does not cause inactivation of the enzyme. Colorimetry was conducted at room temperature in a 1ml cuvette at a wavelength of 460nm and samples were analyzed kinetically at two time points. Results are expressed as follows:

$$\text{Units/ml} = = \frac{\Delta A/\text{min} \times Vol_{tot}}{\Delta t \times Vol_{sample}}$$

Where: $\Delta A/\text{min}$ = A/minute (sample) - A/minute (blank)

$Vol_{tot/sample}$ = total volume of reaction/ volume of enzyme or sample in ml

Δt = time differential between the two time points in min

The purity was accepted, if a 10-fold enrichment of mitochondria in comparison to peroxisome (Lee Sweetlove, personal communication) was observed.

4.3.3 Determination of Cellular Respiration

Respiratory oxygen consumption was determined in a Clark-type oxygen electrode (Bachofer) in 1ml mitochondria containing reaction buffer (10mM KPO_4 pH 7.4, 5mM $MgCl_2$, 20mM KCl, 250mM mannitol, and 20mM succinate) in presence of ADP (0.5mM, pH 7.4). When a certain voltage is applied to the instrument, oxygen is destroyed at the platinum surface of the electrode; the flow of current is then proportional to the rate at which oxygen can diffuse to the platinum surface from the gas or liquid sample outside the membrane, and is thus a measure of the oxygen pressure in the sample. So, after the residual current of the electrode was removed, mitochondria containing fractions were placed in the cuvette and the oxygen pressure in the sample measured. All experiments were repeated three times for each mitochondrial fraction.

4.3.4 2D Gel Electrophoresis

Enriched mitochondria in Mitochondria Wash Buffer were re-suspended in a solution of 10mM TRIS-HCl pH 7.4 after centrifugation at 15000rcf for 15min. Three cycles of freeze-thaw followed by a vortex in 0.4% CHAPS were used to break mitochondrial membranes. Proteins recover was achieved by precipitation for 2h at -20°C in 3 volume of acetone 10% TCA (-20°C), followed by 15000rcf for 10min 4°C centrifugation. This precipitation step was repeated other two times using acetone (-20°C). Precipitated mitochondrial proteins were diluted under agitation in Rehydratation Buffer and total protein concentrations estimated according Bradford protocol (Bradford, 1976). Aliquots containing 300μg protein were further purified by removing contaminants that could disturb the electrophoresis process using a Desalting spin column (BioRad). The first-dimension was performed on the horizontal isoelectric focusing system (IEF) Ettan IPGphor III (GE Healthcare) under utilization of 18cm, pH 3 to 11 nonlinear immobilized pH gradient strips (GE Healthcare). Sample was applied on the anode of a strip rehydrated with 350μl of Rehydratation Buffer (cup loading). The IEF was performed overnight (18h), reaching a total of 52kV h. The pH gradient strips were transferred onto a 12% SDS-gels (24x24cm) in an Ettan Dalt six Electrophoresis System (GE Healthcare). Running conditions were maintained over night at 25mA, 20°C in 2D Running Buffer. Three independent runs of samples on 2D-gels were carried out. After 2D-gel electrophoresis, proteins were stained with Sypro Ruby (Molecular Probes) and then scanned using Typhoon TRIO+ (GE Healthcare).

Solutions Rehydratation Buffer: 8M Urea, 2% CHAPS, 0.5% IGP buffer (respective pH range), 0.4 % DTT (added freshly), water to reach the volume. To 350μl of buffer 2μl of 0.5% Bromophenol Blue were added. 2D Running Buffer: 192mM Glycine, 25mM Tris, 0.1% SDS, pH 8.3 (no adjustment necessary). <u>IEF run</u> 150V 3h, 300V 3h, 1000V 6h, 10000V 3h, 100000V 3h.

4.4   HARPIN PREPARATION and CHEMICALS

4.4.1 Preparation of Harpin Protein

E. coli DH5α cells transformed with a pBluescript vector carrying the full length *Pseudomonas syringae* 61 hrpZ ORF was used for harpin production. Purification steps for the harpin protein were essentially as described by Livaja et al., 2008. 1/200 volume of an over night culture (dYT Amp100, 37°C, 250rpm) was transferred to a new media and grown at 37°C until 0.6 OD_{600}. The expression of harpin protein was induced by 1mM IPTG. After 16h of incubation at 37°C and 250rcf the cells were harvested by centrifugation at 14000rcf at 4°C for 30min. The pellet was re-suspended in 10mM KH_2PO_4 pH 6.5, and sonicated on ice. After

centrifugation at 14000rfc at 4°C for 30min the supernatant was denatured at 95°C for 15min, once again centrifuged at 23000rcf at 4°C for 45min and filtrated through 0.45/0.2µm filters. The protein containing solution was further concentrated with Amicon Ultra-4 cellulose filter tubes (10000NMWL, Millipore) by centrifugation at 7500rcf and 4°C for 15-20min. Prior adding Harpin Storage Buffer, total protein concentration was estimated according Bradford protocol [6] and by SDS-gel analysis. Harpin protein was stored in aliquot at –20°C. *E. coli* DH5α cells transformed with an empty pBluescript vector were used as control.

Solutions Harpin Storage Buffer: 0.5% Tween20, 0.5% Tergiton NP-40, 10mM EDTA, 50% Glycerol, Protease inhibitor cocktail (Roche).

4.4.2 Chemicals

COMPOUND	STOCK	NOTE
Aminoacetonitrile (AAN)	0.5M in H_2O	
Carboxy-PTIO (cPTIO)	500µM in H_2O	Freshly prepared. Store in dark
Catalase	2000units/mg in H_2O	
Cyclosporine A	0.2mM in ethanol	
Dithiothreitol (DTT)	1M in H_2O	Freshly prepared. Store in dark
Glutathione (GSH)	10mM in H_2O	
N-ethylmaleimide (NEM)	20mM in ethanol	
Rotenone	1mM in alcohol	Decomposition upon exposition to light and air
Salicylhydroxamic acid (SHAM)	10mM in H_2O	
S-nitrosoglutathione (GSNO)	10mM in H_2O	Freshly prepared. Store in dark
5,5'-dithiobis-2-nitrobenzoicacid (DTNB)	10mM in ethanol	

4.5 S-NITROSYLATION

4.5.1 S-Nitrosylated Proteins Detection and Purification

Crude mitochondrial extract was diluted with HEN Buffer to a protein concentration of 1mg/ml and then treated with GSNO or GSH 1mM. After incubating samples at RT in the dark, mitochondrial proteins were precipitated with 10 volumes of acetone (-20°C) 20min at

-20°C to remove the excess of GSNO/GSH. The samples were centrifuged at 10000rcf for 10min and pellets re-suspended in HEN buffer (final concentration 1mg/ml). S-nitrosylated proteins where purified using the Biotin-Switch method essentially as described by Jaffrey and Snyder (Jaffrey and Snyder, 2001). All procedures were carried out in the dark. To elute were added 4 volumes of Blocking Buffer at 50°C for 30min with frequent vortex. The MMTS containing solution was then removed by precipitating protein in 3 volumes of acetone (-20°C) for 20min and re-suspending it in 0.1ml HENS Buffer per mg of protein in the starting sample. 1:3 volume of Labelling Solution (containing biotin–HPDP fresh prepared and equilibrated in HENS buffer) and 1:50 volume of Ascorbate Solution were added to blocked proteins and incubated for 1 hour at 25°C. At this point, samples no longer needed to be protected from light.

For detection of biotinylated proteins by immunoblotting, an aliquot of protein was added to Non-Reducing SDS-PAGE Sample Buffer 2X and used to perform a SDS-PAGE followed by western-blot. Biotinylated proteins were detected with anti-biotin mouse monoclonal antibody (AP-coniugated).

To perform the purification of biotinylated proteins, two volumes of −20°C acetone were added and samples incubated for 20min at −20°C to remove the biotin-HPDP. After centrifugation, the walls of the tubes and the surface of the pellets were gently rinsed with −20°C acetone. Neutravidin-agarose (Pierce) was used to purify biotinylated proteins. 10 volumes of Neutralization Buffer and 60µl/mg of Neutravidin-agarose were added to biotinylated proteins (re-suspended in 0.1ml of HENS Buffer per mg of protein in the initial protein sample) and incubated for 2h in the dark at RT in a rotary-shaker.
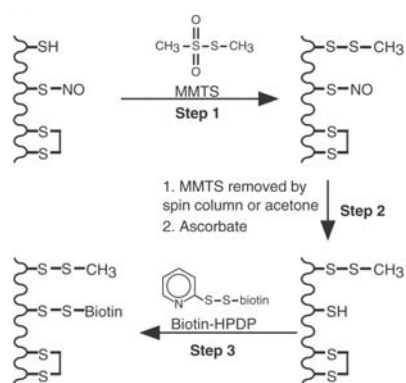
Solutions HEN Buffer: 250mM Hepes-NaOH pH 7.7, 1mM EDTA, 0.1mM Neocuproine; Blocking Buffer: 9 volumes HEN Buffer , 1 volume SDS (25% w/v in H2O), 20mM MMTS (2 M stock in DMF); HENS Buffer: Adjust HEN Buffer to 1% SDS by addition of a 1:25 volume of 25% (w/v) SDS solution;

Ascorbate Solution: 50mM solution of sodium ascorbate in deionised water; Biotin-HPDP: 50mM suspension in DMF; Bromophenol blue 1.2mg; Neutralization Buffer: 25mM Hepes-NaOH, pH 7.7, 100mM NaCl, 1mM EDTA, 0.5% Triton X-100; Washing Buffer: Neutralization Buffer with 600mM NaCl; Elution Buffer: Neutralization Buffer with 150mM 2-Mercaptoethanol (fresh added) instead of Triton X-100. Non-Reducing (Reducing) SDS-PAGE Sample Buffer 2X: 62.5mM TRIS-HCl pH 6.8, 25% Glycerol, 4% SDS, 0.005% Bromophenol Blue (50µl β-Mercaptoethanol added to 450µl Sample Buffer 2X).

The beads were then transferred to a column and the flow trough collected. Three washing steps were performed using 10 volume of Washing Buffer. Finally the beads were incubated with Elution Buffer for 15min to recover the bound proteins. All different fractions were acetone precipitated, re-suspended in HEN buffer and stored at -20°C. The sample were analyzed by SDS-PAGE (reducing condition) or prepared for LC-MS/MS.

4.5.2 Polyacrylamide Gel Electrophoresis

A sodium dodecyl sulfate polyacrylamide gel (SDS-gel) was used for detection of biotinylated proteins and to separate purified S-nitrosylated proteins. The purpose of this method is to separate proteins according to their size as described by Laemli (Laemli, 1970). Prior to load the protein samples, 1 volume of Reducing or Non-Reducing SDS-PAGE Sample Buffer 2X was added and, in case of reducing condition, incubated at 95°C for 5min. The running gel was 1mm thick, 10.5cm x 10cm and contained 12% acrylamide. A constant current of 35mA was applied for approximately 60min. After running, proteins were stained with Colloidal Comassi or with SYPRO Ruby (Molecular Probes[TM]).

Solutions Running Buffer: 25mM TRIS-HCl, 192mM Glycine, 0.1% SDS; SDS-gel Upper Buffer: 0.5M TRIS-HCl pH 6.8, 0.4% SDS; SDS-gel Lower Buffer: 1.5M TRIS-HCl pH 8.8, 0.4% SDS.

	RUNNING GEL	UPPER GEL
H_2O	1.675ml	1.25ml
BUFFER	1.25ml	625µl
ACRILAMIDE 30%	2ml	500µl
SDS 10%	50µl	25µl
TEMED	2.5µl	10µl
APS 10%	25µl	20µl

4.5.3 Staining of Proteins with Sypro® Ruby Protein Gel Stain

The SYPRO Ruby protein gel stain (Molecular Probes) is a ready-to-use, ultrasensitive, luminescent dye for detection of proteins separated in a polyacrylamide gel. After electrophoresis, the gel was placed in Fix Solution and agitated on an orbital shaker (Combishaker KL2, Carl Roth) for 30min. The fixing step was repeated once more with fresh solution. The staining was performed with 50ml SYPRO Ruby protein gel stain over night with gentle agitation. Before imaging the gel was washed for 30min with Wash Solution and rinsed in ultrapure water for at least 5min to prevent possible corrosive damage to the

imager. Proteins were visualized using a Typhoon TRIO+ (GE Healthcare), a 532nm laser-source and a 610nm emission filter.

Solutions Fix Solution: 50% Methanol, 7% Acetic Acid; Wash Solution: 10% Methanol, 7% Acetic Acid.

4.5.4 Staining of Proteins with Colloidal Comassie (Blue Silver)

Blue silver is an organic dyes of the Coomassie family that can reach a sensitivity as high as 1ng protein/band, thus in the range of the most sensitive silver stains. After electrophoresis the gel was placed directly in the Colloidal "blue silver" Solution. The dark green dye solution turn to a deep blue when adsorbed onto the polypeptide chains fixed in the polyacrylamide gel. The staining was performed for at least 2h with gentle agitation. Bands were visible without de-staining but a wash in water was performed to remove the excess of dye.

Solutions Colloidal Solution: 0.12% Comassi G-250, 10% ammonium sulfate, 10% phosphoric acid, and 20% methanol.

4.5.5 Protein Transfer and Immunoblotting

Western blotting is the transfer of electrophoresed proteins (e.g., by SDS-PAGE) to a membrane for further analysis (e.g., by staining, immunodetection, autoradiography, etc). The transfer is induced by electric voltage and the proteins move out towards a membrane where they stick because of hydrophobicity (and electrostatic interactions too with certain types of membranes). After completion of electrophoresis, the gel was removed from the electrophoresis apparatus and a sandwich of the filters, polyvinylidene difluoride membrane (PVDF) and gel was assembled in a semi-dry western apparatus (MilliBlot, Millipore). The blotting was performed in Transfer Buffer for 1h using 2.5mA/cm^2. After transfer of proteins from gels to membranes, the blots (membranes) were removed and rinsed briefly in TBS or water. Ponceau S reversible protein staining was performed at this stage to visualize the proteins. The blots were subsequently blocked in Blocking Buffer for 1-2h at RT or over night at 4°C to prevent non-specific binding of antibodies. Then primary antibodies, that recognize specific proteins or tags on proteins, were allowed to bind to their targets. Blots were washed to remove non-specific binding at least 2 times with TBST and 1 time with TBS (10min each). After washes, secondary antibodies-alkaline phosphatase conjugated, that recognize the primary antibodies and have detection tags on them, were used. After final washes, the detection tags, and thus indirectly the primary antibodies, were detected. Blots were incubated in Developing Buffer for few minutes and then transferred to water.

Solutions Ponceau S: 0.2% w/v Ponceau S in water with 3% acetic acid; TBS: 10mM TRIS-HCl pH 7.4, 0.9% NaCl, 1mM $MgCl_2$; TBST: TBS, 0.5% Tween20; Transfer Buffer: 25mM TRIS-HCl, 192mM Glycine, 0.1% SDS, 20% Methanol (prior to use); Blocking Buffer: TBST, 1% Milk powder, 1% BSA; Anti-Biotin Alkaline Phosphatase Conjugated: 1:10000 dilution in TBST; AP Buffer: 100mM TRIS-HCl pH 8.5, 100mM NaCl, 5mM $MgCl_2$; Developing Buffer: 10ml AP Buffer, 33µl BCIP 50mg/ml, 33µl NBT 100mg/ml.

4.5.6 Maldi-Tof Mass Spectrometry for Peptide Fingerprint Analysis and NanoLC/MS/MS

Proteins were dissolved in 50ml of 0.1M NH_4HCO_3 10% acetonitrile and digested with 3mg of trypsin at 37°C overnight. Protein spots were visualized by colloidal Coomassie staining, excised from SDS-gel and complete destained by washing in 25mM NH_4HCO_3. Digested peptides were extracted by vortexing for 3h with 100ml of 5% formic acid. All tryptic peptide samples were dried and redissolved in 50ml 0.1% trifluoroacetic acid and 5% acetonitrile. Peptides were separated by reversed-phase chromatography using an UltiMate Capillary/Nano liquid chromatography system (LC Packings). Portion of 20µl samples were loaded to a precolumn (300µm * 5mm, 5 µm C18, 100Å, PreMap, LC Packings) and eluted and fractionated on a self-packed analytical column (75 µm * 120mm packed with YMC-Gel ODS-A, 3mm C18, YMC) with a gradient of 5% to 55% acetonitrile at a flow rate of 150nl/min in 40min. Eluted peptides were continuously delivered to a Q-Tof Ultima mass spectrometer (Waters/Micromass) by electrospray and analyzed by MS/MS employing data-dependent analysis (3 most abundant ions in each cycle; 0.3s MS *m/z* 400–2,000 and maximum 4.8s MS/MS *m/z* 50–3,000, continuum mode, 60s dynamic exclusion). The MS/MS raw data were processed and converted into Micromass pkl-format using MassLynx 4.0 ProteinLynx. Resulting pkl-files were compared with those of theoretical trypsin digestions and searched against predicted masses derived from the NCBI genomic database using ProFound software (Genomic Solutions). The MASCOT search engine was used to parse MS data to identify proteins from primary sequence databases. Proteome analysis was carried out by TopLab Company (Martinsried).

4.5.7 Nano-HPLC-MS[2/3] and Data Analysis

For mass spectrometric analyses partially purified P protein was digestion at 37°C for 1h in 100mM TRIS HCl, pH 6.5. The reaction was done in dark to avoid light-dependent decomposition of the modifications. The used trypsin/protein ration was 1/20. All nano-HPLC-MS[2/3]-experiments were performed on a Flux Rheos 2200 nanoflow system connected to a

linear ion trap-Fourier transform (LTQ-Orbitrap) mass spectrometer (Thermo Fisher Scientific, San Jose, CA, USA) equipped with a nanoelectrospray ion source (Proxeon Biosystems).

Protein digests were analyzed by online nano LC-MS/MS. The samples were separated on an in-house made 10cm reversed phase capillary emitter column (inner diameter 75µm, 5µm ProntoSIL 120-5-C18 ace-EPS) using 120min linear gradients from 0 to 40% Acetonitril/0.1% formic acid with a Flux Rheos 2200 nanoflow system (Flux Instruments AG) at a flow rate of 270nl/min. The LC setup was connected to an LTQ-Orbitrap classic (Thermo Fisher) equipped with a nanoelectrospray ion source (Proxeon Biosystems). The mass spectrometer was operated in the data-dependent mode to automatically switch between MS, MS^2, and MS^3 acquisition. Survey full-scan MS spectra (m/z 350–1,800) were acquired in the Orbitrap with resolution R = 7500 at m/z 400. The six most intense ions were then sequentially fragmented in the linear ion trap by using collisionally induced dissociation at normalized collision energy of 35. In the case of a resulting neutral loss of 9.$7m/z$ and 14.5 m/z, respectively in the MS^2 spectra in the three most abundant peaks indicating the loss of NO these fragments were selected for further MS^3 fragmentation. Former target ions selected for MS^2 were dynamically excluded for 30s. Total cycle time was ≈3s. The general mass spectrometric conditions were: spray voltage, 1.4kV; no sheath and auxiliary gas flow; ion transfer tube temperature, 200°C. Ion selection thresholds were: 500 counts for MS^2 and 500 counts for MS^3. An activation q = 0.25 and activation time of 30ms was applied in both MS^2 and MS^3 acquisitions.

Peptides and proteins were identified via automated database searching (Bioworks 3.3.1, SP1) of all MS^2 and MS^3 against an in-house curated database containing the protein entries from The Arabidopsis Information Resource proteome database (version 7), E. coli, porcine trypsin and the human keratins (36361 protein sequences). Spectra were normally searched with a mass tolerance of 1.5amu for the parent mass and 1amu for the MS^2 and MS^3 fragment masses with semitryptic specificity allowing two miscleavages. All modifications were set to be variable: oxidation of methionine, nitrosylation and glutathionylation of cysteine. Proteome analysis was carried out in cooperation with the Helmholtz Zentrum München core facility.

4.6   PURIFICATION OF P-PROTEIN FROM MITOCHONDRIA EXTRACT

P-protein purification from mitochondria extract was essentially as described by Bourguignon et al. (Bourguignon et al., 1988).

4.6.1 Solubilization of Glycine-Cleavage System

Arabidopsis MEF (about 70mg of protein) were diluted in Dilution Buffer to 40mg/ml. The addition of 4µM leupeptin to the lysis buffer provides further protection of the enzymes against endogenous proteinases. Total release of the matrix protein was achieved by three cycles of freeze-thaw (liquid-N_2 for 2 min followed by 30°C until thawed). This procedure breaks about 98% of the mitochondria. The suspension of broken mitochondria was centrifuged at 100000rcf for 2h (24000rpm in a Beckman ultracentrifuge with W28 swilling rotor) to remove all the mitochondrial membranes. The supernatant containing soluble protein was concentrated with a Centricon Plus-20 Pl 10kDa (Millipore) by centrifugation at 3600rcf for 30min in a swilling rotor (Rotanta 460R, Hettich Zentrifugen). All the proteins involved in the conversion of glycine into serine were retained by this selectively retentive membrane (final volume 0.6ml). At this stage, the glycine-cleavage system could be stored at -80 °C under N_2 without deterioration for many months. However, after several cycles of freezing and thawing the glycine-cleavage complex lost part of its activity, owing to P-protein denaturation.

Solutions Dilution Buffer: 5mM MOPS, 5mM TRIS, 1mM β-mercaptoethanol, 1mM EGTA, 20µM Pyridoxal Phosphate, 1mM Serine, 4µM Leupeptin, 0.1% Triton X-100, pH 7.0;

4.6.2 Size Exclusion Chromatography

The matrix extract obtained by ultracentrifugation (0.6ml, 60mg of protein) was applied to a HiPrep 16/60 Sephacryl S-300 HR (GE Healthcare) equilibrated in 0.5 volume of water and 2 volumes of Buffer A at 0.5ml/min. The column connected to an ÄKTAexplorer™ fplc system was eluted with the same buffer at 4°C with a flow rate of 0.5ml/min, a fraction size of 2ml and a void volume (V_0) of 45ml. To predict the protein separation (and the V_0) a Standard Protein Marker (Sigma) was run on the same column prior the sample run. After sample separation different fractions were analyzed on a 12% SDS-gel (20µl *per* sample, visualized by Colloidal Comassie staining). P-protein was eluted in the heavy fractions of the size exclusion chromatography, T- and H-protein in the light fractions and L-protein between light and heavy fractions (intermediary fraction). Heavy fractions were combined and stored at -80°C after the addiction of 20% glycerol.

Solutions Buffer A: 50mMKCl, 5mM Mops, 5mM Tris pH 7.5, 2mM β-mercaptoethanol, 1mM EGTA, 1mM serine, 1mM glycine. Standard Protein Marker (2ml): 2mg/ml Cytochrome C, 10mg/ml BSA, 5mg/ml Alcohol Dehydrogenase.

4.6.3 Anion Exclusion Chromatography

A portion of the size exclusion chromatography heavy fraction (10mg) was applied to a HiTRAP DEAE FF column (GE Healthcare) to further separate proteins according to their charge. The column was first equilibrated with 5 volumes Buffer A containing 10mM phosphate buffer pH 7.5, instead of Tris and Mops buffers (Buffer A*). P-protein was eluted at 4 °C with a continuously increasing KCl gradient (50-1000mM) in the same buffer. The flow rate was maintained at 0.5ml/min, the total volume at 20ml and the fraction size at 0.5ml. After elution a washing step (5 volume Buffer A* 1M KCl) and a re-equilibration step (5 volumes Buffer A* 50mM KCl) were performed to remove residual proteins linked to the column. Twenty µl aliquots of each fraction were analyzed by SDS-PAGE followed by Colloidal Comassie staining. P-protein emerged as a very large peak at ~150mM KCl. Fractions were combined, concentrated with Amicon Ultra-4 10kDa (Millipore) and stored at -80°C (after the addiction of 20% glycerol).

4.7 ASSAYs FOR GDC ACTIVITY

4.7.1 CO$_2$-Glycine Exchange Reaction

The activities of P-protein was determined by measuring the amounts of [^{14}C]bicarbonate fixed to the carboxy-group carbon atom of glycine during the exchange reaction (Hiraga and Kikuchi, 1980). The reaction was conducted in presence of saturating concentration of H-protein. As source of H protein, 100µg of proteins of the light fraction of size exclusion chromatography were used. The reaction was initiated by addition of bicarbonate. The total NaHCO$_3$ concentration in the Reaction Buffer was 20mM with a portion of 0.35µmol of NaH^{14}CO$_3$ (20µCi). After 15min of incubation at RT, the reaction mixture was transferred to a radioactivity-counting vial containing 1ml of acetic acid and the mixture was dried on a hot plate. The radioactivity was determined with a scintillator counter (Beckman LS6000SC) after addition of 10ml of aqueous counting scintillant (Zinsser Analytic).

Solutions Reaction Buffer: 25mM potassium phosphate pH 7.0, 1mM DTT, 50µM pyridoxal phosphate, 25mM glycine and 20mM bicarbonate, 20µCi [^{14}C]bicarbonate, 100µg H-protein, 40µg P-protein .

4.7.2 Glycine Decarboxylase Activity

P-protein activity in Arabidopsis leaf slices and intact mitochondria was performed following the glycine decarboxylase activity in *vitro*:

$$[^{14}C]Glycine + H_4folate + NAD \rightarrow {}^{14}CO_2 + NH_3 + CH_2H_4folate + NADH$$
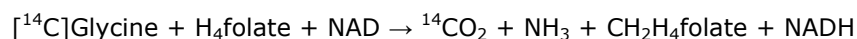
The reaction was started by adding 8mM [^{14}C]glycine (8.75µCi) to 300µl of Assay Buffer containing 100µg of mitochondrial protein or 10 leaf slices. Reaction mixtures were placed in small cups suspended over 1.4ml of Oxysolve c400 scintillator fluid (Zinsser Analytic) in 20ml scintillation vials. Reactions were initiated with glycine and terminated by injecting 100µl of 6M acetic acid into the reaction mixture. The vials were left overnight to allow trapping of $^{14}CO_2$, the reaction cups removed, and the trapped ^{14}C radioactivity determined by scintillation counting (Beckman LS6000SC).

Solutions Reaction Buffer: 0.3M Sorbitol, 20mM MOPS pH 7.2, 8mM KCl, 4mM NaHPO4 pH 7.2, 4mM MgCl2, 0.1% BSA.

4.7.3 Gas-Exchange Measurements

The photorespiration rate *in vivo* was monitor following the response of the photosynthesis (A) to intracellular CO_2 mole fraction (Ci). Rates of photosynthesis and dark respiration of leaves attached to the plants were determined under the growth conditions using a portable infrared gas analyser system LI-6400 (LI-COR Biosciences). A leaf was placed into the leaf chamber of the LICOR-6400 and exposed to light at 75, 250 or 400µmol m^{-2} s^{-1} at a flow rate of 300µmol s^{-1}. Leaf temperature was maintained at 25°C during measurement. The pressure inside the leaf chamber was maintained slightly above ambient, so outside air could not enter the chamber. Leaves were left for 10min in the chamber before the measurement to allow adaptation. To calculate the CO_2 compensation point (Γ) a cycle with six CO_2 references concentrations was used: 400, 300, 200, 100, 50 and 400ppmol.

Photorespiration rate was calculated as photosynthetic CO_2 compensation point in absence of respiration in the light (Γ*). It was defined as the interception point of different curves measured at different light intensities (75, 250, 400µE). The y coordinate of this point gave the respiration in the light (-Rd).

4.7.4 Glycine / Serine Content

For amino acid determination, 100mg leaf material were ground in liquid nitrogen and extracted in 1ml 80% ethanol for 30min. After centrifugation for 10min at the maximum speed, the supernatant was vacuum dried and the dried extract dissolved in 1ml 0.3M Na$_2$PO$_4$ (pH 6.8) and 0.4% tetrahydrofurane. Samples were incubated for 30min and then diluted 1:50 with the same phosphate buffer. Individual amino acids were separated by HPLC

and quantified as described in Hagemann et al., 2005 (Hagemann et al., 2005). Briefly, glycine and serine were assayed after derivatization with o-phthaldialdehyde (OPA) as described by (Geigenberger et al., 1996) Geigenberger et al., 1996 using a Hypersil 120 ODS column (4.6 x 150mM, Knauer) connected to a Class-Vp-HPLC system (Shimadzu) with a fluorescence detector (RF-10A$_{XL}$, Shimadzu).

4.8 FLUORESCENT MICROSCOPY

4.8.1 Mitochondria

Arabidopsis cell culture mitochondria were visualized by confocal microscopy by staining harvested cells with 0.5µM MitoTracker Red 580 (stock 1mM in DMSO, Molecular Probe). After incubation for 20-30min, the fluorescence was excited using a 543nm laser and detected through a long pass (LP) filter 565-615nm.

4.8.2 Nitric Oxide

The detection of NO was done by loading Arabidopsis suspension cells with a NO reactive fluorescent indicator (DAF-2FM DA, Molecular Probe) in conjunction with fluorescence microscopy. This method allowed bioimaging of NO, which is suitable for real-time analysis of intracellular NO. Cell were incubated with 2µM of dye (stock 5mM in DMSO) for 10min and fluorescence analyzed under confocal microscope (Ex: 488nm, band pass filter BP500-550).

4.8.3 Reactive Oxygen Species

To analyze ROS production by fluorescence microscopy, Arabidopsis suspension cells or leaf slices were incubated in a selective dye (H$_2$DCF-DA) at a final concentration of 10µM (stock 1mM in DMSO) for 20 min. Subsequently, samples were washed by short centrifugation or by filtration and transferred to a microscope slide. The fluorescence was excited using a 488nm laser and detected through LP560nm filter.

To quantify the ROS production in Arabidopsis cell culture, a fluorescence microplate reader (Tecan GENios, TECAN) was used. After treatment with H$_2$DCF-DA (10µM) for 30min, cells were washed and 200µl aliquot transferred in a black 96-well plate (Nunc). The excitation wavelength was set at 488nm, the emission at 535nm and the detection gain at 60. ROS production was estimated by measuring fluorescence intensity every 2min over time (60min). The plate was shaken before and between measurement for 60sec to prevent cell stress and death. The values are obtained by subtraction of cells autofluorescence.

4.8.4 Mitochondrial Transmembrane Potential $\Delta\Psi_m$

Changes in mitochondrial transmembrane potential $\Delta\Psi_m$ in response to different elicitors were monitored using the mitochondrial potential sensor JC1 (Invitrogen), a dye that exhibits a potential-dependent accumulation in mitochondria (Yao et al., 2002). The green-fluorescent JC1 probe (emission at 525nm) exists as a monomer at low concentrations or at low membrane potential. However, at higher concentrations or higher potentials, JC1 forms red-fluorescent "J-aggregates" that exhibit a broad excitation spectrum and an emission maximum at 590 nm. Thus, the emission of this cyanine dye can be used as a sensitive measure of mitochondrial membrane potential. Arabidopsis cells were stained with the 5 µg/ml JC1 dye (stock 1mg/ml in DMSO) and incubated for 30min in the dark with continuous shaking. Stained cells were diluted with PS medium, placed in a black 96 well microplate (Nunc) and treated with the elicitors. Changes in fluorescence intensities were measured immediately after treatment using an excitation wavelength of 488nm and two emission filters. Fluorescence intensities were detected every 5min over 100min. To ensure aeration of the medium, microplates were rocked for 5min between subsequent measurements and for 10sec between green and red fluorescence scanning. The ratio of red-to-green JC1 fluorescence is dependent only on the membrane potential and not on other factors that may influence single-component fluorescence signals, such as mitochondrial size, shape and density.

4.8.5 Cell Death Assay

Cell death was measured as loss of plasma membrane integrity and detected by staining Arabidopsis suspension cells with Evans blue and Fluorescein diacetate. Evans blue is commonly used to assay death cell, whereas Fluoresceine is used to stain live cells (Huang et al., 2002). The excitation and emission wavelength of the two dyes were different and not interfering (Evans blue: Ex=543nm laser and a long pass filter LP650nm; Fluorescein diacetate: Ex=488 laser and BP filter 505-530nm). Harvested suspension cells were stained with 0.005% Evans blue solution (stock 1% [w/v] in 0.1mM $CaCl_2$ pH 5.6) for 5min. Then stained cells were incubated for further 5min with 0.01% Fluorescein diacetate (stock 1% [w/v] in DMSO) and treated with different inhibitors or water. Confocal microscopy images were obtained using Zeiss LSM 510 NLO (Zeiss) with a 63X water lens.

4.9   STATISTICAL ANALYSIS

The t-test was used only for appropriate situations where there were only two levels of one independent variable. In the case where there were more than two levels of the independent variable the statistical analysis had to go through two steps. First, it was necessary to carry out an over-all F test to determine if there was any significant difference existing among any of the means. If this F score was statistically significant, then it was carried out a second step in which sets of two means at a time were compared in order to determine specifically, where the significance difference lies.

4.9.1   Anova Test

A One-Way Analysis of Variance is a way to test the equality of three or more means at one time by using variances (using the F distribution).

Assumptions:

- The populations from which the samples were obtained must be normally or approximately normally distributed
- The samples must be independent
- The variances of the populations must be equal

The ANOVA produces an F statistic, the ratio of the variance among the means to the variance within the samples. Essentially, the ratio of variance is a comparison of the variance amongst the different groups to the variance amongst all the individuals within those groups. The degrees of freedom (d_f) for the numerator are I-1, where I is the number of groups (means). The degrees of freedom for the denominator is N - I, where N is the total of all the sample sizes. Tests were performed using the trial version of the statistical software SPC XL add-in to Microsoft Excel.

4.9.2   Tukey's Hsd Post Hoc Test

To answer the pair comparisons questions a series of Tukey's post-hoc (Honestly Significantly Different) tests were run, which are like a series of t-tests. The post-hoc tests are more stringent than the regular t-tests however, due to the fact that the more tests you perform the more likely it is that you will find a significant difference just by chance. It is based on what is called the "studentized range distribution." To test all pairwise comparisons among means using the Tukey HSD, it is necessary to compute t for each pair of means using the formula:

$$t_s = \frac{M_1 - M_2}{\sqrt{MS_w \, (1/n)}}$$

M = treatment mean

MS_w = is the Mean Square Error (from ANOVA)

n = number per treatment/group

The Tukey's score (t_s) must be statistically significant with Tukey's probability/critical value table taking into account appropriate df_{within} (ANOVA) and number of treatments ($P< 0.05$).

Part II

NITRIC OXIDE RESPONSIVE GENES AND PROMOTERS IN *ARABIDOPSIS THALIANA*: A BIOINFORMATICS APPROACH

This part of the thesis was made in collaboration with:

Huang X and Sell S., who performed the **microarray analysis** on Arabidopsis plant/cells. The dataset is in part published in *Huang X, von Rad U, Durner J (2002) Nitric oxide induces transcriptional activation of the nitric oxide-tolerant alternative oxidase in Arabidopsis suspension cells. Planta 215: 914-923*

Scherf M. and Werner T., who developed the **sequence analysis software** for Genomatix GmbH. *Quandt K, Frech K, Karas H, Wingender E, Werner T (1995) MatInd and MatInspector: new fast and versatile tools for detection of consensus matches in nucleotide sequence data. Nucleic Acids Res 23: 4878-4884*

The adjustments and application of the program to plant derived expression data and promoter sequences were done by myself only. The presented results and discussion have been obtained and written by myself only.

5 Methods and Results

A major task in biology is to identify binding sites for transcription factors (TFBS) in gene promoter regions to understand the mechanisms that regulate the interactions between gene expression and regulatory networks. Recent advances in genome sequence availability and in high-throughput gene expression analysis technologies have allowed for the development of computational methods for promoter modules finding.

5.1 MICROARRAY DATA ANALYSES

For detection of common TFBS and promoter modules in the promoter region of NO-regulated genes *A. thaliana* whole genome microarray data were used. These microarray were generated in our laboratory by Huang Xi, who analysed Arabidopsis cell suspension cultures and plants in response to the NO donor (±)-(E)-ethyl-2-[(E)-hydroxyimino]-5-nitro-3-hexeneamide (NOR-3) and gaseous NO. To obtain specific gene expression, the NO treatment was adjusted by Huang to yield only moderate changes in transcriptional activity. In the conditions applied (ca. 100 ppm NO or 0.5mM NOR-3 for 10 min) the cells did not show any symptoms such as cell death. To avoid false-positive results, a crucial step in promoter analysis is the selection of gene clusters. For this reason, microarray data were rearranged in clusters and those genes with relatively low basal expression ratios, even if those genes showed high induction by NO were ignored. In summary, 28 genes which were up-regulated in almost all experiments were observed (Figure 29 and Appendix D). Furthermore, 79 and 121 genes were exclusively induced in cell culture and plant experiments, respectively. Additionally, 26 genes down-regulated in cell culture experiments were found. The difference in the set of regulated genes is probably due to the difference between the biological system used (plant/cell culture) but also due to the different way of action of the NO-applications (NO-donor NOR-3/gaseous NO).
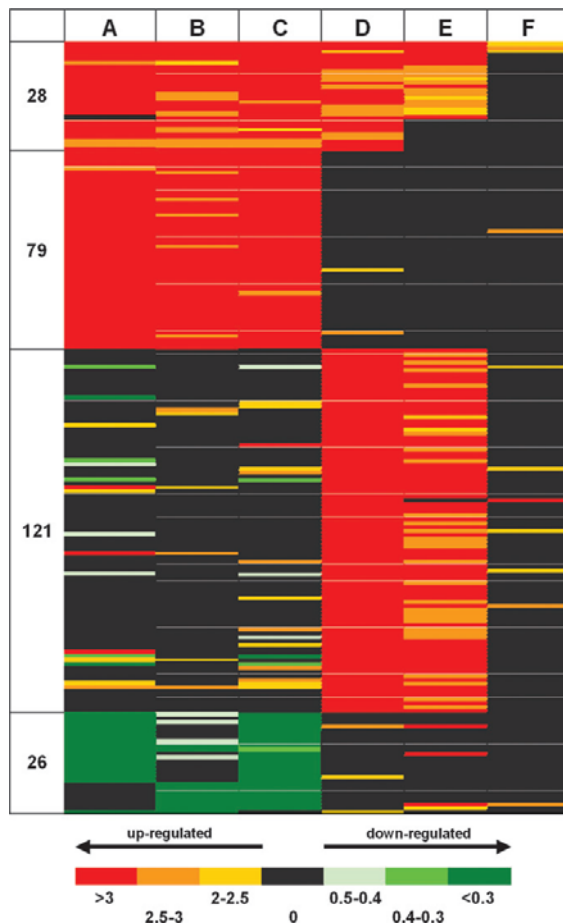
Figure 29. Schematic display of the expression profile of NO-regulated Arabidopsis genes

Expression profile of NO-regulated genes in cell cultures (A-C) and plants (D-F) treated with 0.5mM NOR-3 or gaseous NO, respectively. The transcriptional profile of the cell cultures and plants was analyzed using Agilent microarrays (generation 1 for A and D and generation 2 for B, C, E, and F). Cell cultures and plants were treated for 1h (A, B, D, E) or 3h (C, F). NO-regulated genes were grouped in genes, which were up-regulated in almost all experiments (28), up-regulated in cell culture experiments only (79), up-regulated in plant experiments only (121), and down-regulated genes (26).

5.2   COMMON TFBS IN NO-REGULATED GENES

5.2.1 Gene2Promoter

After the rearrangement of the microarray analyses data, the corresponding promoter sequences of the significantly regulated transcripts were analyzed with the Gene2Promoter "tool" of the Genomatix software (developed and released by Genomatix GmbH). The Gene2promotor was used to locate the correlated genes within the genome and define the promoter for each gene. First of all, microarray data were uploaded into the Genomatix portal as distinct cluster depending on their modulation after NO- treatment:

- UP-REGULATED GENES: cell cultures + plants, plants, cell cultures;

- DOWN-REGULATED GENES**:** cell cultures.

Using the default "Extract and interactively analyze up to 1000 promoters" option it was possible to select "*Arabidopsis thaliana*" among the organisms and the input genes promoters for subsequent analysis (Figure 30).
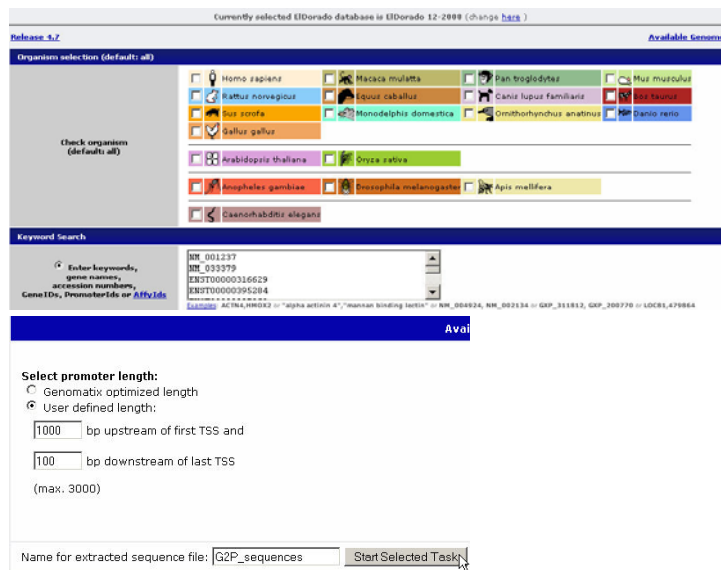
Figure 30. Overview of parameters for Gene2promotor

Arabidopsis thaliana was selected among the organisms, genes name uploaded and the promoter region was defined as 601 base pairs of the promoter regions: 500 bp upstream of and 100 bp into the transcription start site.

The promoter region was defined as 601 base pairs of the promoter regions: 500 base pairs upstream of and 100 base pairs into the transcription start site, for each gene (Figure 30). The promoters of input transcripts were displayed in the next step and saved for the subsequent analysis.

5.2.2 MatInspector

The 601 base pair sequences obtained from the Gene2promotor program were then used as the target sequences for putative transcription factor recognition site identification using the Genomatix MatInspector Version 4.3 program. This program gives all physical TF binding sites in a given sequence. The matrices in the MatInspector library are derived from single publications. In contrast to other programs, the library is not representing all literature regarding a single TFBS but rather the best of current knowledge in terms of specificity and sensitivity. Thus, putatively erroneous binding sites are not represented. Moreover, by using an optimized thresholds and comparative analysis, MatInspector can scan sequences of unlimited length for pattern matches and produces concise results avoiding redundant and false-positive matches. The optimized thresholds are obtained using a matrix threshold for each individual matrix in the library. Without this approach, matches to a long and highly conserved matrix would have a lower probability to reach any fixed threshold, as compared with matches to short, less conserved matrices.

The parameters used to analyse the 601 bp sequences with MatInspector were the standard 0.75 core similarity and the optimized matrix similarity (Quandt et al., 1995). The "core sequence" of a matrix is defined as the highest conserved positions of the matrix. The

maximum core similarity of 1.0 is only reached when the highest conserved bases of a matrix match exactly in the sequence. So, only matches that contain the "core sequence" of the matrix with a score higher than the core similarity will be listed in the output file.

As control genes, 120 genes were randomly selected from the Arabidopsis genome and analysed using the same parameters. The MatInspector analyses showed a high number of putative TFBSs in the promoter of the NO-regulated genes (Fig. 31).
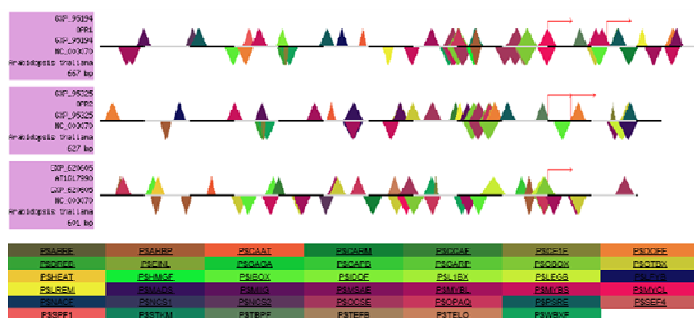
Figure 31. Example of MatInspesctor output file
Common Transcription Factor Binding Sites in three genes overexpressed in NO-treated Arabidopsis cell cultures. Different colours denote different transcription factor families.

In the table 4 all TFBS are listed, which were common to at least 25% of the analysed promoters. The given values represent the percentage of promoters, in which a match to the matrix family is found with optimized matrix similarity. The detailed and complete results are given online http://jxb.oxfordjournals.org/ cgi/content/full/erm345/DC1.

Table 4. Frequency of occurrence of different TFBS in the promoter region of NO-regulated genes

The promoter regions of the different groups of NO-regulated genes were screened for common transcription factor binding sites using the Genomatix program tools. Promoter regions of 120 randomly picked Arabidopsis genes were used to determine the unspecified distribution of the transcription binding sites (control). Transcription factor binding sites occurring at least 20% more often in the promoter regions of the NO-regulated genes compared to the control are highlighted in red.

TRANSCRIPTION FACTOR	UP-REGULATED GENES			DOWN-REGULATED GENES	CONTROL
	Cell cultures and plants	Plants	Cell cultures	Cell cultures	Randomly selected genes
WRKY	50%	**71%**	49%	42%	39%
GBOX	**85%**	70%	**90%**	65%	53%
OCSE	**82%**	76%	**82%**	61%	62%
TBPF	75%	**82%**	**82%**	**88%**	62%

L1BX	**75%**	61%	58%	65%	52%
MYCL	53%	47%	**66%**	38%	35%
MIIG	35%	35%	33%	**57%**	27%
GAGA	21%	37%	31%	42%	26%
GAPB	32%	44%	33%	65%	46%
HMGF	57%	51%	39%	50%	40%
OPAQ	75%	69%	82%	73%	66%
AHBP	92%	91%	92%	100%	90%
CCAF	57%	65%	45%	53%	63%
DOFF	71%	89%	86%	84%	82%
GTBX	92%	98%	98%	96%	95%
HEAT	46%	35%	41%	34%	47%
IBOX	60%	77%	76%	73%	76%
IDDF	42%	40%	45%	26%	42%
LREM	57%	65%	74%	73%	67%
MADS	85%	83%	84%	92%	82%
MSAE	42%	46%	45%	38%	47%
MYBL	100%	92%	88%	88%	94%
MYBS	60%	68%	56%	57%	56%
NCS1	57%	70%	62%	46%	63%
NCS2	46%	41%	49%	46%	43%
PSRE	32%	50%	47%	23%	38%
SPF1	35%	55%	56%	65%	51%
STKM	32%	47%	45%	30%	43%
CAAT	39%	53%	54%	44%	52%

Most of the TFBSs were found to occur with the same frequency as the 120 control genes, e. g. MADS-, OPAQ-, AHBP-, IBOX-elements. However, seven families of TFBSs occurred at least 20% more often in the promoter regions of the analyzed groups of genes in comparison to the promoter regions of the control genes. GBOX-, OCSE-, and L1BX-elements were found enriched in genes up-regulated in both cell culture and plant experiments. Moreover, GBOX- and OCSE-elements, together with TBPF and MYCL, were highly present in promoters of up-regulated cell culture genes. In genes induced in plants only WRKY and TBPF binding sites

were enriched in their promoters. In the down-regulated genes of cell cultures an increased occurrence of TBPF- and MIIG-elements was observed. In figure 32 putative GBOX- and WRKY binding sites in the promoter region of NO-induced Arabidopsis genes are illustrated.

5.3   COMMON TFBS MODULES

Co-regulation of genes usually depends on sets of transcription factors rather than individual factors alone. Regulatory sequence elements are often organized into defined frameworks of two or more transcription factor binding sites and clusters of such motifs. Interestingly, in the microarray analysis, several genes of the JA biosynthetic pathway were found up-regulated after NO-treatment: all the three 12-oxophytodienoate reductases (OPR1, OPR2, OPR3) and two lipoxygenases (LOX3 and a putative lipoxygenase protein).
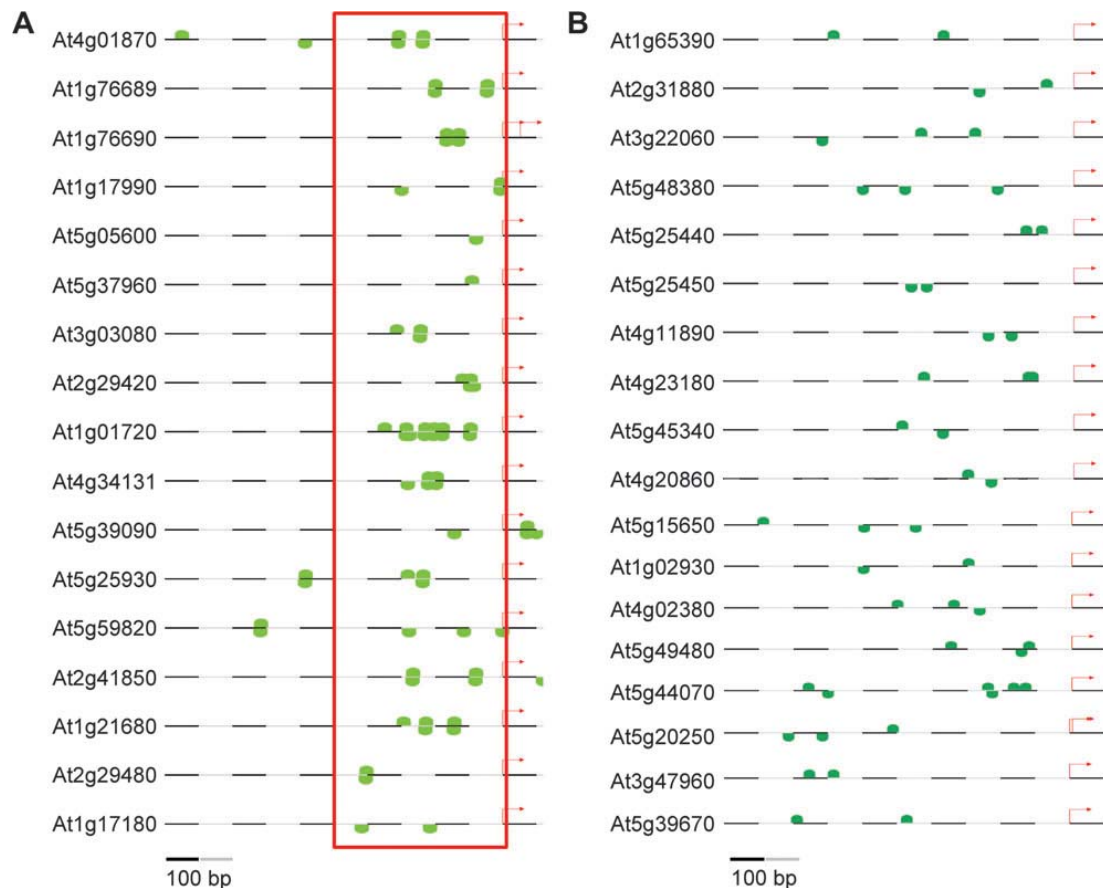
Figure 32. Illustration of putative TFBS in the promoter regions of NO-induced Arabidopsis genes

For each gene the promoter region 500bp upstream and 100bp downstream from the putative transcription start site (arrow) is shown. The position of significant binding sites for GBOX transcription factors (A) and WRKY proteins (B) are indicated. Gene, which were up-regulated in almost all experiments are enriched in GBOX-elements (A), whereas genes induced in plant experiments only were charged with multiple WRKY-elements (B).

To identify common TFBS modules in the promoter regions of the JA biosynthetic pathway genes the Frameworker "tool" of the Genomatix program was used. The first step in the search for common frameworks in multiple promoter regions was the selection of the matrix library. A matrix is a description of a TF binding site that takes into account how well conserved each position in the sequence is. Generally, TF binding sites are phylogenetically well conserved, which means that they can be divided into relatively large phylogenetic groups. For the analysis of Arabidopsis promoters the "Plant matrix library" was selected (Figure 33).

Figure 33.
Frameworker parameters
Screen showing several options for FrameWorker. This program allows the identification of common TFBS modules in the promoter regions of given genes.

Frameworker can analyse all possible combinations of alternative promoters of the input genes. In this way, it avoids comparing alternative promoters of the same gene with one another. After selecting the library, the following screen gave several options for FrameWorker parameters (Figure 33). The "quorum constraint" determines the lower limit of loci within the input set that has to contain the common framework and was set up to 27%. Moreover there are 3 "distance constraints". The first sets the maximum difference of the distances between elements and it was set up to 25bp. The other two distance constraints set the minimum and maximum distance between elements and were left at the default values. The output was an overview of the results for each of the promoter combinations that were possible. Two modules common to three genes each and consisting of four TFBS-elements (Figure 34) were identified. One is present in the promoter region of LOX3, OPR1

and of a putative OPR, and is formed by OPAQ, OCSE, GBOX and MYBL elements (Figure 34A). The second module is present in LOX3, OPR3 and a putative LOX gene, and is composed of MADS, GBOX, MYBL (Figure 34B).
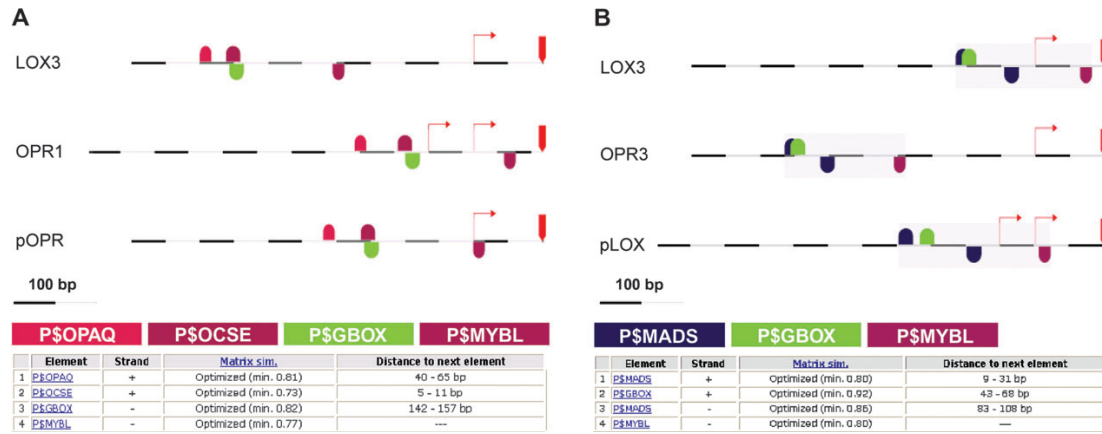
Figure 34. Illustration of common framework of elements from the promoter region of several genes of the JA biosynthetic pathway

Genomatix program Frameworker was used to search for common frameworks between the promoter regions of the JA biosynthetic pathway genes. A, 4-element module present in the promoter region of LOX3 (At1g17420), OPR1 (At1g76680) and of a putative OPR (At1g17990). It's composed by OPAQ, OCSE, GBOX and MYBL elements. B, 4-element module present in LOX3 (At1g17420), OPR3 (At2g06050) and a putative LOX gene (At1g72520), and is composed by MADS, GBOX, MYBL.

6 Discussion

NO is an important signalling molecule, which fulfils many different physiological functions in plants. Gene expression in response to NO was analyzed in several laboratories, where an induction of several pathogenesis-related proteins and an array of anti-oxidant genes encoding peroxidases, glutathione S-transferases, protein kinases and transcription factors could be demonstrated. Unfortunately, results from these high-throughput methods do not immediately yield information about transcription control or regulatory networks. These approaches observe dynamic changes in transcripts without offering any explanation on how this is all orchestrated by the genome and its interactions with environmental conditions. Nevertheless, such data provide an excellent launch pad for new tools and strategies to elucidate underlying molecular mechanisms. In the last years, the use of whole genome transcript analyses to identify common transcription factor binding site (TFBS) and promoter modules in the promoter region of co-regulated genes has been rapidly becoming a widespread approach to understand the regulation of physiological processes. These new approach was used in this work to analyze the whole genome microarray data obtained by Huang Xi, to search for common TFBS and promoter modules in the promoter region of NO-regulated genes.

Using the Genomatix software package, it was possible to analyse the promoter region of NO-modulated genes and to identify common TFBS. Among these GBOX-, OCSE-, and L1BX-elements were found enriched in genes up-regulated in both cell culture and plant experiments. Moreover, GBOX- and OCSE-elements, together with TBPF and MYCL, were highly present in promoters of up-regulated cell culture genes. In genes induced in plants only WRKY and TBPF binding sites were enriched in their promoters. In the down-regulated genes of cell cultures an increased occurrence of TBPF- and MIIG-elements was observed (Table 4).

bZIP Family

In plants basic region/leucine zipper motif (bZIP) transcription factors are involved in regulation of many different physiological processes such as biotic and abiotic stress signalling, seed maturation, flowering and light signalling (Lebel et al., 1998; Hobo et al., 1999; Ratcliffe and Riechmann, 2002). The bZIP transcription factors contain a DNA binding

motif and a leucine zipper domain, which is responsible for dimerization (Ellenberger et al., 1992; Izawa et al., 1993; Metallo and Schepartz, 1997; Choi et al., 2000). The core motif for DNA-binding is ACGT. However, using recombinant bZIP proteins it has been demonstrated that neighboring nucleotides affect binding affinity. Dependent on the nucleotide flanking the 3´-site of the motif three different types of ACGT elements have been defined: G-box (CACGTG), C-box (GACGTG), and A-box (TACGTA). bZIP transcription factors seem to play a pivotal role in the regulation of plant physiology, since Arabidopsis has about four times as many bZIP encoding genes as yeast, worm, and human (Riechmann et al., 2000). The bZIP family of the G-box binding factors has been implicated in the expression of a number of genes during pathogen attack (Kim et al., 1992). Interestingly, in almost all promoters of the genes up-regulated in plant and cell culture treated with NO, GBOX-elements were located within the first 250bp upstream of the putative transcription start (Figure 32A).

Another class of bZIP binding elements implicated in the plant defence response is formed by octopine synthase (ocs). In Arabidopsis, ocs element-like sequences (OCSE) are important for the expression of specific glutathione S-transferase (GST) and pathogenesis-related genes such as the GST6 and the PR1 genes (Lebel et al., 1998; Chen and Singh, 1999). This relation between ocs elements and plant defence responses was supported by the discovery that Arabidopsis TGA/ocs element binding factors (OBF) interact with NPR1, a key component in the salicylic acid defence signalling pathway (Zhou et al., 2000). Moreover there are several members of the TGA/OBF family, which plays a role in xenobiotic stress responses and development (Johnson et al., 2001).

Opaque-2 like transcriptional activators are also a well characterized family of plant bZIPs with an extended leucine zipper with up to nine heptad repeats. Opaque-2 and closely related genes seems to play a role in the regulation of seed storage protein production, whereas other members such as CPFR2 and G/HBF-1 might be involved in responses to environmental or pathogen challenge (Dröge-Laser et al., 1997; Lara et al., 2003).

WRKY Family

Similar to bZIP proteins WRKY family members are involved in the regulation of various physiological processes, including pathogen defence, senescence and trichome development (Robatzek and Somssich, 2001; Johnson et al., 2002; Dong et al., 2003). Their DNA-binding domain (WRKY domain) comprises approximately 60 amino acids, but the overall structures of WRKY proteins are highly divergent and can be categorized into distinct groups, which might reflect their different functions (Eulgem et al., 2000). Additional domains of WRKYs are restricted to subgroups of this family and include e. g. conserved regions of nuclear localization signals, calmodulin binding sites, or putative leucine zippers (Cormack et al.

2002; Sun et al., 2003; Park et al., 2005). Multiple studies have demonstrated the ability of WRKYs to bind the W box elements (TTGACC/T) (Rushton et al., 2002; Yamasaki et al., 2005), which is found in the promoters of many plant defence genes (Maleck et al., 2000; Chen et al., 2002). W box or W box-like sequences often occur in clusters within promoters, suggesting a possible synergistic action with other WRKY proteins and or other classes of transcription factors (Maleck et al., 2000). The transcription of WRKY genes is strongly and rapidly up-regulated in numerous plant species in response to wounding, pathogen infection or abiotic stresses, such as drought, cold adaptation or heat-induced chilling tolerance (Eulgem et al., 2000; Robatzek and Somssich, 2001; Rizhsky et al., 2002). 74 Arabidopsis WRKY genes respond to bacterial infection or SA treatment (Dong et al., 2003) and Arabidopsis WRKY70 was identified as a common regulatory component of SA- and jasmonic acid (JA)-dependent defence signalling, mediating cross-talk between these antagonistic pathways. Overexpression and antisense lines indicated that WRKY70 plays a positive role in SA signalling and functions as a negative regulator of JA-inducible genes (Li et al., 2004). Contrarily, WRKY18, WRKY40 and WRKY60 may function redundantly as negative regulators in SA-dependent pathways but play a positive role in JA-mediated pathways (Xu et al., 2006). Moreover, NPR1 is functionally linked to WRKYs during plant immune responses. Intriguingly, WRKYs control NPR1 expression on one hand, while on the other hand they seem to operate downstream from NPR1 (Yu et al., 2001; Wang et al., 2006). Additionally, WRKY transcription factors are involved in coordination of plant development and/or aging, since the expression of several Arabidopsis WRKY genes is strongly up-regulated during plant senescence (Robatzek and Somssich, 2001).

Many of the genes induced in Arabidopsis plants after NO treatment have more than one WRKY binding site in their promoter region (Figure 32B). Typically, WRKY promoters are enriched for W boxes and multiple studies have revealed interactions of WRKYs with either their own promoters or those of other family members, suggesting that these transcription factors extensively engage in auto- and cross-regulation (Eulgem et al., 1999; Turck et al., 2004).

L1BX Family

The L1 box (L1BX) was identified as essential promoter sequence for the expression of the *Arabidopsis thaliana* protodermal factor1 (PDF1). The PDF1 gene encodes a putative extracellular proline-rich protein that is exclusively expressed in the L1 layer of shoot apices and the protoderm of organ primordia. Electrophoretic mobility shift assays demonstrated that the L1-specific homeodomain protein ATML1 can bind to the L1 box sequence in vitro (Abe et al., 2001). This protein belongs to the HD-ZIP IV class homeodomain (HD) proteins

that are expressed exclusively in the L1 layer of the shoot apical meristem (Lu et al., 1996). The homeodomain consists of about 60 amino acids starting with the N-terminal arm followed by three helical regions. Helix 3 of the homeodomain binds in the major groove of DNA, with helices 1 and 2 lying outside the double helix. The N-terminal arm is located in the major groove and makes additional contacts.

Different genes codifying for the HD-ZIP IV class have been shown in the Arabidopsis genome. Intriguingly, a similar target sequence of the L1 box has been identified in the upstream region of a parsley PR2 gene (Korfhage et al., 1994). Interaction of this element with PRHP, an HD protein isolated as a binding factor to it, has been suggested to play a role in the elicitor-inducible expression of PR2 (Korfhage et al., 1994).

TBP Family

TATA box is a cis-regulatory element found in the promoter region of many eukaryotic genes. This binding site can interact with transcription factors or histones (Godde et al., 1995; Smale and Kadonaga, 2003). It is normally bound by the TATA binding protein (TBP) in the process of transcription. The segment coding for the evolutionarily conserved C-terminal DNA-binding domain is unique. Binding of TBP is the first step in the assembly of a transcription complex and is essentially the only step where the particular base sequence of the DNA is read and recognized during this process (Smale and Kadonaga, 2003).

MYCL Family

The characteristic feature of the MYCL transcription factors is their basic helix-loop-helix structure, a stretch of 40-50 amino acids contains two amphipathic alpha-helices separated by a linker region (the loop) of varying length. Basic HLH proteins have a region with conserved positive charges immediately adjacent to the first helix (Murre et al., 1994). Proteins in this group form both homodimers and heterodimers by means of interactions between the hydrophobic residues on the corresponding faces of the two helices. A dimer in which both subunits have the basic region can bind to DNA. While the bHLH domain is evolutionarily conserved, there is little sequence similarity between clades beyond the domain (Morgenstern and Atchley, 1999). The bHLHs that have been characterized function in the transcriptional regulation of genes associated with anthocyanin biosynthesis, phytochrome signalling, globulin expression, fruit dehiscence, carpel and epidermal development and circadian clock (Heisler et al., 2001; Rajani and Sundaresan, 2001; Makino et al., 2002). AtMYC2, a bHLH transcription factor, has been shown to be functioning in ABA-inducible gene expression under drought stress in plants. Moreover, as a positive regulator of ABA signalling, it plays a role in negative regulation of JA-ethylene responsive defence genes

Discussion

in Arabidopsis (Abe et al., 2003; Anderson et al., 2004; Boter et al., 2004; Lorenzo et al., 2004).

MYB Family

The myb domain of vertebrates consists of three imperfect tandem repeats (R1, R2, R3), each forming a helix-turn-helix structure of about 53 amino acids. Three regularly spaced tryptophan residues, which form a tryptophan cluster in the three-dimensional helix-turn-helix structure, are characteristic of a MYB repeat. Myb proteins usually have only one (1R) or two imperfect tandem repeats (R2, R3). MYB genes containing two repeats constitute the largest MYB gene family in plants. An important function for R2R3-type MYB factors is the control of development and determination of cell fate and identity (Oppenheimer et al., 1991; Lee and Schiefelbein, 1999); some are activated in plants in response to environmental factors and hormones (Iturriaga et al., 1996; Hoeren et al., 1998). Most members of the family seem to be involved in control of secondary metabolism or response to secondary metabolites such as flavonoid and phenylpropanoid metabolism and the anthocyanin pathway (Logemann et al., 1995; Moyano et al., 1996; Grotewold et al., 1998). Moreover, MYB factors play a role in the plant defence reactions. NtMYB2 is involved in the stress response of the retrotransposon and defence-related genes. Overexpression of NtMYB2 cDNA in transgenic tobacco plants induced expression of Tto1 and a phenylalanine ammonia lyase, a gene involved in the defence response to plant development and in response to light, pathogen ingress, mechanical damage and other stresses (Sugimoto et al., 2000).

MatInspector can find the potential binding sites of various activators and repressors that bind to specific DNA regulatory sequences. However, the concurrent expression of genes as observed in expression array analysis, in particular is in part orchestrated by sets of common regulatory elements. These regulatory modules can be discovered using specific library (Fig. 34) and, in a further step of investigation, used to identify additional target genes with similar regulatory properties in genomic sequence databases. In particular, the Frameworker tool of the Genomatix program was used to search for common TFBS modules in the promoter regions of the NO-modulated JA biosynthetic pathway genes. Two modules common to three genes each and consisting of four TFBS-elements were identified (Figure 34). One is present in the promoter region of LOX3, OPR1 and of a putative OPR, and is formed by OPAQ, OCSE, GBOX and MYBL elements (Figure 34A). The second module is present in LOX3, OPR3 and a putative LOX gene, and is composed of MADS, GBOX, MYBL (Figure 34B). These modules inside the promoters represent a possible explanation of the

co-expression of some genes of the JA biosynthetic pathway after the NO treatment. As already shown, a particular physiological process can induce a distinct set of genes responsible for the elevation of JA levels in plants (He et al., 2002). For example, LOX2 is required for the wound-induced synthesis of the JA in leaves (Bell et al., 1995). Furthermore, OPR1, OPR3 and LOX3 are reported to be over-expressed during leaf senescence, while OPR2 appears to be constitutively expressed through the different stages of leaf development and LOX2 down-regulated in senescence leaf (He et al., 2002). In several reports the correlation between NO and JA is discussed controversially. Huang et al. (2004) showed JA- and wounding-dependent NO production by diamino-fluoresceins (DAFs). Using a cDNA microarray made up of about 330 defence-related genes, they observed the induction of three genes involved wounding-induced JA biosynthesis (Allene oxide synthase, LOX2 and OPR3). Although NO activates genes involved in JA biosynthesis, it did not affect JA levels in Arabidopsis and showed an extremely weak or almost no accumulation of JA-dependent late defence genes (Huang et al., 2004). In Taxus cell cultures, exogenously supplied methyl jasmonate (MeJA) induced rapid production of NO and the MeJA-induced intracellular malondialdehyde (MDA), LOX and phenylalanine ammonium-lyase were all enhanced by a NO donor, but suppressed by NO inhibitors underlining the connection between NO- and JA-signalling (Wang and Wu, 2005).

In leaf senescence the role of NO and JA is still controversial. Although it was demonstrated that exogenous application of JA or of MeJA induces leaf senescence (Ueda and Kato, 1980) and that endogenous JA level in senescing leaves increased to nearly 500% of that in non-senescence leaves (He et al., 2002), the role for JA in this process remains unclear. Nitric oxide also seems to affect this phase of the plant life cycle. It's hypothesized that a stoichiometric relationship between the two gases, NO and ethylene, probably determined whether senescence took place or not (Leshem and Haramaty, 1996; Leshem and Pinchasov, 2000).

CONCLUSION

Taken together, such a bioinformatics approach is a useful tool to identify common transcription factor binding sites and promoter modules in co-regulated genes, which might be involved in establishing specific expression profiles. It should be stressed that such an analysis is complicated by the fact that co-expressed genes in an expression array experiment are not all necessarily co-regulated, as different regulation mechanisms can lead to the same expression pattern. Effects like a secondary cascade of transcription activation during the time course can divide a co-expressed cluster of genes in subsets regarding co-

regulation. For this reason a careful analysis of microarray results and a careful selection of gene clusters is a crucial step for a successful promoter analysis. However, such promoter analyses may be a fist step to provide the basis to understand regulatory networks involved in gene expression profiles.

7 Concluding Remarks

The biological activities of NO are numerous and complex. Although the importance of this molecule for many physiological reactions is demonstrated, in most cases its exact way of function is still unknown. It seems unlikely that 'specific receptors' exist for NO sensing. However, various cellular activities are modulated by NO demonstrating that cells react to this molecule. The currently available data illustrate that NO has multiple molecular targets that act as cellular 'NO sensor' and are able to activate signal cascades.

NO can control physiological processes directly by encroaching upon gene transcription (Huang et al., 2002). Until now, there are no experimental evidences for the existence of DNA elements within the promoter regions of eukaryotic genes that respond directly to NO. The bioinformatic approach was a useful tool to identify common transcription factor binding sites and promoter modules in NO co-regulated genes, providing the basis to understand regulatory networks involved in gene expression profiles. However, most of the effects of NO are based on the modulation of transcription factors. This can be achieved by acting upstream of the signalling cascade or by modulating its transcription, mRNA stability and translation (Figure 32) (Bogdan, 2001).
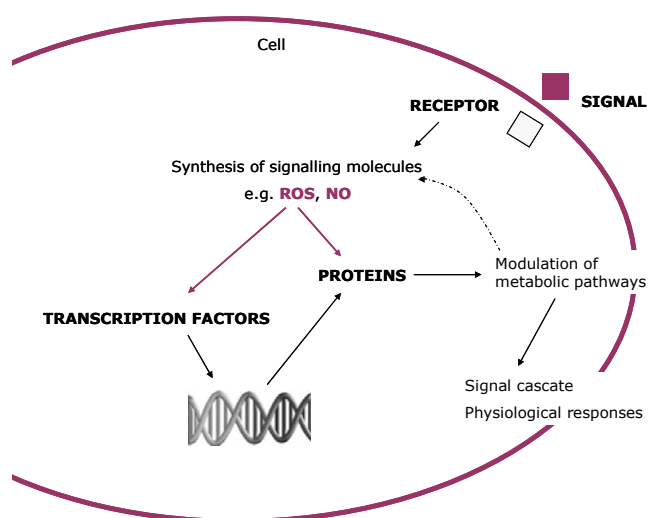
Figure 32. Transcriptional and post-translational redox-signalling NO production is induced by exogenous or endogenous signals. The produced NO can activate transcription factors directly - by acting on mRNA or protein level - or indirectly – regulating upstream signals. In both cases, the transcription factors bind to its specific NO-responsive element in the promoter regions of eukaryotic genes. Moreover, NO can affect cellular functions acting directly on essential metabolic pathway, by modulating the activity of specific enzymes.

Moreover, NO can directly influence the activity of transcription factors by modifying their affinity to transcription factor binding sites or affecting their translocation into the nucleus, e.g. by S-nitrosylation of crucial cysteine residues (Tada et al., 2008).

Upon regulation of gene expression, NO can affect cellular functions by acting directly on essential metabolic pathway. Modulating the mitochondrial KCN-sensitive respiration (dark respiration and photorespiration) *via* thiol modification, for example, causes a perturbation of the redox state of the entire cell. This induces a further accumulation of redox signal molecules (NO, ROS) with a concomitant activation of signal cascades (Figure 32). The identification of NO sensitive proteins represents a promising starting point to get insight in signalling pathways downstream of NO as well as physiological and regulatory functions of NO in plants.

8 Appendix

8.1 APPENDIX A

MALDI-TOF-TOF ON THE 110KDa BAND IN THE S-NITROSYLATED-PROTEIN

GEL (analysis was carried out by TopLab Company)

8.1.1 Mascot Search Results

Search Parameters

Type of search: MS/MS Ion Search

Enzyme: Trypsin

Fixed modifications: Carbamidomethyl (C)

Variable modifications: Oxidation (M), Oxidation (HW)

Mass values: Monoisotopic

Protein Mass: Unrestricted

Peptide Mass Tolerance: ± 100ppm

Fragment Mass Tolerance: ± 0.6Da

Max Missed Cleavages: 1

Instrument type: MALDI-TOF-TOF

Number of queries: 1

Peptide Summary Report

- gi|14596025 **Mass:** 113852 **Score:** 16 **Queries matched:** 1

  P-Protein - like protein [Arabidopsis thaliana]

Query	Observed	Mr (expt)	Mr (calc)	Delta	Miss	Score	Expect	Rank	Peptide
1	1320.800	1319.7927	1319.6662	0.1265	0	16	1.8	1	R.EYA

Proteins matching the same set of peptides:

- gi|15225249 **Mass:** 114672 **Score:** 16 **Queries matched:** 1

  glycine dehydrogenase (decarboxylating) [Arabidopsis thaliana]

- gi|15234036 **Mass:** 113822 **Score:** 16 **Queries matched:** 1

  glycine dehydrogenase (decarboxylating) [Arabidopsis thaliana]

- gi|16604476 **Mass:** 75747 **Score:** 16 **Queries matched:** 1

  AT4g33010/F26P21_130 [Arabidopsis thaliana]

- gi|18086383 **Mass:** 113841 **Score:** 16 **Queries matched:** 1

  AT4g33010/F26P21_130 [Arabidopsis thaliana]

- gi|110742034 **Mass:** 114702 **Score:** 16 **Queries matched:** 1

  putative glycine dehydrogenase [Arabidopsis thaliana]

8.1.2 ProFound - Search Result Details

List of peptides identified that match with the glycine dehydrogenase P protein.
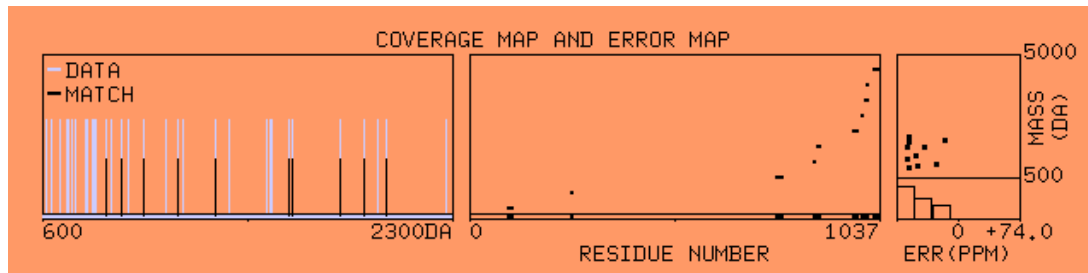
MEASURED MASS (M)	AVG/ MONO	COMPUTED MASS	ERROR (PPM)	RESIDUES START	TO	MISSED CUT	PEPTIDE SEQUENCE
863.379	M	863.429	-58	1004	1010	0	FWPTTGR
930.462	M	930.507	-48	870	876	0	HYPVLFR
1021.493	M	1021.519	-26	255	263	1	TRADGFDLK
1165.516	M	1165.588	-62	1001	1010	1	SSKFWPTTGR

Coverage map and error map of sequenced peptides on glycine dehydrogenase P protein.

8.2 APPENDIX B

MASS SPECTROMETRIC ANALYSES ON THE PARTIALLY PURIFIED P$_{AEC}$ PROTEIN (analysis was carried out in cooperation with the Helmholtz Zentrum München core facility)

- Cysteine 943
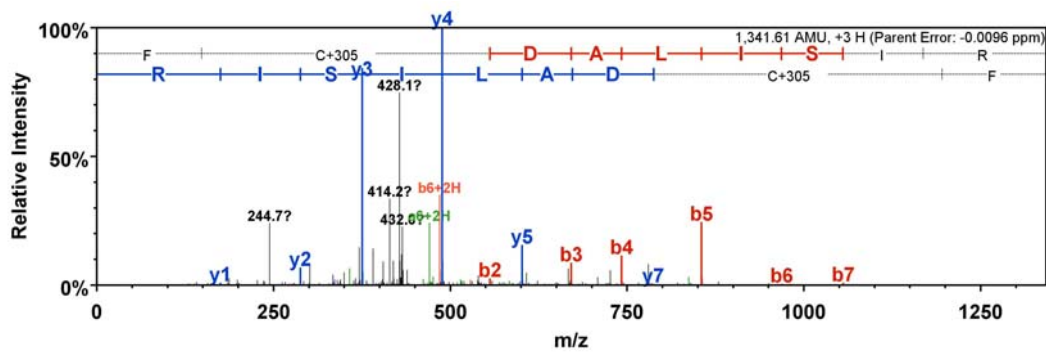
- Cysteine 98
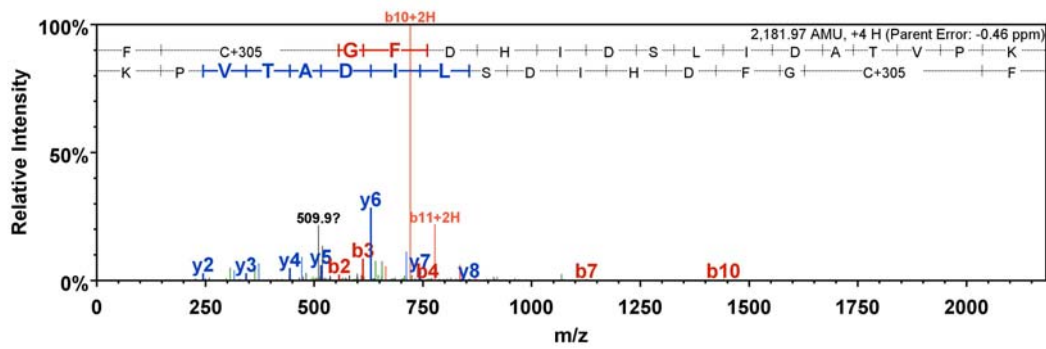
- Cysteine 777
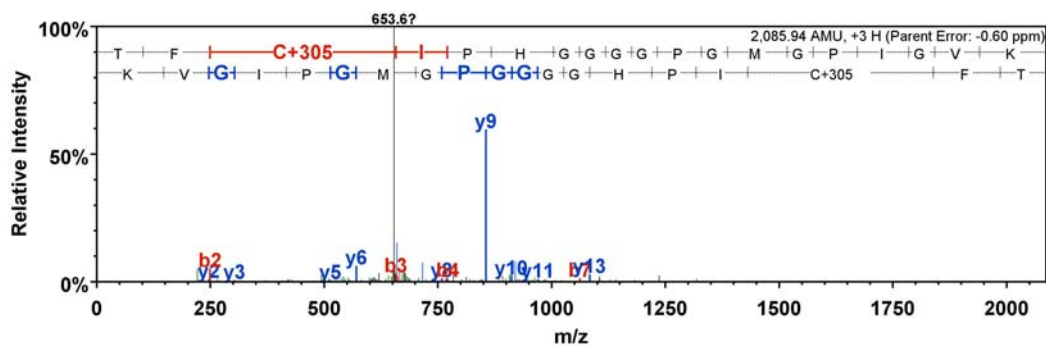
- Cysteine 402
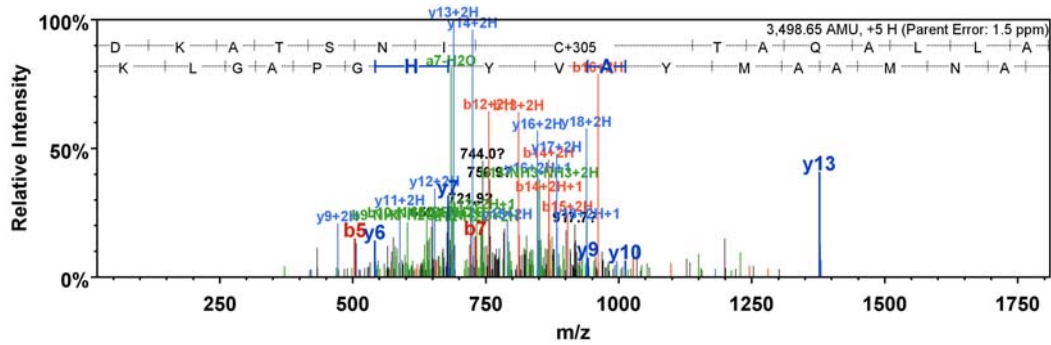
- Cysteine 463
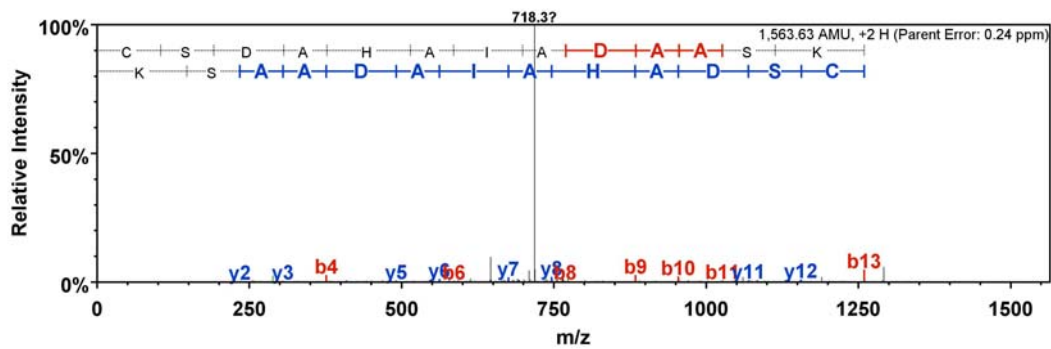
- Cysteine 1022
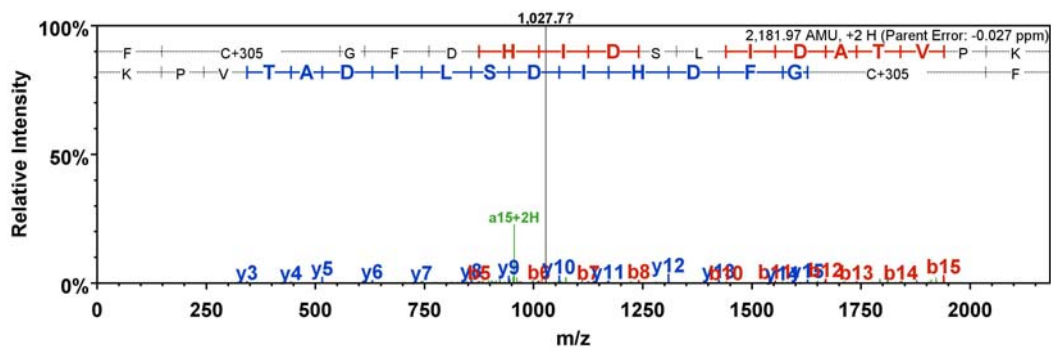
For mass spectrometric analyses partially purified P protein was digested with trypsin at 37°C for 1h, pH 6.5. Digested proteins were analyzed by online nano LC-MS/MS, with an automatic switch between MS, MS^2, and MS^3 acquisition. In the case of a resulting neutral loss in the MS^2 spectra - corresponding to the NO masses (29kDa) - the three most abundant peaks indicating the loss of NO were selected for further MS^3 fragmentation. The S-glutathionylation was detected in the MS^2 as gain of 305kDa in masses. The spectra represent the MS^3 fragmentation of the peptides containing modified cysteine (numbers near the cysteines indicate the position in the protein sequence).

8.3   APPENDIX C

GAS EXCHANGE MEASUREMENTS ON ARABIDOPSIS PLANTS

C

E. coli 4h 75µE

E. coli 4h 250µE

E. coli 4h 400uE

E.Coli 4h

$y = 0.0231x - 1.8664$

$y = 0.0232x - 1.9057$

$y = 0.0108x - 1.5488$

D

Harpin 30min 75µE

Harpin 30min 250µE

Harpin 30min 400uE

Harpin 30min

$y = 0.0115x - 1.3566$

$y = 0.0097x - 1.2472$

$y = 0.0071x - 1.3045$

E

E

Harpin 4h 400uE

Harpin 4h

$y = 0.0045x - 0.9366$

$y = 0.0039x - 0.8795$

$y = 0.0035x - 0.9416$

Chart axes: A (μmol CO$_2$ m^{-2} s^{-1}) vs Ci (μm CO$_2$ mol^{-1})

F

	Light (μE)	Average Γ (μl⁻¹ CO₂)	Average A (μmol CO₂ m⁻² s⁻¹)	Average Γ* (μl⁻¹ CO₂)	Std Deviation Γ (μl⁻¹ CO₂)	Std Deviation A (μmol CO₂ m⁻² s⁻¹)	Std Deviation Γ* (μl⁻¹ CO₂)
Untreated	75	81.02	2.22	46.05	7.67	0.08	10.82
	250	72.20	3.95		5.93	0.65	
	400	72.57	3.94		1.07	0.42	
E.coli 30min	75	148.12	1.34	30.8	27.56	0.20	2.5
	250	95.71	3.08		11.47	0.83	
	400	99.5	2.68		5.9	0.26	
E.coli 4h	75	144.35	1.68	25.80	8.46	0.43	1.25
	250	81.36	5.06		6.36	0.88	
	400	79.93	4.16		9.56	0.66	
Harpin 30min	75	191.25	1.17	4.68	19.44	0.28	3.78
	250	118.17	2.60		14.90	0.54	
	400	130.77	2.20		8.72	0.47	
Harpin 4h	75	255.73	0.45	-2.06	39.00	0.20	4.45
	250	275.84	0.46		29.85	0.73	
	400	224.38	0.53		1.14	0.11	

The photorespiration rate *in vivo* was monitor following the response of the photosynthesis (A) to intracellular CO_2 mole fraction (Ci). Five weeks old Arabidopsis plants were used in combination with an Infrared Gas Analyzer (IRGA) system (LICOR 6400, Licor Bioscience). Apparent CO_2 exchange rates (A) were measured at 6 different CO_2 concentrations (400, 300, 200, 100, 50, 400ppmol). The Ci was used to eliminate effects of boundary layer and stomata aperture (transpiration). Extrapolation to zero yields the rate of CO_2 released from the leaf, the sum of photorespiration and respiration in the light (compensation point Γ). Each point represents the mean of at least 3 independent replications. Photorespiration rate was calculated as photosynthetic CO_2 compensation point in absence of respiration in the light (Γ*). It was defined as the interception point of different curves measured at different light intensities (75, 250, 400μE). The y coordinate of this point gave the respiration in the light (-Rd). Each curve represents the mean of at least 3 independent replications. **A-E.** Calculation of Γ* in untreated, E. coli or harpin treated plants. **F.** Table summarizing average and standard deviation of Γ, A and Γ* values.

8.4 APPENDIX D

CLUSTERS OF NO REGULATED GENE IN *ARABIDOPSIS THALIANA*

8.4.1 Genes Up-Regulated in Cell Cultures and Plants

ID	NAME	A	B	C	D	E	F
AT4G01870	hypothetical protein, similar to bacterial tolB (virus, ozone)	4,255	3,931	4,208	10,26	4,878	2,057
AT1G76680	12-oxophytodienoate reductase (OPR1)	5,997	8,648	4,768	4,056	10,649	2,866
AT1G76690	12-oxophytodienoate reductase (OPR2)	3,949	8,452	4,601	2,027	11,027	2,07
AT1G17990	12-oxophytodienoate reductase, putative	5,266	10,151	4,828	4,934	6,939	1,343
AT5G05600	2-oxoglutarate-dependent dioxygenase family	6,633	3,527	6,391	9,943	4,077	1,917
AT3G11180	2-oxoglutarate-dependent dioxygenase family	2,975	2,3	3,679	6,544	4,035	1,62
AT5G37960	NADP-dependent oxidoreductase, putative (quinine oxidoreduc.)	5,654	4,488	6,59	5,083	2,986	1,25
AT3G03080	putative NADP-dependent oxidoreductase	4,476	4,013	5,666	2,893	2,602	1,165
AT2G47730	glutathione transferase, putative (GST6)	4,332	6,172	7,947	2,979	2,722	1,966
AT2G29450	Glutathione transferase (103-1A)	8,776	4,823	5,449	2,729	2,251	0,877
AT2G29420	Glutathione transferase, putative	4,588	3,594	4,421	5,334	2,888	1,591
AT2G29440	Glutathione transferase, putative	3,328	3,802	3,001	2,56	4,505	
AT3G50260	AP2 domain transcription factor, putative	6,247	3,774	3,777	3,248	2,772	
AT1G01720	NAC domain protein, putative	4,574	2,756	4,469	6,64	2,732	1,111
AT1G63840	putative RING zinc finger protein	4,435	2,932	5,03	5,412	2,038	1,406
AT4G34131	similar to glucosyltransferase -like protein	3,297	3,051	2,696	5,718	2,765	1,222
AT1G52560	chloroplast-localized small heat shock protein, putative	6,702	3,067	4,767	2,877	2,562	
AT3G44190	pyridine nucleotide-disulphide oxidoreductase family	7,5	4,097	3,616	2,681	2,006	1,072
AT5G39090	acyltransferase -like protein	4,312	2,791	3,53	2,699	2,031	1,343
AT2G06050	12-oxophytodienoate reductase (OPR3)(DDE1)	1,891	10,585	4,85	9,554	9,366	1,311
AT4G37370	cytochrome p450 family	8,474	4,091	5,391	4,418		0,902
AT5G25930	receptor-like protein kinase - like	7,727	8,043	4,723	4,477		1,02
AT5G59820	zinc finger protein Zat12	8,052	2,549	2,259	4,844	1,569	1,355

AT2G41850	polygalacturonase, putative	**3,539**	**4,277**	**6,989**	**2,786**		
AT1G21680	probable tolB protein precursor	**7,018**	**5,664**	**8,771**	**2,615**		1,362
AT2G29460	Glutathione transferase, putative	**2,724**	**2,645**	**2,621**	**3,478**		
AT2G29480	Glutathione transferase, putative	**2,839**	**2,946**	**2,923**	**3,149**		
AT1G17180	Glutathione transferase, putative	**3,885**	**3,4**		**5,693**	**31,25**	

8.4.2 Genes Up-Regulated in Cell Cultures

ID	NAME	A	B	C	D	E	F
AT4G37340	Cytochrome P450 monooxygenase, putative	**7,294**	**5,076**	**3,966**	1,771		
AT3G28740	Cytochrome p450 family	**26,282**	**8,929**	**6,806**			
AT3G14660	Cytochrome P450, putative	**8,512**	**9,434**	**8,605**	1,668		
AT2G46950	Cytochrome p450, putative	**3,144**	**3,409**	**3,116**	1,553		
AT4G37360	Cytochrome p450 family	**2,56**	**5,525**	**7,576**			
AT3G14630	Cytochrome P450, putative	**4,301**	**2,525**	**6,986**	0,915	0,637	1,046
AT1G17170	Glutathione transferase, putative	**4,677**	**4,174**	**5,713**	1,299		
AT2G29470	Glutathione transferase, putative	**8,321**	**3,658**	**4,798**	1,001		
AT1G78320	Glutathione transferase, putative	**4,253**	**3,474**	**4,571**	1,215	0,913	
AT1G78370	Glutathione transferase, putative	**3,966**	**3,525**	**5,336**	0,909	0,996	0,701
AT1G78380	Glutathione transferase, putative	**3,798**	**3,903**	**4,728**	1,252	1,26	1,189
AT5G63530	copper chaperone (CCH)-related	**3,419**	**3,214**	**3,346**	0,645	0,861	0,995
AT1G71050	copper chaperone (CCH)-related	**3,178**	**2,505**	**4,368**	1,41		
AT3G46230	heat shock protein 17	**6,056**	**3,486**	**6,081**	0,856		
AT1G59860	heat shock protein, putative	**6,603**	**5,259**	**4,012**	0,979	0,944	1,136
AT2G19310	putative small heat shock protein	**6,406**	**4,27**	**4,77**	0,826	0,877	1,06
AT2G29500	putative small heat shock protein	**3,665**	**2,515**	**3,064**	1,644	1,56	1,016
AT1G10140	expressed protein	**10,135**	**4**	**8,216**	1,301		1,202
AT1G23710	expressed protein	**4,787**	**3,615**	**4,059**	1,628		0,883
AT2G36950	expressed protein	**5,394**	**6,107**	**8,197**	1,239		1,131
AT1G69490	expressed protein	**9,585**	**5,025**	**6,086**	0,963	0,662	**2,151**
AT1G79710	hypothetical protein	**3,421**	**4,082**	**3,401**	1,414		1,093
AT4G30490	putative protein	**4,236**	**3,604**	**5,822**	1,694		0,799
AT1G15380	expressed protein	**3,634**	**3,076**	**7,121**	0,669		1,122
AT5G14470	putative protein	**7,749**	**2,523**	**3,042**			

ID	NAME	A	B	C	D	E	F
AT5G07860	N-hydroxycinnamoyl benzoyltransferase-like protein	**6,076**	**5,625**	**3,269**	0,856		
AT5G07870	N-hydroxycinnamoyl benzoyltransferase-like protein	**15,816**	**10,757**	**3,278**	1,329		
AT3G46080	zinc finger -like protein	**6,136**	**4,632**	**4,738**	1,764		1,139
AT2G47890	CONSTANS B-box zinc finger family protein	**6,089**	**5,341**	**4,583**	**0,473**		0,985
AT1G55530	putative zinc finger protein	**4,292**	**3,401**	**3,082**	0,931		1,441
AT3G27620	alternative oxidase 1c precursor	**4,918**	**3,818**	**3,99**	**2,184**	1,345	1,324
AT3G22370	alternative oxidase 1a precursor	**5,963**	**3,842**	**4,493**	1,737	1,989	1,34
AT1G75280	isoflavone reductase homolog P3	**3,104**	**5,208**	**3,711**	1,554	1,274	1,091
AT1G19540	isoflavone reductase homolog P3, putative	**3,188**	**4,902**	**3,683**	1,28	1,432	1,071
AT3G25250	protein kinase, putative	**8,386**	**3,563**	**3,467**	0,73		1,007
AT1G05100	putative NPK1-related MAP kinase	**23,824**	**7,092**	**4,537**			
AT4G28350	receptor protein kinase like protein	**9,88**	**3,205**	**2,96**			1,024
AT2G47520	putative AP2 domain transcription factor	**11,086**	**3,281**	**4,065**			
AT4G36040	DnaJ-like protein	**10,131**	**5,682**	**6,386**	1,802	1,702	1,243
AT3G02100	putative UDP-glucosyl transferase	**6,905**	**3,064**	**4,343**	1,057	1,446	0,995
AT1G14130	2-oxoglutarate-dependent dioxygenase, putative	**5,863**	**3,814**	**5,074**	1,141		
AT1G76080	chloroplast drought-induced stress protein, putative	**4,932**	**3,339**	**5,711**	0,837	0,992	0,981
AT3G15500	putative jasmonic acid regulatory protein	**4,301**	**3,571**	**7,103**	0,806		
AT3G10740	glycosyl hydrolase family 51	**3,751**	**4,651**	**4,302**	1,059	0,553	0,749
AT5G25880	malate dehydrogenase - like protein	**3,687**	**4,167**	**3,129**			1,172
AT5G64250	2-nitropropane dioxygenase-like protein	**3,665**	**3,188**	**3,932**	1,04	0,959	1,06
AT2G41850	polygalacturonase, putative	**3,539**	**4,277**	**6,989**	**2,786**		
AT1G30400	glutathione S-conjugate ABC transporter (AtMRP1)	**3,208**	**2,56**	**3,935**	1,491	0,908	1,025
AT1G08920	putative sugar transport protein, ERD6	**3,406**	**3,727**	**5,442**	1,439	0,981	1,031
AT1G68620	putative cell death associated protein	**14,231**	**3,269**	**4,475**			
AT1G73260	putative trypsin inhibitor	**3,116**	**3,281**	**4,561**	0,859		

8.4.3 Genes Up-Regulated in Plants

ID	NAME	A	B	C	D	E	F
AT1G65390	disease resistance protein (TIR class), putative				**11,519**	**8,392**	
AT1G56510	disease resistance protein (TIR-NBS-LRR class), putative				**3,872**	**2,836**	

AT1G09970	leucine-rich repeat transmembrane protein kinase, putative	1,202	1,291	1,265	**4,387**	**4,844**	1,589
AT2G31880	leucine-rich repeat transmembrane protein kinase, putative	0,946		1,125	**3,226**	**2,978**	0,873
AT2G34930	disease resistance protein family	**0,376**	0,721	**0,457**	**6,475**	**7,353**	**2,254**
AT3G22060	receptor kinase common family, putative	1,431			**3,651**	**2,504**	1,46
AT4G08850	receptor protein kinase-like protein	0,737		0,642	**3,425**	**3,52**	0,956
AT5G48380	receptor-like protein kinase	1,064	0,985	1,364	**16,703**	**3,398**	1,257
AT5G25440	putative protein kinase	0,937	0,889	0,757	**6,267**	**3,821**	1,125
AT4G11890	protein kinase - like protein	1,299			**3,649**	**2,696**	1,345
AT4G23180	serine/threonine kinase -like protein				**3,847**	**3,215**	0,579
AT5G66210	calcium-dependent protein kinase	0,975		1,203	**9,422**	**6,49**	0,684
AT5G45340	Cytochrome p450 family	**0,227**			**7,226**	**3,751**	
AT4G20830	FAD-linked oxidoreductase family	1,798	1,467	**2,085**	**6,477**	**4,66**	1,308
AT4G20840	FAD-linked oxidoreductase family	1,878	1,246	**2,248**	**3,115**	**4,161**	1,172
AT5G44360	FAD-linked oxidoreductase family	1,462	2,572	1,847	**7,852**	**4,058**	
AT4G20860	FAD-linked oxidoreductase family	1,376	**2,385**	1,535	**4,333**	**3,252**	1,251
AT4G23810	WRKY family transcription factor				**7,181**	**2,367**	0,952
AT1G80840	WRKY family transcription factor	0,978			**5,409**	**5,092**	
AT2G30250	WRKY family transcription factor	**2,182**	1,761	1,792	**4,436**	**3,361**	1,215
AT2G23320	WRKY family transcription factor	1,152	1,113	1,152	**4,178**	**2,466**	0,717
AT3G11820	syntaxin SYP121	1,276	1,081	1,312	**3,775**	**2,901**	1,017
AT3G52400	syntaxin SYP122	1,512	1,543	1,677	**5,364**	**3,329**	1,053
AT5G61210	syntaxin SNAP33	1,522		1,888	**3,43**	**3,357**	0,983
AT1G17420	Lipoxygenase			4,049	**10,851**	**4,97**	1,084
AT1G72520	putative lipoxygenase	1,338	1,052	1,532	**4,302**	**2,855**	1,141
AT2G22500	mitochondrial carrier protein family	0,517		1,483	**5,082**	**3,262**	0,815
AT5G27520	mitochondrial carrier protein family	1,125	1,014	1,362	**5,333**	**3,067**	1,194
AT3G02230	reversibly glycosylated polypeptide-1	**0,341**	0,586	0,516	**3,265**	**2,658**	1,502
AT5G15650	reversibly glycosylated polypeptide-3	**0,455**	0,734	0,709	**3,104**	**3,458**	1,555
AT1G02930	glutathione transferase, putative	1,865		**2,062**	**4,099**	**4,506**	**2,129**
AT1G02920	glutathione transferase, putative	1,842	1,751	**2,634**	**3,626**	**4,017**	1,911
AT2G17840	putative senescence-associated protein 12	1,221	0,917	1,758	**7,883**	**3,388**	1,155
AT5G48070	xyloglucan endotransglycosylase, putative	**0,376**	0,695	**0,338**	**7,25**	**3,947**	
AT4G02380	late embryogenesis abundant protein-related	1,852	0,869	0,592	**7,107**	**5,32**	1,332
AT5G49480	NaCl-inducible Ca2+-binding protein-like; calmodulin-like	**4,563**	**2,153**	1,837	**6,767**	**5,675**	1,402

AT5G54170	membrane related protein-like	2,027		1,711	6,59	3,267	1,088
AT4G21870	heat shock protein - like				6,522	3,545	
AT2G38240	2-oxoglutarate-dependent dioxygenase family				6,442		3,641
AT3G51660	Macrophage migration inhibitory factor (MIF) family	1,996		1,829	6,283	4,514	0,676
AT1G08930	zinc finger protein ATZF1, putative	1,007	0,882	0,819	5,624	6,938	1,391
AT2G41430	ERD15 protein	1,136	0,851	1,13	5,232	5,478	0,959
AT1G51780	auxin conjugate hydrolase (ILL5)	0,84	0,86	1,13	5,173	2,664	1,631
AT1G71697	choline kinase, putative	1,576	1,189	1,391	5,168	3,581	1,084
AT5G47240	mutT domain protein-like	0,869			5,006	2,813	1,154
AT4G12720	growth factor like protein	1,787	1,065	0,757	4,944	4,863	1,25
AT4G34710	arginine decarboxylase SPE2	1,204	1,201	1,835	4,927	2,688	2,119
AT5G45750	GTP-binding protein, putative	0,435		0,93	4,559	3,236	0,945
AT2G46370	putative auxin-responsive protein	0,611	1,263	1,456	4,524	2,881	1,213
AT2G24850	putative tyrosine aminotransferase				4,468	2,783	1,89
AT5G44070	phytochelatin synthase (gb|AAD41794.1)	0,728			4,579	2,763	1,281
AT5G20230	blue copper binding protein	0,982	1,586	1,685	11,247	4,04	1,945
AT4G21990	PRH26 protein	4,104	2,963	1,927	4,668	4,704	0,921
AT1G51760	IAA-Ala hydrolase (IAR3)	0,838	0,831	1,202	4,404	3,41	1,652
AT5G07440	glutamate dehydrogenase 2	1,432	1,533	2,682	4,374	2,576	1,555
AT5G26030	ferrochelatase-I	1,028	0,915	1,133	4,356	3,114	1,08
AT1G18210	calcium-binding protein, putative	1,108	0,69	1,013	4,181	6,066	2,163
AT1G76160	multi-copper oxidase type I family protein	0,423	0,727	0,412	3,145	4,173	1,011
AT2G39210	nodulin-like protein				3,134	3,241	1,374
AT4G22590	trehalose-6-phosphate phosphatase - like protein	0,7	0,824	1,31	3,12	2,703	0,94
AT1G11260	glucose transporter	1,042	1,813	1,841	4,118	3,661	0,809
AT1G71880	sucrose transport protein SUC1	0,812			4,116	3,965	1,819
AT4G36010	thaumatin-like protein	0,827	1,142	1,813	4,087	3,236	1,103
AT5G20250	glycosyl hydrolase family 36	1,72	1,75	2,05	4,063	3,817	1,865
AT3G47960	putative peptide transporter	1,027	1,157	1,368	4,016	2,962	0,979
AT3G16530	putative lectin	1,295			3,813	3,839	2,704
AT3G55430	glycosyl hydrolase family 17 (beta-1,3-glucanase)	1,075	0,949	1,585	3,757	2,584	1,042
AT5G06860	polygalacturonase inhibiting protein (PGIP1)	1,167	1,122	1,107	3,725	2,667	1,46
AT2G46140	putative desiccation related protein	0,933	1,023	1,131	3,718	2,665	1,376
AT4G24960	abscisic acid-induced - like protein	0,67	1,245	1,242	3,587	2,578	1,435

AT3G51450	Strictosidine synthase-related	0,614		1,038	**3,541**	**3,13**	1,895
AT1G22400	UDP-glucose glucosyltransferase, putative	1,079	0,913	**2,526**	**3,519**	**2,83**	1,084
AT2G38290	putative ammonium transporter	1,36		1,925	**3,496**	**2,935**	1,547
AT5G39670	calcium-binding protein - like	0,87		**0,431**	**3,414**	**2,593**	1,108
AT3G01290	expressed protein	1,339	1,022	1,041	**5,421**	**5,757**	1,048
AT5G56980	putative protein	1,431	1,364	**2,291**	**5,724**	**4,127**	0,734
AT1G20450	expressed protein	1,115	0,878	1,223	**3,938**	**3,229**	0,997
AT1G55450	expressed protein	**3,61**			**4,1**	**3,362**	0,633
AT3G45970	putative protein	**0,334**	0,641	**0,262**	**4,298**	**4,96**	0,792
AT5G63790	putative protein	**2,289**	**2,448**	1,58	**6,549**	**4,51**	1,389
AT1G19380	hypothetical protein	**0,216**	0,574	**0,349**	**17,503**	**7,892**	1,435
AT5G64750	putative protein	1,917	1,404	**2,678**	**13,232**	**8,065**	
AT1G65400	hypothetical protein				**4,907**	**3,212**	0,937
AT4G21570	putative protein	0,739	0,859	0,899	**4,833**	**2,925**	1,232
AT1G09070	expressed protein	1,819	1,538	**2,722**	**4,608**	**3,937**	1,097
AT1G32460	expressed protein	**2,108**	1,297	**2,016**	**4,597**	**2,635**	1,243
AT4G24160	putative protein	**2,849**	**2,845**	**2,113**	**4,559**	**3,708**	1,009
AT3G19010	expressed protein				**3,649**	**3,068**	0,841
AT4G18010	putative protein	0,904			**3,66**	**3,193**	
AT4G30530	putative protein	1,055	1,215	1,096	**3,312**	**2,81**	1,026
AT1G20510	4-coumarate--CoA ligase family protein	0,619	1,597		**3,304**	**3,157**	0,926
AT1G01470	late embryogenesis abundant protein, putative	1,07	1,006	1,132	**3,303**	**2,848**	1,413
AT1G69840	unknown protein; band 7 family protein	0,958	0,868	1,021	**3,206**	**3,585**	1,184

8.4.4 Genes Down-Regulated in Cell Cultures

ID	NAME	A	B	C	D	E	F
AT1G41830	pectinesterase (pectin methylesterase), putative	**0,172**	**0,473**	**0,315**	0,728	1,103	0,696
AT5G66920	pectinesterase (pectin methylesterase) family	**0,205**	**0,511**	**0,234**			
AT2G36880	putative s-adenosylmethionine synthetase 2	**0,314**	0,433	**0,265**	1,229	1,477	1,227
AT3G17390	putative s-adenosylmethionine synthetase 3	**0,215**	0,55	**0,18**	**2,576**	**3,965**	0,952
AT5G17920	5-methyltetrahydropteroyltriglutamate-homocysteine S-methyltransferase	**0,261**	0,595	**0,293**	0,965	1,375	1,13
AT4G13930	hydroxymethyltransferase	**0,207**	0,537	**0,296**	1,11	1,422	0,942
AT3G23730	xyloglucan endotransglycosylase, putative	**0,112**	0,582	**0,275**	1,022		

Gene	Description	A	B	C	D	E	F
AT2G34080	cysteine proteinase	0,169	0,499	0,292	0,958		
AT4G10270	probable wound-induced protein	0,228	0,252	0,335	0,705		1,008
AT3G54810	GATA zinc finger protein	0,205	0,31	0,392	0,802		0,84
AT4G38400	putative pollen allergen	0,21	0,618	0,244	1,744	4,721	0,827
AT1G01300	chloroplast nucleoid DNA binding protein, putative	0,139	0,453	0,278	1,502	1,56	1,167
AT1G04430	ankyrin-like protein	0,261	0,584	0,244	1,268	1,865	0,839
AT3G54400	nucleoid DNA-binding - like protein	0,319	0,734	0,251	1,366	0,817	1,147
AT5G47370	homeobox-leucine zipper protein-like	0,223		0,297	1,235	0,854	1,119
AT4G27260	GH3 like protein	0,312	0,628	0,218			
AT1G15210	ABC transporter family protein	0,216		0,297	2,012		
AT2G14960	putative auxin-regulated protein	0,262	0,534	0,236	1,775		
AT4G14980	CHP-rich zinc finger protein, putative		0,29	0,326			
AT3G29970	gene_id:K17E7.15~unknown protein		0,326	0,321			
AT1G78100	expressed protein		0,296	0,286		0,945	1,206
AT1G51010	hypothetical protein	0,675	0,259	0,215			
AT4G33560	putative protein		0,256	0,292			
AT3G25770	AOC3		0,277	0,242		3,941	2,512
AT4G34950	putative protein	0,543	0,244	0,3	1,79	2,034	1,395
AT3G58790	Transferring glycosyl groups / transferase	0,295	0,226		2,143		

The whole genome microarray (Agilent 1/2) was used by Huang Xi to explore transcriptional changes in Arabidopsis cell suspension cultures and plants in response to the NO donor (±)-(E)-ethyl-2-[(E)-hydroxyimino]-5-nitro-3-hexeneamide (NOR-3) and gaseous NO. Here the up (orange-red) down (green) regulated genes are presented: 28 genes up-regulated in almost all experiments; 79 and 121 genes exclusively induced in cell culture and plant experiments; 26 genes down-regulated in cell culture experiments.

Legend:

A: Agilent array 1; Cell cultures + NOR3 1h

B: Agilent array 2; Cell cultures + NOR3 1h

C: Agilent array 2; Cell cultures + NOR3 3h

D: Agilent array 1; Plants + NOR3 1h

E: Agilent array 2; Plants + NOR3 1h

F: Agilent array 2; Plants + NOR3 3h

up-regulated | down-regulated
>3 | 2-2.5 | 0.5-0.4 | <0.3
2.5-3 | 0 | 0.4-0.3
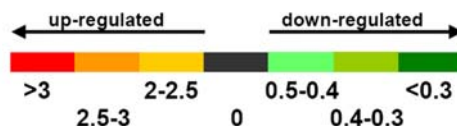
8.5 APPENDIX E

- ARABIDOPSIS THALIANA GLYCINE DECARBOXYLASE P PROTEIN 1

  UniProtKB: Q94B78

```
            10         20         30         40         50         60
        MERARRLAYR GIVKRLVNDT KRHRNAETPH LVPHAPARYV SSLSPFISTP RSVNHTAAFG

            70         80         90        100        110        120
        RHQQTRSISV DAVKPSDTFP RRHNSATPDE QTHMAKFCGF DHIDSLIDAT VPKSIRLDSM

           130        140        150        160        170        180
        KFSKFDAGLT ESQMIQHMVD LASKNKVFKS FIGMGYYNTH VPTVILRNIM ENPAWYTQYT

           190        200        210        220        230        240
        PYQAEISQGR LESLLNFQTV ITDLTGLPMS NASLLDEGTA AAEAMAMCNN ILKGKKKTFV

           250        260        270        280        290        300
        IASNCHPQTI DVCKTRADGF DLKVVTSDLK DIDYSSGDVC GVLVQYPGTE GEVLDYAEFV

           310        320        330        340        350        360
        KNAHANGVKV VMATDLLALT VLKPPGEFGA DIVVGSAQRF GVPMGYGGPH AAFLATSQEY

           370        380        390        400        410        420
        KRMMPGRIIG ISVDSSGKQA LRMAMQTREQ HIRRDKATSN ICTAQALLAN MAAMYAVYHG

           430        440        450        460        470        480
        PAGLKSIAQR VHGLAGIFSL GLNKLGVAEV QELPFFDTVK IKCSDAHAIA DAASKSEINL

           490        500        510        520        530        540
        RVVDSTTITA SFDETTTLDD VDKLFKVFAS GKPVPFTAES LAPEVQNSIP SSLTRESPYL

           550        560        570        580        590        600
        THPIFNMYHT EHELLRYIHK LQSKDLSLCH SMIPLGSCTM KLNATTEMMP VTWPSFTDIH

           610        620        630        640        650        660
        PFAPVEQAQG YQEMFENLGD LLCTITGFDS FSLQPNAGAA GEYAGLMVIR AYHMSRGDHH

           670        680        690        700        710        720
        RNVCIIPVSA HGTNPASAAM CGMKIITVGT DAKGNINIEE VRKAAEANKD NLAALMVTYP

           730        740        750        760        770        780
        STHGVYEEGI DEICNIIHEN GGQVYMDGAN MNAQVGLTSP GFIGADVCHL NLHKTFCIPH

           790        800        810        820        830        840
        GGGGPGMGPI GVKNHLAPFL PSHPVIPTGG IPQPEKTAPL GAISAAPWGS ALILPISYTY

           850        860        870        880        890        900
        IAMMGSGGLT DASKIAILNA NYMAKRLEKH YPVLFRGVNG TVAHEFIIDL RGFKNTAGIE

           910        920        930        940        950        960
        PEDVAKRLMD YGFHGPTMSW PVPGTLMIEP TESESKAELD RFCDALISIR EEIAQIEKGN

           970        980        990       1000       1010       1020
        ADVQNNVLKG APHPPSLLMA DTWKKPYSRE YAAFPAPWLR SSKFWPTTGR VDNVYGDRKL

          1030
        VCTLLPEEEQ VAAAVSA
```

Cysteine residues are underlined. By MS analysis 6 modified cysteine residues were identified (red).

- ARABIDOPSIS THALIANA GLYCINE DECARBOXYLASE P PROTEIN 2

  UniProtKB: O80988

```
        10         20         30         40         50         60
MERARRLAYR GIVKRLVNET KRHRNGESSL LPTTTVTPSR YVSSVSSFLH RRRDVSGSAF

        70         80         90        100        110        120
TTSGRNQHQT RSISVDALKP SDTFPRRHNS ATPDEQAQMA NYCGFDNLNT LIDSTVPKSI

       130        140        150        160        170        180
RLDSMKFSGI FDEGLTESQM IEHMSDLASK NKVFKSFIGM GYYNTHVPPV ILRNIMENPA

       190        200        210        220        230        240
WYTQYTPYQA EISQGRLESL LNYQTVITDL TGLPMSNASL LDEGTAAAEA MAMCNNILKG

       250        260        270        280        290        300
KKKTFVIASN CHPQTIDVCK TRADGFDLKV VTVDIKDVDY SSGDVCGVLV QYPGTEGEVL

       310        320        330        340        350        360
DYGEFVKNAH ANGVKVVMAT DLLALTMLKP PGEFGADIVV GSGQRFGVPM GYGGPHAAFL

       370        380        390        400        410        420
ATSQEYKRMM PGRIIGVSVD SSGKQALRMA MQTREQHIRR DKATSNICTA QALLANMTAM

       430        440        450        460        470        480
YAVYHGPEGL KSIAQRVHGL AGVFALGLKK LGTAQVQDLP FFDTVKVTCS DATAIFDVAA

       490        500        510        520        530        540
KKEINLRLVD SNTITVAFDE TTTLDDVDKL FEVFASGKPV QFTAESLAPE FNNAIPSSLT

       550        560        570        580        590        600
RESPYLTHPI FNMYHTEHEL LRYIHKLQNK DLSLCHSMIP LGSCTMKLNA TTEMMPVTWP

       610        620        630        640        650        660
SFTNMHPFAP VEQAQGYQEM FTNLGELLCT ITGFDSFSLQ PNAGAAGEYA GLMVIRAYHM

       670        680        690        700        710        720
SRGDHHRNVC IIPVSAHGTN PASAAMCGMK IVAVGTDAKG NINIEELRNA AEANKDNLAA

       730        740        750        760        770        780
LMVTYPSTHG VYEEGIDEIC NIIHENGGQV YMDGANMNAQ VGLTSPGFIG ADVCHLNLHK

       790        800        810        820        830        840
TFCIPHGGGG PGMGPIGVKQ HLAPFLPSHP VIPTGGIPEP EQTSPLGTIS AAPWGSALIL

       850        860        870        880        890        900
PISYTYIAMM GSGGLTDASK IAILNANYMA KRLESHYPVL FRGVNGTVAH EFIIDLRGFK

       910        920        930        940        950        960
NTAGIEPEDV AKRLMDYGFH GPTMSWPVPG TLMIEPTESE SKAELDRFCD ALISIREEIS

       970        980        990       1000       1010       1020
QIEKGNADPN NNVLKGAPHP PSLLMADTWK KPYSREYAAF PAPWLRSSKF WPTTGRVDNV

      1030       1040
YGDRNLVCTL QPANEEQAAA AVSA
```

Cysteine residues are underlined. By MS analysis 3 modified cysteine residues were identified (red).

9 References

Abe H, Urao T, Ito T, Seki M, Shinozaki K, Yamaguchi-Shinozaki K (2003) Arabidopsis AtMYC2 (bHLH) and AtMYB2 (MYB) function as transcriptional activators in abscisic acid signaling. Plant Cell **15:** 63-78

Abe M, Takahashi T, Komeda Y (2001) Identification of a cis-regulatory element for L1 layer-specific gene expression, which is targeted by an L1-specific homeodomain protein. Plant J **26:** 487-494

Allan AC, Fluhr R (1997) Two Distinct Sources of Elicited Reactive Oxygen Species in Tobacco Epidermal Cells. Plant Cell **9:** 1559-1572

Anderson JP, Badruzsaufari E, Schenk PM, Manners JM, Desmond OJ, Ehlert C, Maclean DJ, Ebert PR, Kazan K (2004) Antagonistic interaction between abscisic acid and jasmonate-ethylene signaling pathways modulates defense gene expression and disease resistance in Arabidopsis. Plant Cell **16:** 3460-3479

Barchowsky A, Klei LR, Dudek EJ, Swartz HM, James PE (1999) Stimulation of reactive oxygen, but not reactive nitrogen species, in vascular endothelial cells exposed to low levels of arsenite. Free Radic Biol Med **27:** 1405-1412

Bauwe H, Kolukisaoglu U (2003) Genetic manipulation of glycine decarboxylation. J Exp Bot **54:** 1523-1535

Belenghi B, Romero-Puertas MC, Vercammen D, Brackenier A, Inze D, Delledonne M, Van Breusegem F (2007) Metacaspase activity of Arabidopsis thaliana is regulated by S-nitrosylation of a critical cysteine residue. J Biol Chem **282:** 1352-1358

Beligni MV, Lamattina L (2001) Nitric oxide: a non-traditional regulator of plant growth. Trends Plant Sci **6:** 508-509

Bethke PC, Badger MR, Jones RL (2004) Apoplastic synthesis of nitric oxide by plant tissues. Plant Cell **16:** 332-341

Blackwell RD, Murray AJ, Lea PJ (1990) Photorespiratory Mutants of the Mitochondrial Conversion of Glycine to Serine. Plant Physiol **94:** 1316-1322

Bogdan C (2001) Nitric oxide and the regulation of gene expression. Trends Cell Biol **11:** 66-75

Bolwell GP, Bindschedler LV, Blee KA, Butt VS, Davies DR, Gardner SL, Gerrish C, Minibayeva F (2002) The apoplastic oxidative burst in response to biotic stress in plants: a three-component system. J Exp Bot **53:** 1367-1376

Borutaite V, Brown GC (2006) S-nitrosothiol inhibition of mitochondrial complex I causes a reversible increase in mitochondrial hydrogen peroxide production. Biochim Biophys Acta **1757:** 562-566

Boter M, Ruiz-Rivero O, Abdeen A, Prat S (2004) Conserved MYC transcription factors play a key role in jasmonate signaling both in tomato and Arabidopsis. Genes Dev **18:** 1577-1591

Bourguignon J, Neuburger M, Douce R (1988) Resolution and characterization of the glycine-cleavage reaction in pea leaf mitochondria. Properties of the forward reaction catalysed by glycine decarboxylase and serine hydroxymethyltransferase. Biochem J **255:** 169-178

Bradford MM (1976) A rapid and sensitive method for the quantitation of microgram quantities of protein utilizing the principle of protein-dye binding. Anal Biochem **72:** 248-254

Brooks A, Farquhar GD (1985) Effect of temperature on the CO2/O2 specificity of ribulose-1,5-bisphosphate carboxylase/oxygenase and the rate of respiration in the light. Planta **165:** 397-406

Brunori M, Giuffre A, Sarti P, Stubauer G, Wilson MT (1999) Nitric oxide and cellular respiration. Cell Mol Life Sci **56:** 549-557

Burwell LS, Nadtochiy SM, Tompkins AJ, Young S, Brookes PS (2006) Direct evidence for S-nitrosation of mitochondrial complex I. Biochem J **394:** 627-634

Cardinale F, Jonak C, Ligterink W, Niehaus K, Boller T, Hirt H (2000) Differential activation of four specific MAPK pathways by distinct elicitors. J Biol Chem **275:** 36734-36740

Chen W, Provart NJ, Glazebrook J, Katagiri F, Chang HS, Eulgem T, Mauch F, Luan S, Zou G, Whitham SA, Budworth PR, Tao Y, Xie Z, Chen X, Lam S, Kreps JA, Harper JF, Si-Ammour A, Mauch-Mani B, Heinlein M, Kobayashi K, Hohn T, Dangl JL, Wang X, Zhu T (2002) Expression profile matrix of Arabidopsis transcription factor genes suggests their putative functions in response to environmental stresses. Plant Cell **14:** 559-574

Chen WQ, Singh KB (1999) The auxin, hydrogen peroxide and salicylic acid induced expression of the Arabidopsis GST6 promoter is mediated in part by an ocs element. Plant Journal **19:** 667-677

Chen Y, Gibson SB (2008) Is mitochondrial generation of reactive oxygen species a trigger for autophagy? Autophagy **4:** 246-248

Chivasa S, Carr JP (1998) Cyanide restores N gene-mediated resistance to tobacco mosaic virus in transgenic tobacco expressing salicylic acid hydroxylase. Plant Cell **10:** 1489-1498

Choi H, Hong J, Ha J, Kang J, Kim SY (2000) ABFs, a family of ABA-responsive element binding factors. J Biol Chem **275:** 1723-1730

References

Clarke A, Desikan R, Hurst RD, Hancock JT, Neill SJ (2000) NO way back: nitric oxide and programmed cell death in Arabidopsis thaliana suspension cultures. Plant J **24:** 667-677

Cleeter MW, Cooper JM, Darley-Usmar VM, Moncada S, Schapira AH (1994) Reversible inhibition of cytochrome c oxidase, the terminal enzyme of the mitochondrial respiratory chain, by nitric oxide. Implications for neurodegenerative diseases. FEBS Lett **345:** 50-54

Clementi E, Brown GC, Feelisch M, Moncada S (1998) Persistent inhibition of cell respiration by nitric oxide: crucial role of S-nitrosylation of mitochondrial complex I and protective action of glutathione. Proc Natl Acad Sci U S A **95:** 7631-7636

Clyde Hill A, Bennett JH (1970) Inhibition of apparent photosynthesis by nitrogen oxides. Atmospheric Environment (1967) **4:** 341-348

Cohen G, Kim M, Ogwu V (1996) A modified catalase assay suitable for a plate reader and for the analysis of brain cell cultures. J Neurosci Methods **67:** 53-56

Cormack RS, Eulgem T, Rushton PJ, Kochner P, Hahlbrock K, Somssich IE (2002) Leucine zipper-containing WRKY proteins widen the spectrum of immediate early elicitor-induced WRKY transcription factors in parsley. Biochim Biophys Acta **1576:** 92-100.

Crawford NM, Galli M, Tischner R, Heimer YM, Okamoto M, Mack A (2006) Response to Zemojtel et al: Plant nitric oxide synthase: back to square one. Trends in Plant Science **11:** 526-527

Creach E, Stewart CR (1982) Effects of Aminoacetonitrile on Net Photosynthesis, Ribulose-1,5-Bisphosphate Levels, and Glycolate Pathway Intermediates. Plant Physiol **70:** 1444-1448

Dahm CC, Moore K, Murphy MP (2006) Persistent S-nitrosation of complex I and other mitochondrial membrane proteins by S-nitrosothiols but not nitric oxide or peroxynitrite: implications for the interaction of nitric oxide with mitochondria. J Biol Chem **281:** 10056-10065

Delledonne M (2005) NO news is good news for plants. Curr Opin Plant Biol **8:** 390-396

Delledonne M, Xia Y, Dixon RA, Lamb C (1998) Nitric oxide functions as a signal in plant disease resistance. Nature **394:** 585-588

Delledonne M, Zeier J, Marocco A, Lamb C (2001) Signal interactions between nitric oxide and reactive oxygen intermediates in the plant hypersensitive disease resistance response. Proc Natl Acad Sci U S A **98:** 13454-13459

Desikan R, Griffiths R, Hancock J, Neill S (2002) A new role for an old enzyme: nitrate reductase-mediated nitric oxide generation is required for abscisic acid-induced stomatal closure in Arabidopsis thaliana. Proc Natl Acad Sci U S A **99:** 16314-16318

Desikan R, Reynolds A, Hancock JT, Neill SJ (1998) Harpin and hydrogen peroxide both initiate programmed cell death but have differential effects on defence gene expression in Arabidopsis suspension cultures. Biochem J **330 (Pt 1):** 115-120

Dong J, Chen C, Chen Z (2003) Expression profiles of the Arabidopsis WRKY gene superfamily during plant defense response. Plant Mol Biol **51:** 21-37

Douce R, Bourguignon J, Neuburger M, Rebeille F (2001) The glycine decarboxylase system: a fascinating complex. Trends Plant Sci **6:** 167-176

Dröge-Laser W, Kaiser A, Lindsay WP, Halkier BA, Loake GJ, Doerner P, Dixon RA, Lamb C (1997) Rapid stimulation of a soybean protein-serine kinase which phosphorylates a novel bZIP DNA-binding protein, G/HBF-1, in the iduction of early transcription-dependent defenses. EMBO J. **16:** 726-738

Durner J, Klessig DF (1999) Nitric oxide as a signal in plants. Curr Opin Plant Biol **2:** 369-374

Durner J, Wendehenne D, Klessig DF (1998) Defense gene induction in tobacco by nitric oxide, cyclic GMP, and cyclic ADP-ribose. Proc Natl Acad Sci U S A **95:** 10328-10333

Eaton P, Jones ME, McGregor E, Dunn MJ, Leeds N, Byers HL, Leung KY, Ward MA, Pratt JR, Shattock MJ (2003) Reversible cysteine-targeted oxidation of proteins during renal oxidative stress. J Am Soc Nephrol **14:** S290-296

Ellenberger TE, Brandl CJ, Struhl K, Harrison SC (1992) The GCN4 basic region leucine zipper binds DNA as a dimer of uninterrupted alpha helices: crystal structure of the protein-DNA complex. Cell **71:** 1223-1237

Eubel H, Lee CP, Kuo J, Meyer EH, Taylor NL, Millar AH (2007) Free-flow electrophoresis for purification of plant mitochondria by surface charge. Plant J **52:** 583-594

Eulgem T, Rushton PJ, Robatzek S, Somssich IE (2000) The WRKY superfamily of plant transcription factors. Trends Plant Sci **5:** 199-206

Eulgem T, Rushton PJ, Schmelzer E, Hahlbrock K, Somssich IE (1999) Early nuclear events in plant defence signalling: rapid gene activation by WRKY transcription factors. Embo J **18:** 4689-4699

Farquhar GD (1979) Models describing the kinetics of ribulose biphosphate carboxylase-oxygenase. Arch Biochem Biophys **193:** 456-468

Farquhar GD, Caemmerer S, Berry JA (1980) A biochemical model of photosynthetic CO2 assimilation in leaves of C3 species. Planta **149:** 78-90

Feechan A, Kwon E, Yun BW, Wang Y, Pallas JA, Loake GJ (2005) A central role for S-nitrosothiols in plant disease resistance. Proc Natl Acad Sci U S A **102:** 8054-8059

Foissner I, Wendehenne D, Langebartels C, Durner J (2000) In vivo imaging of an elicitor-induced nitric oxide burst in tobacco. Plant J **23:** 817-824

Foster MW, Stamler JS (2004) New insights into protein S-nitrosylation. Mitochondria as a model system. J Biol Chem **279:** 25891-25897

Foyer CH, Parry M, Noctor G (2003) Markers and signals associated with nitrogen assimilation in higher plants. J Exp Bot **54:** 585-593

Fukao Y, Hayashi M, Nishimura M (2002) Proteomic analysis of leaf peroxisomal proteins in greening cotyledons of Arabidopsis thaliana. Plant Cell Physiol **43:** 689-696

Furchgott RF (1995) A research trail over half a century. Annu Rev Pharmacol Toxicol **35:** 1-27

References

Garcia-Mata C, Gay R, Sokolovski S, Hills A, Lamattina L, Blatt MR (2003) Nitric oxide regulates K+ and Cl- channels in guard cells through a subset of abscisic acid-evoked signaling pathways. Proc Natl Acad Sci U S A **100:** 11116-11121

Garcia-Mata C, Lamattina L (2002) Nitric oxide and abscisic acid cross talk in guard cells. Plant Physiol **128:** 790-792

Geigenberger P, Lerchi J, Stitt M, Sonnewald U (1996) Phloem-specific expression of pyrophosphatase inhibits long distance transport of carbohydrates and amino acids in tobacco plants. Plant, Cell and Environment **19:** 43-55

Godde JS, Nakatani Y, Wolffe AP (1995) The amino-terminal tails of the core histones and the translational position of the TATA box determine TBP/TFIIA association with nucleosomal DNA. Nucleic Acids Res **23:** 4557-4564

Goldstein JC, Waterhouse NJ, Juin P, Evan GI, Green DR (2000) The coordinate release of cytochrome c during apoptosis is rapid, complete and kinetically invariant. Nat Cell Biol **2:** 156-162

Gould KS, Lamotte O, Klinguer A, Pugin A, Wendehenne D (2003) Nitric oxide production in tobacco leaf cells: a generalized stress response? Plant, Cell & Environment **26:** 1851-1862

Green DR, Reed JC (1998) Mitochondria and apoptosis. Science **281:** 1309-1312

Grotewold E, Chamberlin M, Snook M, Siame B, Butler L, Swenson J, Maddock S, St Clair G, Bowen B (1998) Engineering secondary metabolism in maize cells by ectopic expression of transcription factors. Plant Cell **10:** 721-740

Guo FQ, Okamoto M, Crawford NM (2003) Identification of a plant nitric oxide synthase gene involved in hormonal signaling. Science **302:** 100-103

Gupta KJ, Stoimenova M, Kaiser WM (2005) In higher plants, only root mitochondria, but not leaf mitochondria reduce nitrite to NO, in vitro and in situ. J Exp Bot **56:** 2601-2609

Hagemann M, Vinnemeier J, Oberpichler I, Boldt R, Bauwe H (2005) The glycine decarboxylase complex is not essential for the cyanobacterium Synechocystis sp. strain PCC 6803. Plant Biol (Stuttg) **7:** 15-22

Halliwell B, Whiteman M (2004) Measuring reactive species and oxidative damage in vivo and in cell culture: how should you do it and what do the results mean? Br J Pharmacol **142:** 231-255

Hanafy KA, Krumenacker JS, Murad F (2001) NO, nitrotyrosine, and cyclic GMP in signal transduction. Med Sci Monit **7:** 801-819

Hasse D, Mikkat S, Thrun HA, Hagemann M, Bauwe H (2007) Properties of recombinant glycine decarboxylase P- and H-protein subunits from the cyanobacterium Synechocystis sp. strain PCC 6803. FEBS Lett **581:** 1297-1301

Hausladen A, Privalle CT, Keng T, DeAngelo J, Stamler JS (1996) Nitrosative stress: activation of the transcription factor OxyR. Cell **86:** 719-729

He Y, Fukushige H, Hildebrand DF, Gan S (2002) Evidence supporting a role of jasmonic acid in Arabidopsis leaf senescence. Plant Physiol **128:** 876-884

Heazlewood JL, Tonti-Filippini JS, Gout AM, Day DA, Whelan J, Millar AH (2004) Experimental analysis of the Arabidopsis mitochondrial proteome highlights signaling and regulatory components, provides assessment of targeting prediction programs, and indicates plant-specific mitochondrial proteins. Plant Cell **16:** 241-256

Heidrich HG, Stahn R, Hannig K (1970) The surface charge of rat liver mitochondria and their membranes. Clarification of some controversies concerning mitochondrial structure. J Cell Biol **46:** 137-150

Heineke D, Bykova N, Gardestrom P, Bauwe H (2001) Metabolic response of potato plants to an antisense reduction of the P-protein of glycine decarboxylase. Planta **212:** 880-887

Heisler MG, Atkinson A, Bylstra YH, Walsh R, Smyth DR (2001) SPATULA, a gene that controls development of carpel margin tissues in Arabidopsis, encodes a bHLH protein. Development **128:** 1089-1098

Hess DT, Matsumoto A, Kim SO, Marshall HE, Stamler JS (2005) Protein S-nitrosylation: purview and parameters. Nat Rev Mol Cell Biol **6:** 150-166

Hiraga K, Kikuchi G (1980) The mitochondrial glycine cleavage system. Functional association of glycine decarboxylase and aminomethyl carrier protein. J Biol Chem **255:** 11671-11676

Hiraga K, Kikuchi G (1980) The mitochondrial glycine cleavage system. Purification and properties of glycine decarboxylase from chicken liver mitochondria. J Biol Chem **255:** 11664-11670

Hiraga K, Kikuchi G (1982) The mitochondrial glycine cleavage system: differential inhibition by divalent cations of glycine synthesis and glycine decarboxylation in the glycine-CO2 exchange. J Biochem **92:** 937-944

Hobo T, Kowyama Y, Hattori T (1999) A bZIP factor, TRAB1, interacts with VP1 and mediates abscisic acid-induced transcription. Proc Natl Acad Sci U S A **96:** 15348-15353

Hoeren FU, Dolferus R, Wu Y, Peacock WJ, Dennis ES (1998) Evidence for a role for AtMYB2 in the induction of the Arabidopsis alcohol dehydrogenase gene (ADH1) by low oxygen. Genetics **149:** 479-490

Huang X, Stettmaier K, Michel C, Hutzler P, Mueller MJ, Durner J (2004) Nitric oxide is induced by wounding and influences jasmonic acid signaling in Arabidopsis thaliana. Planta **218:** 938-946

Huang X, von Rad U, Durner J (2002) Nitric oxide induces transcriptional activation of the nitric oxide-tolerant alternative oxidase in Arabidopsis suspension cells. Planta **215:** 914-923

Igamberdiev AU, Bykova NV, Lea PJ, Gardestrom P (2001) The role of photorespiration in redox and energy balance of photosynthetic plant cells: A study with a barley mutant deficient in glycine decarboxylase. Physiol Plant **111:** 427-438

Iturriaga G, Leyns L, Villegas A, Gharaibeh R, Salamini F, Bartels D (1996) A family of novel myb-related genes from the resurrection plant Craterostigma plantagineum are

specifically expressed in callus and roots in response to ABA or desiccation. Plant Mol Biol **32:** 707-716

Izawa T, Foster R, Chua NH (1993) Plant bZIP protein DNA binding specificity. J Mol Biol **230:** 1131-1144

Jaffrey SR, Snyder SH (2001) The biotin switch method for the detection of S-nitrosylated proteins. Sci STKE **2001:** PL1

Jasid S, Simontacchi M, Bartoli CG, Puntarulo S (2006) Chloroplasts as a nitric oxide cellular source. Effect of reactive nitrogen species on chloroplastic lipids and proteins. Plant Physiol **142:** 1246-1255

Johnson CS, Kolevski B, Smyth DR (2002) TRANSPARENT TESTA GLABRA2, a trichome and seed coat development gene of Arabidopsis, encodes a WRKY transcription factor. Plant Cell **14:** 1359-1375

Keech O, Dizengremel P, Gardestr, ouml, m P (2005) Preparation of leaf mitochondria from Arabidopsis thaliana. Physiologia Plantarum **124:** 403-409

Kim TS, Russell SJ, Collins MK, Cohen EP (1992) Immunity to B16 melanoma in mice immunized with IL-2-secreting allogeneic mouse fibroblasts expressing melanoma-associated antigens. Int J Cancer **51:** 283-289

Klessig DF, Durner J, Noad R, Navarre DA, Wendehenne D, Kumar D, Zhou JM, Shah J, Zhang S, Kachroo P, Trifa Y, Pontier D, Lam E, Silva H (2000) Nitric oxide and salicylic acid signaling in plant defense. Proc Natl Acad Sci U S A **97:** 8849-8855

Kopyra M, Gwó d E (2004) The role of nitric oxide in plant growth regulation and responses to abiotic stresses. Acta Physiologiae Plantarum **26:** 459-473

Korfhage U, Trezzini GF, Meier I, Hahlbrock K, Somssich IE (1994) Plant homeodomain protein involved in transcriptional regulation of a pathogen defense-related gene. Plant Cell **6:** 695-708

Kozlov AV, Staniek K, Nohl H (1999) Nitrite reductase activity is a novel function of mammalian mitochondria. FEBS Lett **454:** 127-130

Krause M, Durner J (2004) Harpin inactivates mitochondria in Arabidopsis suspension cells. Mol Plant Microbe Interact **17:** 131-139

Kruft V, Eubel H, Jansch L, Werhahn W, Braun HP (2001) Proteomic approach to identify novel mitochondrial proteins in Arabidopsis. Plant Physiol **127:** 1694-1710

Laemli UK (1970) Most commonly used discontinuous buffer system for SDS electrophoresis. Nature **227:** 680-685

Lam E, del Pozo O (2000) Caspase-like protease involvement in the control of plant cell death. Plant Mol Biol **44:** 417-428

Lara P, Onate-Sanchez L, Abraham Z, Ferrandiz C, Diaz I, Carbonero P, Vicente-Carbajosa J (2003) Synergistic activation of seed storage protein gene expression in Arabidopsis by ABI3 and two bZIPs related to OPAQUE2. J Biol Chem **278:** 21003-21011

Lebel E, Heifetz P, Thorne L, Uknes S, Ryals J, Ward E (1998) Functional analysis of regulatory sequences controlling PR-1 gene expression in Arabidopsis. Plant Journal **16:** 223-233

Lee MM, Schiefelbein J (1999) WEREWOLF, a MYB-related protein in Arabidopsis, is a position-dependent regulator of epidermal cell patterning. Cell **99:** 473-483

Lee U, Wie C, Fernandez BO, Feelisch M, Vierling E (2008) Modulation of Nitrosative Stress by S-Nitrosoglutathione Reductase Is Critical for Thermotolerance and Plant Growth in Arabidopsis. Plant Cell **20:** 786-802

Lennon AM, Neuenschwander UH, Ribas-Carbo M, Giles L, Ryals JA, Siedow JN (1997) The Effects of Salicylic Acid and Tobacco Mosaic Virus Infection on the Alternative Oxidase of Tobacco. Plant Physiol **115:** 783-791

Leshem Y, Haramaty E (1996) The characterization and contrasting effects of the nitric oxide free radical in vegetative stress and senescence of Pisum sativum Linn. foliage. Journal of Plant Physiology **148:** 258-263

Leshem YY, Pinchasov Y (2000) Non-invasive photoacoustic spectroscopic determination of relative endogenous nitric oxide and ethylene content stoichiometry during the ripening of strawberries *Fragaria anannasa* (Duch.) and avocados *Persea americana* (Mill.). J. Exp. Bot. **51:** 1471-1473

Lindermayr C, Saalbach G, Bahnweg G, Durner J (2006) Differential inhibition of Arabidopsis methionine adenosyltransferases by protein S-nitrosylation. J Biol Chem **281:** 4285-4291

Lindermayr C, Saalbach G, Durner J (2005) Proteomic identification of S-nitrosylated proteins in Arabidopsis. Plant Physiol **137:** 921-930

Liu L, Hausladen A, Zeng M, Que L, Heitman J, Stamler JS (2001) A metabolic enzyme for S-nitrosothiol conserved from bacteria to humans. Nature **410:** 490-494

Livaja M, Palmieri MC, von Rad U, Durner J (2008) The effect of the bacterial effector protein harpin on transcriptional profile and mitochondrial proteins of Arabidopsis thaliana. J Proteomics **71:** 148-159

Logemann E, Wu S-H, Schröder J, Schmelzer E, Somsich IE, Hahlbrock K (1995) Gene activation by UV light, fungal elicitor or fungal infection in Petroselinum crispum is correlated with repression of cell cycle-related genes. Plant J. **8:** 865-876

Lorenzo O, Chico JM, Sanchez-Serrano JJ, Solano R (2004) JASMONATE-INSENSITIVE1 encodes a MYC transcription factor essential to discriminate between different jasmonate-regulated defense responses in Arabidopsis. Plant Cell **16:** 1938-1950

Madore M, Grodzinski B (1984) Effect of Oxygen Concentration on C-Photoassimilate Transport from Leaves of Salvia splendens L. Plant Physiol **76:** 782-786

Makino S, Matsushika A, Kojima M, Yamashino T, Mizuno T (2002) The APRR1/TOC1 quintet implicated in circadian rhythms of Arabidopsis thaliana: I. Characterization with APRR1-overexpressing plants. Plant Cell Physiol **43:** 58-69

References

Maleck K, Levine A, Eulgem T, Morgan A, Schmid J, Lawton KA, Dangl JL, Dietrich RA (2000) The transcriptome of Arabidopsis thaliana during systemic acquired resistance. Nat Genet **26:** 403-410.

Mannick JB, Schonhoff C, Papeta N, Ghafourifar P, Szibor M, Fang K, Gaston B (2001) S-Nitrosylation of mitochondrial caspases. J Cell Biol **154:** 1111-1116

Mannick JB, Schonhoff CM (2004) NO means no and yes: regulation of cell signaling by protein nitrosylation. Free Radic Res **38:** 1-7

Martinez-Ruiz A, Lamas S (2007) Signalling by NO-induced protein S-nitrosylation and S-glutathionylation: convergences and divergences. Cardiovasc Res **75:** 220-228

Metallo SJ, Schepartz A (1997) Certain bZIP peptides bind DNA sequentially as monomers and dimerize on the DNA. Nat Struct Biol **4:** 115-117

Millar AH, Day DA (1996) Nitric oxide inhibits the cytochrome oxidase but not the alternative oxidase of plant mitochondria. FEBS Lett **398:** 155-158

Millar AH, Sweetlove LJ, Giege P, Leaver CJ (2001) Analysis of the Arabidopsis mitochondrial proteome. Plant Physiol **127:** 1711-1727

Millar TM, Stevens CR, Benjamin N, Eisenthal R, Harrison R, Blake DR (1998) Xanthine oxidoreductase catalyses the reduction of nitrates and nitrite to nitric oxide under hypoxic conditions. FEBS Lett **427:** 225-228

Mittler R (2002) Oxidative stress, antioxidants and stress tolerance. Trends Plant Sci **7:** 405-410

Modolo LV, Cunha FQ, Braga MR, Salgado I (2002) Nitric oxide synthase-mediated phytoalexin accumulation in soybean cotyledons in response to the Diaporthe phaseolorum f. sp. meridionalis elicitor. Plant Physiol **130:** 1288-1297

Moller IM (2001) PLANT MITOCHONDRIA AND OXIDATIVE STRESS: Electron Transport, NADPH Turnover, and Metabolism of Reactive Oxygen Species. Annu Rev Plant Physiol Plant Mol Biol **52:** 561-591

Moreau M, Lee GI, Wang Y, Crane BR, Klessig DF (2008) AtNOS/AtNOA1 is a functional Arabidopsis thaliana cGTPase and not a nitric-oxide synthase. J Biol Chem **283:** 32957-32967

Morgenstern B, Atchley WR (1999) Evolution of bHLH transcription factors: modular evolution by domain shuffling? Mol Biol Evol **16:** 1654-1663

Morot-Gaudry-Talarmain Y, Rockel P, Moureaux T, Quillere I, Leydecker MT, Kaiser WM, Morot-Gaudry JF (2002) Nitrite accumulation and nitric oxide emission in relation to cellular signaling in nitrite reductase antisense tobacco. Planta **215:** 708-715

Moyano E, Martinez-Garcia JF, Martin C (1996) Apparent redundancy in myb gene function provides gearing for the control of flavonoid biosynthesis in antirrhinum flowers. Plant Cell **8:** 1519-1532

Mur LA, Kenton P, Lloyd AJ, Ougham H, Prats E (2008) The hypersensitive response; the centenary is upon us but how much do we know? J Exp Bot **59:** 501-520

Murre C, Bain G, van Dijk MA, Engel I, Furnari BA, Massari ME, Matthews JR, Quong MW, Rivera RR, Stuiver MH (1994) Structure and function of helix-loop-helix proteins. Biochim Biophys Acta **1218:** 129-135

Nakagami H, Pitzschke A, Hirt H (2005) Emerging MAP kinase pathways in plant stress signalling. Trends in Plant Science **10:** 339-346

Nakai T, Nakagawa N, Maoka N, Masui R, Kuramitsu S, Kamiya N (2005) Structure of P-protein of the glycine cleavage system: implications for nonketotic hyperglycinemia. Embo J **24:** 1523-1536

Navarre DA, Wolpert TJ (1995) Inhibition of the glycine decarboxylase multienzyme complex by the host-selective toxin victorin. Plant Cell **7:** 463-471

Neill S, Barros R, Bright J, Desikan R, Hancock J, Harrison J, Morris P, Ribeiro D, Wilson I (2008) Nitric oxide, stomatal closure, and abiotic stress. J. Exp. Bot. **59:** 165-176

Neill SJ, Desikan R, Clarke A, Hurst RD, Hancock JT (2002) Hydrogen peroxide and nitric oxide as signalling molecules in plants. J Exp Bot **53:** 1237-1247

Neill SJ, Desikan R, Hancock JT (2003) Nitric oxide signalling in plants. New Phytologist **159:** 11-35

Neuburger M, Day DA, Douce R (1985) Transport of NAD in Percoll-Purified Potato Tuber Mitochondria: Inhibition of NAD Influx and Efflux by N-4-Azido-2-nitrophenyl-4-aminobutyryl-3'-NAD. Plant Physiol **78:** 405-410

Neuburger M, Journet EP, Bligny R, Carde JP, Douce R (1982) Purification of plant mitochondria by isopycnic centrifugation in density gradients of Percoll. Arch Biochem Biophys **217:** 312-323

Neuburger M, Polidori AM, Pietre E, Faure M, Jourdain A, Bourguignon J, Pucci B, Douce R (2000) Interaction between the lipoamide-containing H-protein and the lipoamide dehydrogenase (L-protein) of the glycine decarboxylase multienzyme system. 1. Biochemical studies. Eur J Biochem **267:** 2882-2889

Nishimura H, Hayamizu T, Yanagisawa Y (1986) Reduction of nitrogen oxide (NO2) to nitrogen oxide (NO) by rush and other plants. Environmental Science & Technology **20:** 413-416

Noctor G, Foyer CH (1998) ASCORBATE AND GLUTATHIONE: Keeping Active Oxygen Under Control. Annu Rev Plant Physiol Plant Mol Biol **49:** 249-279

Okamura-Ikeda K, Hosaka H, Yoshimura M, Yamashita E, Toma S, Nakagawa A, Fujiwara K, Motokawa Y, Taniguchi H (2005) Crystal structure of human T-protein of glycine cleavage system at 2.0 A resolution and its implication for understanding non-ketotic hyperglycinemia. J Mol Biol **351:** 1146-1159

Oppenheimer DG, Herman PL, Sivakumaran S, Esch J, Marks MD (1991) A myb gene required for leaf trichome differentiation in Arabidopsis is expressed in stipules. Cell **67:** 483-493

Orozco-Cardenas ML, Ryan CA (2002) Nitric oxide negatively modulates wound signaling in tomato plants. Plant Physiol **130:** 487-493

References

Overmyer K, Brosche M, Kangasjarvi J (2003) Reactive oxygen species and hormonal control of cell death. Trends Plant Sci **8:** 335-342

Palmer RM, Ferrige AG, Moncada S (1987) Nitric oxide release accounts for the biological activity of endothelium-derived relaxing factor. Nature **327:** 524-526

Parani M, Rudrabhatla S, Myers R, Weirich H, Smith B, Leaman DW, Goldman SL (2004) Microarray analysis of nitric oxide responsive transcripts in Arabidopsis. Plant Biotechnol J **2:** 359-366

Pares S, Cohen-Addad C, Sieker L, Neuburger M, Douce R (1994) X-ray structure determination at 2.6-A resolution of a lipoate-containing protein: the H-protein of the glycine decarboxylase complex from pea leaves. Proc Natl Acad Sci U S A **91:** 4850-4853

Park CY, Lee JH, Yoo JH, Moon BC, Choi MS, Kang YH, Lee SM, Kim HS, Kang KY, Chung WS, Lim CO, Cho MJ (2005) WRKY group IId transcription factors interact with calmodulin. FEBS Lett **579:** 1545-1550

Parnik T, Ivanova H, Keerberg O (2007) Photorespiratory and respiratory decarboxylations in leaves of C3 plants under different CO2 concentrations and irradiances. Plant Cell Environ **30:** 1535-1544

Pedroso MC, Magalhaes JR, Durzan D (2000) A nitric oxide burst precedes apoptosis in angiosperm and gymnosperm callus cells and foliar tissues. J Exp Bot **51:** 1027-1036

Pedroso MC, Magalhaes JR, Durzan D (2000) Nitric oxide induces cell death in Taxus cells. Plant Sci **157:** 173-180

Peeters N, Small I (2001) Dual targeting to mitochondria and chloroplasts. Biochim Biophys Acta **1541:** 54-63

Pellinen R, Palva T, Kangasjarvi J (1999) Short communication: subcellular localization of ozone-induced hydrogen peroxide production in birch (Betula pendula) leaf cells. Plant J **20:** 349-356

Perez-Mato I, Castro C, Ruiz FA, Corrales FJ, Mato JM (1999) Methionine adenosyltransferase S-nitrosylation is regulated by the basic and acidic amino acids surrounding the target thiol. J Biol Chem **274:** 17075-17079

Petit PX, Lecoeur H, Zorn E, Dauguet C, Mignotte B, Gougeon ML (1995) Alterations in mitochondrial structure and function are early events of dexamethasone-induced thymocyte apoptosis. J Cell Biol **130:** 157-167

Planchet E, Jagadis Gupta K, Sonoda M, Kaiser WM (2005) Nitric oxide emission from tobacco leaves and cell suspensions: rate limiting factors and evidence for the involvement of mitochondrial electron transport. Plant J **41:** 732-743

Planchet E, Kaiser WM (2006) Nitric oxide (NO) detection by DAF fluorescence and chemiluminescence: a comparison using abiotic and biotic NO sources. J Exp Bot **57:** 3043-3055

Polverari A, Molesini B, Pezzotti M, Buonaurio R, Marte M, Delledonne M (2003) Nitric oxide-mediated transcriptional changes in Arabidopsis thaliana. Mol Plant Microbe Interact **16:** 1094-1105

Puntarulo S, Sanchez RA, Boveris A (1988) Hydrogen Peroxide Metabolism in Soybean Embryonic Axes at the Onset of Germination. Plant Physiol **86:** 626-630

Qiao W, Fan LM (2008) Nitric oxide signaling in plant responses to abiotic stresses. J Integr Plant Biol **50:** 1238-1246

Quandt K, Frech K, Karas H, Wingender E, Werner T (1995) MatInd and MatInspector: new fast and versatile tools for detection of consensus matches in nucleotide sequence data. Nucleic Acids Res **23:** 4878-4884

Rajani S, Sundaresan V (2001) The Arabidopsis myc/bHLH gene ALCATRAZ enables cell separation in fruit dehiscence. Curr Biol **11:** 1914-1922

Ratcliffe OJ, Riechmann JL (2002) Arabidopsis transcription factors and the regulation of flowering time: a genomic perspective. Curr Issues Mol Biol **4:** 77-91

Rhoads DM, Umbach AL, Subbaiah CC, Siedow JN (2006) Mitochondrial reactive oxygen species. Contribution to oxidative stress and interorganellar signaling. Plant Physiol **141:** 357-366

Riechmann JL, Heard J, Martin G, Reuber L, Jiang C, Keddie J, Adam L, Pineda O, Ratcliffe OJ, Samaha RR, Creelman R, Pilgrim M, Broun P, Zhang JZ, Ghandehari D, Sherman BK, Yu G (2000) Arabidopsis transcription factors: genome-wide comparative analysis among eukaryotes. Science **290:** 2105-2110

Rizhsky L, Liang H, Mittler R (2002) The combined effect of drought stress and heat shock on gene expression in tobacco. Plant Physiol **130:** 1143-1151

Robatzek S, Somssich IE (2001) A new member of the Arabidopsis WRKY transcription factor family, AtWRKY6, is associated with both senescence- and defence-related processes. Plant J **28:** 123-133

Robson CA, Vanlerberghe GC (2002) Transgenic plant cells lacking mitochondrial alternative oxidase have increased susceptibility to mitochondria-dependent and -independent pathways of programmed cell death. Plant Physiol **129:** 1908-1920

Romero-Puertas MC, Campostrini N, Matte A, Righetti PG, Perazzolli M, Zolla L, Roepstorff P, Delledonne M (2008) Proteomic analysis of S-nitrosylated proteins in Arabidopsis thaliana undergoing hypersensitive response. Proteomics **8:** 1459-1469

Romero-Puertas MC, Delledonne M (2003) Nitric oxide signaling in plant-pathogen interactions. IUBMB Life **55:** 579-583

Romero-Puertas MC, Laxa M, Matte A, Zaninotto F, Finkemeier I, Jones AM, Perazzolli M, Vandelle E, Dietz KJ, Delledonne M (2007) S-nitrosylation of peroxiredoxin II E promotes peroxynitrite-mediated tyrosine nitration. Plant Cell **19:** 4120-4130

Romero-Puertas MC, Perazzolli M, Zago ED, Delledonne M (2004) Nitric oxide signalling functions in plant-pathogen interactions. Cell Microbiol **6:** 795-803

Rushton PJ, Reinstadler A, Lipka V, Lippok B, Somssich IE (2002) Synthetic plant promoters containing defined regulatory elements provide novel insights into pathogen- and wound-induced signaling. Plant Cell **14:** 749-762

References

Rusterucci C, Espunya MC, Diaz M, Chabannes M, Martinez MC (2007) S-nitrosoglutathione reductase affords protection against pathogens in Arabidopsis, both locally and systemically. Plant Physiol **143:** 1282-1292

Ryerson DE, Heath MC (1996) Cleavage of Nuclear DNA into Oligonucleosomal Fragments during Cell Death Induced by Fungal Infection or by Abiotic Treatments. Plant Cell **8:** 393-402

Saviani EE, Orsi CH, Oliveira JF, Pinto-Maglio CA, Salgado I (2002) Participation of the mitochondrial permeability transition pore in nitric oxide-induced plant cell death. FEBS Lett **510:** 136-140

Schmidt HH, Walter U (1994) NO at work. Cell **78:** 919-925

Schonhoff CM, Gaston B, Mannick JB (2003) Nitrosylation of cytochrome c during apoptosis. J Biol Chem **278:** 18265-18270

Schopfer FJ, Baker PR, Freeman BA (2003) NO-dependent protein nitration: a cell signaling event or an oxidative inflammatory response? Trends Biochem Sci **28:** 646-654

Shingles R, Roh MH, McCarty RE (1996) Nitrite Transport in Chloroplast Inner Envelope Vesicles (I. Direct Measurement of Proton-Linked Transport). Plant Physiol **112:** 1375-1381

Shiva S, Brookes PS, Patel RP, Anderson PG, Darley-Usmar VM (2001) Nitric oxide partitioning into mitochondrial membranes and the control of respiration at cytochrome c oxidase. Proc Natl Acad Sci U S A **98:** 7212-7217

Siedow JN, Umbach AL (1995) Plant Mitochondrial Electron Transfer and Molecular Biology. Plant Cell **7:** 821-831

Skulachev VP (1996) Why are mitochondria involved in apoptosis? Permeability transition pores and apoptosis as selective mechanisms to eliminate superoxide-producing mitochondria and cell. FEBS Lett **397:** 7-10

Smale ST, Kadonaga JT (2003) The RNA polymerase II core promoter. Annu Rev Biochem **72:** 449-479

Stamler JS, Lamas S, Fang FC (2001) Nitrosylation. the prototypic redox-based signaling mechanism. Cell **106:** 675-683

Stamler JS, Singel DJ, Loscalzo J (1992) Biochemistry of nitric oxide and its redox-activated forms. Science **258:** 1898-1902

Stamler JS, Toone EJ, Lipton SA, Sucher NJ (1997) (S)NO signals: translocation, regulation, and a consensus motif. Neuron **18:** 691-696

Stohr C, Stremlau S (2006) Formation and possible roles of nitric oxide in plant roots. J Exp Bot **57:** 463-470

Stohr C, Strube F, Marx G, Ullrich WR, Rockel P (2001) A plasma membrane-bound enzyme of tobacco roots catalyses the formation of nitric oxide from nitrite. Planta **212:** 835-841

Sugimoto K, Takeda S, Hirochika H (2000) MYB-related transcription factor NtMYB2 induced by wounding and elicitors is a regulator of the tobacco retrotransposon Tto1 and defense-related genes. Plant Cell **12:** 2511-2528

Sun C, Palmqvist S, Olsson H, Boren M, Ahlandsberg S, Jansson C (2003) A novel WRKY transcription factor, SUSIBA2, participates in sugar signaling in barley by binding to the sugar-responsive elements of the iso1 promoter. Plant Cell **15:** 2076-2092

Tada Y, Kusaka K, Betsuyaku S, Shinogi T, Sakamoto M, Ohura Y, Hata S, Mori T, Tosa Y, Mayama S (2005) Victorin triggers programmed cell death and the defense response via interaction with a cell surface mediator. Plant Cell Physiol **46:** 1787-1798

Tada Y, Spoel SH, Pajerowska-Mukhtar K, Mou Z, Song J, Wang C, Zuo J, Dong X (2008) Plant immunity requires conformational charges of NPR1 via S-nitrosylation and thioredoxins. Science **321:** 952-956

Taylor NL, Day DA, Millar AH (2002) Environmental stress causes oxidative damage to plant mitochondria leading to inhibition of glycine decarboxylase. J Biol Chem **277:** 42663-42668

Taylor NL, Day DA, Millar AH (2004) Targets of stress-induced oxidative damage in plant mitochondria and their impact on cell carbon/nitrogen metabolism. J Exp Bot **55:** 1-10

Thornberry NA, Lazebnik Y (1998) Caspases: enemies within. Science **281:** 1312-1316

Tischner R, Planchet E, Kaiser WM (2004) Mitochondrial electron transport as a source for nitric oxide in the unicellular green alga Chlorella sorokiniana. FEBS Lett **576:** 151-155

Tiwari BS, Belenghi B, Levine A (2002) Oxidative stress increased respiration and generation of reactive oxygen species, resulting in ATP depletion, opening of mitochondrial permeability transition, and programmed cell death. Plant Physiol **128:** 1271-1281

Toshio Murashige FS (1962) A Revised Medium for Rapid Growth and Bio Assays with Tobacco Tissue Cultures. Physiologia Plantarum **15:** 473-497

Turck F, Zhou A, Somssich IE (2004) Stimulus-dependent, promoter-specific binding of transcription factor WRKY1 to Its native promoter and the defense-related gene PcPR1-1 in Parsley. Plant Cell **16:** 2573-2585

Turrens JF (2003) Mitochondrial formation of reactive oxygen species. J Physiol **552:** 335-344

Ueda J, Kato J (1980) Isolation and Identification of a Senescence-promoting Substance from Wormwood (Artemisia absinthium L.). Plant Physiol **66:** 246-249

Usuda H, Edwards GE (1980) Localization of Glycerate Kinase and Some Enzymes for Sucrose Synthesis in C(3) and C(4) Plants. Plant Physiol **65:** 1017-1022

References

Valderrama R, Corpas FJ, Carreras A, Fernandez-Ocana A, Chaki M, Luque F, Gomez-Rodriguez MV, Colmenero-Varea P, Del Rio LA, Barroso JB (2007) Nitrosative stress in plants. FEBS Lett **581:** 453-461

Vanlerberghe GC, Robson CA, Yip JY (2002) Induction of mitochondrial alternative oxidase in response to a cell signal pathway down-regulating the cytochrome pathway prevents programmed cell death. Plant Physiol **129:** 1829-1842

Vranova E, Inze D, Van Breusegem F (2002) Signal transduction during oxidative stress. J Exp Bot **53:** 1227-1236

Walker GH, Sarojini G, Oliver DJ (1982) Identification of a glycine transporter from pea leaf mitochondria. Biochem Biophys Res Commun **107:** 856-861

Walker JL, Oliver DJ (1986) Glycine decarboxylase multienzyme complex. Purification and partial characterization from pea leaf mitochondria. J Biol Chem **261:** 2214-2221

Walker JL, Oliver DJ (1986) Light-induced increases in the glycine decarboxylase multienzyme complex from pea leaf mitochondria. Arch Biochem Biophys **248:** 626-638

Wang D, Amornsiripanitch N, Dong X (2006) A genomic approach to identify regulatory nodes in the transcriptional network of systemic acquired resistance in plants. PLoS Pathog **2:** e123

Wang JW, Wu JY (2005) Nitric oxide is involved in methyl jasmonate-induced defense responses and secondary metabolism activities of Taxus cells. Plant Cell Physiol **46:** 923-930

Wendehenne D, Durner J, Klessig DF (2004) Nitric oxide: a new player in plant signalling and defence responses. Curr Opin Plant Biol **7:** 449-455

Wendehenne D, Pugin A, Klessig DF, Durner J (2001) Nitric oxide: comparative synthesis and signaling in animal and plant cells. Trends Plant Sci **6:** 177-183

Wingler A, Lea PJ, Quick WP, Leegood RC (2000) Photorespiration: metabolic pathways and their role in stress protection. Philos Trans R Soc Lond B Biol Sci **355:** 1517-1529

Xie Z, Chen Z (2000) Harpin-induced hypersensitive cell death is associated with altered mitochondrial functions in tobacco cells. Mol Plant Microbe Interact **13:** 183-190

Xu X, Chen C, Fan B, Chen Z (2006) Physical and functional interactions between pathogen-induced Arabidopsis WRKY18, WRKY40, and WRKY60 transcription factors. Plant Cell **18:** 1310-1326

Yamamoto A, Katou S, Yoshioka H, Doke N, Kawakita K (2003) Nitrate reductase, a nitric oxide-producing enzyme: induction by pathogen signals. Journal of General Plant Pathology **69:** 218-229

Yamasaki H, Sakihama Y (2000) Simultaneous production of nitric oxide and peroxynitrite by plant nitrate reductase: in vitro evidence for the NR-dependent formation of active nitrogen species. FEBS Lett **468:** 89-92

Yamasaki H, Shimoji H, Ohshiro Y, Sakihama Y (2001) Inhibitory effects of nitric oxide on oxidative phosphorylation in plant mitochondria. Nitric Oxide **5:** 261-270

Yamasaki K, Kigawa T, Inoue M, Tateno M, Yamasaki T, Yabuki T, Aoki M, Seki E, Matsuda T, Tomo Y, Hayami N, Terada T, Shirouzu M, Tanaka A, Seki M, Shinozaki K, Yokoyama S (2005) Solution structure of an Arabidopsis WRKY DNA binding domain. Plant Cell **17:** 944-956

Yang AJ, Mulligan RM (1996) Identification of a 4.5S-like ribonucleoprotein in maize mitochondria. Nucleic Acids Res **24:** 3601-3606

Yao N, Imai S, Tada Y, Nakayashiki H, Tosa Y, Park P, Mayama S (2002) Apoptotic cell death is a common response to pathogen attack in oats. Mol Plant Microbe Interact **15:** 1000-1007

Yao N, Tada Y, Sakamoto M, Nakayashiki H, Park P, Tosa Y, Mayama S (2002) Mitochondrial oxidative burst involved in apoptotic response in oats. Plant J **30:** 567-579

Yu D, Chen C, Chen Z (2001) Evidence for an important role of WRKY DNA binding proteins in the regulation of NPR1 gene expression. Plant Cell **13:** 1527-1540

Zemojtel T, Frohlich A, Palmieri MC, Kolanczyk M, Mikula I, Wyrwicz LS, Wanker EE, Mundlos S, Vingron M, Martasek P, Durner J (2006) Plant nitric oxide synthase: a never-ending story? Trends Plant Sci **11:** 524-525; author reply 526-528

Zhang C, Czymmek KJ, Shapiro AD (2003) Nitric oxide does not trigger early programmed cell death events but may contribute to cell-to-cell signaling governing progression of the Arabidopsis hypersensitive response. Mol Plant Microbe Interact **16:** 962-972

Zhao L, Zhang F, Guo J, Yang Y, Li B, Zhang L (2004) Nitric oxide functions as a signal in salt resistance in the calluses from two ecotypes of reed. Plant Physiol **134:** 849-857

Zhao Z, Chen G, Zhang C (2001) Interaction between reactive oxygen species and nitric oxide in drought-induced abscisic acid synthesis in root tips of wheat seedlings. Functional Plant Biology **28:** 1055-1061

Zhou JM, Trifa Y, Silva H, Pontier D, Lam E, Shah J, Klessig DF (2000) NPR1 differentially interacts with members of the TGA/OBF family of transcription factors that bind an element of the PR-1 gene required for induction by salicylic acid. Mol Plant Microbe Interact **13:** 191-202

Zischka H, Weber G, Weber PJ, Posch A, Braun RJ, Buhringer D, Schneider U, Nissum M, Meitinger T, Ueffing M, Eckerskorn C (2003) Improved proteome analysis of Saccharomyces cerevisiae mitochondria by free-flow electrophoresis. Proteomics **3:** 906-916

Zottini M, Formentin E, Scattolin M, Carimi F, Lo Schiavo F, Terzi M (2002) Nitric oxide affects plant mitochondrial functionality in vivo. FEBS Lett **515:** 75-78

Acknowledgements

I would like to thank:

Curriculum Vitae

E-mail: mcristina.palmieri@gmail.com

Nationalität: Italienisch

Geburtsort: in Grumo Appula (BA) on 07/29/1980

L e b e n s l a u f   v o n

MARIA CRISTINA PALMIERI, Dipl.Biotechnologin Univ.

Beruflicher Werdegang

Januar 2006 – März 2009   Helmholtz Zentrum München – München, Deutchland

Institut für Biochemische Pflanzenpathologie, Redox signalling and proteomics unit, apl. Univ.- Prof. Dr. Joerg Durner

Doktorarbeit

NITRIC OXIDE AND MITOCHONDRIA: MODULATION OF PHOTORESPIRATION BY S-NITROSYLATION

Juni 2005 – November 2005   Universität von Verona – Verona, Italien

Scientific and Technological Department, Division of Genetic Biotechnology, Univ.- Prof. Dr. Massimo Delledonne

Wissenschaftlicher Mitarbeiter

STUDY OF INDUCED SYSTEMIC RESISTANCE (ISR)

März 2005 – April 2005   Universität von Verona – Verona, Italien

'Biomolecular technology course', Univ.- Prof. Dr. Massimo Delledonne

Wissenschaftlicher Mitarbeiter

März 2004 – März 2005 Universität von Verona – Verona, Italien

Scientific and Technological Department, Division of Genetic Biotechnology, Univ.- Prof. Dr. Massimo Delledonne

Diplomarbeit

CHARACTERIZATION OF THE TRANSCRIPTION FACTOR NOi-ERF FROM *ARABIDOPSIS THALIANA* DURING PLANT-PATHOGEN INTERACTION

Ausbildung

Oktober 1999 – März 2005   Universität von Verona – Verona, Italien

Diplom Biotechnologie; Endnote:1,0

1994 – 1999   Liceo scientifico 'G. Tarantino' **–** Gravina di Puglia (Bari), Italien

Naturwissenschaftliches Gymnasium; Endnote: 86/100

Veröffentlichungen

NITRIC OXIDE RESPONSIVE GENES AND PROMOTERS IN ARABIDOPSIS THALIANA: A BIOINFORMATICS APPROACH.
Lindermayr C, Palmeri MC, and Durner J
Plant Signaling & Behavior. 2008

THE EFFECT OF THE BACTERIAL EFFECTOR PROTEIN HARPIN ON TRANSCRIPTIONAL PROFILE AND MITOCHONDRIAL PROTEINS OF ARABIDOPSIS THALIANA.
Livaja M, Palmieri MC, von Rad U, Durner J
Journal of proteomics. 2008 Jul 21;71(2):148-59

NITRIC OXIDE-RESPONSIVE GENES AND PROMOTERS IN ARABIDOPSIS THALIANA: A BIOINFORMATICS APPROACH.
Palmieri MC, Sell S, Huang X, Scherf M, Werner T, Durner J, Lindermayr C
Journal of experimental botany. 2008;59(2):177-86

PLANT NITRIC OXIDE SYNTHASE: A NEVER-ENDING STORY?
Zemojtel T, Fröhlich A, Palmieri MC, Kolanczyk M, Mikula I, Wyrwicz LS, Wanker EE, Mundlos S, Vingron M, Martasek P, Durner J
Trends in plant science. 2006 Nov;11(11):524-5; author reply 526-8

Kongressteilnahmen

Juli 2008
2nd Nitric Oxide Meeting
NITRIC OXIDE AND MITOCHONDRIA: MODULATION OF PHOTORESPIRATION BY S-NITROSYLATION (Präsentation)
M. Cristina Palmieri, Christian Lindermayr, Joerg Durner

September 2007

Reactive Oxygen Species meeting 2007

IDENTIFICATION OF THE S-NITROSYLATED PROTEINS IN ARABIDOPSIS THALIANA LEAVES MITOCHONDRIA (Poster)

M. Cristina Palmieri, Christian Lindermayr, Joerg Durner

September 2006

1st Nitric Oxide Meeting

September 2005

XLIX Annual Congress of SIGA (Italian Society of Agriculture Geneticists)

IDENTIFICATION OF GENES MODULATED BY NITRIC OXIDE IN MEDICAGO TRUNCATULA DURING SYMBIOSIS AND/OR PATHOGENESIS (Poster)

M. De Stefano, M.C. Palmieri, A. Ferrarini, F. Zaninotto, E. Baudouin, M. Delledonne

September 2005

VII National Congress of FISV (Italian Federation of Life Science)

FUNCTIONAL CHARACTERIZATION OF THE TRANSCRIPTION FACTOR NOi-ERF FROM A. THALIANA DURING PLANT- PATHOGEN INTERACTION (Präsentation und Poster)

M.C. Palmieri, M.C. Romero-Puertas, A. Mattè, F. Zaninotto, M. Delledonne

September 2004

XLVII Annual Congress of SIGA (Italian Society of Agriculture Geneticists)

Fremdsprachen

Italienisch: Muttersprache

Englisch: Flüssig in Sprache und Schrift

Französisch: Grundkenntnisse in Sprache und Schrift

Deutsch: Grundkenntnisse in Sprache und Schrift